

**USE OF FOURIER-TRANSFORM INFRARED SPECTROSCOPY TO DETERMINE  
IMMUNOGLOBULIN STATUS IN CAMELID AND EQUINE SPECIES**

A Thesis  
Submitted to the Graduate Faculty  
in Partial Fulfillment of the Requirements  
for the Degree of

MASTER OF SCIENCE

Department of Health Management  
Faculty of Veterinary Medicine  
University of Prince Edward Island

**Jennifer Joyce Burns**  
Charlottetown, P.E.I.  
April 14, 2014

© 2014. J.J. Burns

## **CONDITIONS OF USE**

The author has agreed that the Library, University of Prince Edward Island, may make this thesis freely available for inspection. Moreover, the author has agreed that permission for extensive copying of this thesis for scholarly purposes may be granted by the professor or professors who supervised the thesis work recorded herein or, in their absence, by the Chair of the Department or the Dean of the Faculty in which the thesis work was done. It is understood that due recognition will be given to the author of this thesis and to the University of Prince Edward Island in any use of the material in this thesis. Copying or publication or any other use of the thesis for financial gain without approval by the University of Prince Edward Island and the author's written permission is prohibited.

Requests for permission to copy or to make any other use of material in this thesis in whole or in part should be addressed to:

Chair of the Department of Health Management  
Faculty of Veterinary Medicine  
University of Prince Edward Island  
Charlottetown, PE  
Canada  
C1A 4P3

## PERMISSION TO USE POSTGRADUATE THESES

Title of Thesis: **“USE OF FOURIER-TRANSFORM INFRARED SPECTROSCOPY TO DETERMINE IMMUNOGLOBULIN STATUS IN CAMELID AND EQUINE SPECIES”**

Name of Author: Jennifer Joyce Burns

Department: Health Management

Degree: Master of Science Year: 2014

In presenting this thesis in partial fulfillment of the requirements for a postgraduate degree from the University of Prince Edward Island, I agree that the Libraries of this University may make it freely available for inspection. I further agree that permission for extensive copying of this thesis for scholarly purposes may be granted by the professor or professors who supervised my thesis work, or, in their absence, by the Chair of the Department or the Dean of the Faculty in which my thesis work was done. It is understood any copying or publication or use of this thesis or parts thereof for financial gain shall not be allowed without my written permission. It is also understood that due recognition shall be given to me and to the University of Prince Edward Island in any scholarly use which may be made of any material in my thesis.

Signature:

Address: Department of Health Management  
Faculty of Veterinary Medicine  
University of Prince Edward Island  
550 University Avenue  
Charlottetown, PE  
Canada  
C1A 4P3

Date: April 2014

**University of Prince Edward Island**

**Faculty of Veterinary Medicine**

**Charlottetown**

**CERTIFICATION OF THESIS WORK**

We, the undersigned, certify that **Jennifer Joyce Burns**, DVM, candidate for the degree of Master of Science, has presented his/her thesis with the following title:

**“Use of Fourier-transform infrared spectroscopy to determine immunoglobulin status  
in equine and camelid species”**

and that the thesis is acceptable in form and content, and that a satisfactory knowledge of the field covered by the thesis was demonstrated by the candidate through an oral examination held on **April 14, 2014**.

Examiners' Names

Examiners' Signatures

Dr. J McClure

\_\_\_\_\_

Dr. Anthony Shaw

\_\_\_\_\_

Dr. Jeanne Lofstedt

\_\_\_\_\_

Dr. Tammy Muirhead

\_\_\_\_\_

Dr. Daniel Hurnik

\_\_\_\_\_

Date: April 14, 2014

## **ABSTRACT**

Measurement of systemic immunoglobulin (Ig) concentrations in horses and camelids is important for early and accurate diagnosis of immunodeficiencies in order to provide proper medical intervention. As a consequence, there is a demand for up-to-date, economic, rapid and precise diagnostic assays for Igs. Accordingly, multiple methods for the evaluation of Ig concentrations have been evaluated in equine and camelid species, each with particular advantages and disadvantages.

Fourier-transform infrared (FTIR) spectroscopy has recently emerged as a powerful diagnostic tool for the quantitative characterization of biological fluids in human and veterinary medicine. In particular, FTIR spectroscopy has proven to be an accurate, economical and reagent-free method for immunoglobulin G (IgG) quantitation in horses. Further research to investigate its potential application in the quantitation of other equine Ig isotypes and IgG subclasses is warranted. Additionally, as rapid quantitative assays for the measurement of camelid serum IgG are limited, further work to assess the use of FTIR spectroscopy in this area is desirable.

The objectives of this thesis were: (1) to develop an FTIR-based assay for the measurement of IgG concentrations in alpaca serum and to compare its performance to that of the radial immunodiffusion (RID) assay, and (2) to develop FTIR-based assays for the measurement IgGa, IgGb, IgG(T), IgA, and IgM for equine plasma using ELISA assays as reference tests.

The first objective of this thesis was achieved by performing RID IgG assays and collecting FTIR spectra for 175 alpaca serum samples. A FTIR-based assay was built using

partial least squares regression to convert the spectroscopic data into quantitative IgG values which were compared to the RID results. Correlation coefficients and scatter plots indicated good to excellent levels of agreement between the assays. The results suggest that FTIR spectroscopy may be a useful method for IgG measurement in alpaca serum.

For the second objective, IgGa, IgGb, IgG(T), IgA, and IgM concentrations were determined by ELISA assays and FTIR spectra were collected for 100 equine plasma samples. The spectra were randomly divided into training and prediction sets. The training set was used to build a calibration model for each Ig isotype or IgG subclass using partial least squares regression, while the prediction set was used to test the performance of the developed models. Pearson correlation coefficients and scatter plots displayed moderate to good agreement between FTIR and ELISA IgGb assay results but poor overall agreement for IgGa, IgG(T), IgA and IgM assay results. As well, significant differences were noted between the ELISA results of this study and the reviewed studies from the published literature. At present, a FTIR spectroscopic approach is an inaccurate technique for the measurement of Ig isotypes or IgG subclasses in equine plasma.

## **ACKNOWLEDGEMENTS (amended November 23, 2015)**

First and foremost, I would like to thank my supervisors, Dr. J McClure and Dr. Chris Riley, for their guidance throughout the duration of this project. They have encouraged and pushed me through the various ups and downs of the past three years and I am truly grateful for their continued support.

A sincere thank you is also extended to the members of my supervisory committee: Dr. Greg Keefe, Dr. Fred Markham and Dr. Anthony Shaw. Their knowledge and advice was always greatly appreciated.

Additionally I would like to thank Dr. Siyuan Hou for the advice, time and effort he contributed to this project. His work, particularly the data processing, calibration model development, assay validation and precision evaluation of the FTIR spectroscopic analysis using MATLAB script written by him for an equine project and modified for this project, was invaluable to the progression and completion of this thesis project. I would also like to recognize his creation of figures 2.1-2.5 in Chapter 2.

A special thank you also goes to Cynthia Mitchell and Judy Sheppard for their technical assistance with this project. Although things did not always go as planned, their patience and good humor helped make the best out of every situation.

Lastly, I would like to acknowledge my husband, Adam, for his never-ending love and encouragement. This thesis would not have been completed without his continued support. Thank you for all you do.

## **DEDICATION**

This thesis is dedicated to my mother, Barbara. Thank you for showing me the true meaning of strength, resiliency, and perseverance.



## TABLE OF CONTENTS

|   |              |
|---|--------------|
| TITLE PAGE .....  | I            |
| CONDITIONS OF USE.....  | II           |
| PERMISSION TO USE POSTGRADUATE THESIS .....   | III          |
| CERTIFICATION OF THESIS WORK.....   | IV           |
| ABSTRACT .....  | V            |
| ACKNOWLEDGEMENTS.....   | VII          |
| DEDICATION.....   | VIII         |
| TABLE OF CONTENTS .....   | IX           |
| LIST OF TABLES.....   | XII          |
| LIST OF FIGURES .....   | XIII         |
| LIST OF ABBREVIATIONS .....   | XV           |
| <br><b>CHAPTER 1. GENERAL DISCUSSION .....</b>  | <br><b>1</b> |
| 1.1. Immunology in camelid and equine species.....  | 2            |
| 1.1.1. Protection from infectious agents .....  | 2            |
| 1.1.2. Innate immune system.....  | 2            |
| 1.1.3. Adaptive immune system.....  | 4            |
| 1.1.3.1. Overview .....   | 4            |
| 1.1.3.2. Humoral immunity .....   | 8            |
| 1.1.3.2.1. Antibody overview .....  | 8            |
| 1.1.3.2.2. Antibody structure.....  | 9            |
| 1.1.3.2.3. Antibody classification and function .....   | 10           |
| 1.1.3.2.4. Species-specific differences .....   | 12           |
| 1.2. Immunodeficiency disorders .....   | 13           |
| 1.2.1. Overview .....   | 13           |
| 1.2.2. Failure of transfer of passive immunity .....  | 14           |
| 1.2.3. Severe combined immunodeficiency disorder .....  | 17           |
| 1.2.4. Selective immunoglobulin M deficiency .....  | 19           |
| 1.2.5. Foal immunodeficiency syndrome .....   | 21           |
| 1.2.6. Juvenile llama immunodeficiency syndrome .....   | 22           |
| 1.2.7. Other immunologic disorders .....  | 23           |
| 1.3. Diagnostic testing methods to determine immunoglobulin status .....                          | 24           |
| 1.3.1. Introduction.....  | 24           |
| 1.3.2. Testing methods currently available for immunoglobulin measurement in equine species ..... | 25           |

|  |           |
|--|-----------|
| 1.3.3. Testing methods currently available for immunoglobulin measurement in camelid species .....                                 | 29        |
| 1.4. Fourier-transform infrared spectroscopy.....  | 31        |
| 1.4.1. Overview .....  | 31        |
| 1.4.2. Principles of use .....   | 33        |
| 1.4.3. Advantages of Fourier-transform infrared spectroscopy .....   | 36        |
| 1.4.4. Practical applications of infrared spectroscopy in human medicine.....  | 38        |
| 1.4.4.1. Overview .....  | 38        |
| 1.4.4.2. Infrared clinical chemistry .....   | 38        |
| 1.4.4.3. Infrared pathology .....  | 40        |
| 1.4.4.4. Other applications in human medicine .....  | 44        |
| 1.4.5. Practical applications of infrared spectroscopy in veterinary medicine.....   | 44        |
| 1.4.5.1. Overview .....  | 44        |
| 1.4.5.2. Arthrology .....  | 45        |
| 1.4.5.3. Transmissible spongiform encephalopathies .....   | 46        |
| 1.4.5.4. Dairy herd health management.....   | 47        |
| 1.4.5.4. Urolithiasis .....  | 49        |
| 1.4.6. Application of infrared spectroscopy in immunoglobulin quantification.....  | 50        |
| 1.5. Objectives of current study .....   | 51        |
| 1.6. References .....  | 52        |
| <b>CHAPTER 2. USE OF FOURIER-TRANSFORM INFRARED SPECTROSCOPY TO QUANTIFY IMMUNOGLOBULIN G CONCENTRATIONS IN ALPACA SERUM .....</b> | <b>64</b> |
| 2.1. Abstract.....   | 65        |
| 2.2. Introduction .....  | 66        |
| 2.3. Materials and Methods .....   | 68        |
| 2.3.1. Experimental animals.....   | 68        |
| 2.3.2. Serum sampling protocol .....   | 68        |
| 2.3.3. Radial immunodiffusion assay for immunoglobulin G antibodies.....   | 69        |
| 2.3.4. Fourier-transform Infrared spectroscopy for immunoglobulin G antibodies..   | 69        |
| 2.3.5. Data processing.....  | 70        |
| 2.3.6. Calibration model development and assay validation.....   | 70        |
| 2.3.7. Precision of Fourier-transform infrared spectroscopic analyses .....  | 72        |
| 2.3.8. Diagnostic sensitivity and specificity.....   | 72        |
| 2.4. Results.....  | 72        |
| 2.4.1. Demographic data and RID-derived IgG concentration results .....  | 72        |
| 2.4.2. Analysis of agreement between FTIR and RID IgG quantitation methods .....   | 73        |
| 2.4.3. Precision of the FTIR Spectroscopic Analyses .....  | 74        |
| 2.4.4. Diagnostic sensitivity and specificity.....   | 74        |

|  |            |
|--|------------|
| 2.5. Discussion .....  | 75         |
| 2.6. Footnotes .....   | 80         |
| 2.7. Acknowledgements .....  | 81         |
| 2.8. References .....  | 82         |
| <b>CHAPTER 3 - EXPLORATORY STUDY EVALUATING THE USE OF FOURIER TRANSFORM<br/>INFRARED SPECTROSCOPY FOR THE QUANTIFICATION OF IMMUNOGLOBULIN<br/>ISOTYPES IGGA, IGGB, IGG(T), IGA, AND IGM IN EQUINE PLASMA .....</b> | <b>91</b>  |
| 3.1. Abstract .....  | 92         |
| 3.2. Introduction .....  | 93         |
| 3.3. Materials and Methods .....   | 96         |
| 3.3.1. Experimental animals and sample collection .....  | 96         |
| 3.3.2. Enzyme-linked immunosorbant assays for equine plasma IgG subclasses, IgM<br>and IgA .....   | 96         |
| 3.3.2.1. Plasma sample dilutions .....   | 96         |
| 3.3.2.2. Standard dilutions .....  | 97         |
| 3.3.2.3. Detection antibody dilutions .....  | 98         |
| 3.3.2.4. Procedure Overview .....  | 98         |
| 3.3.3. Radial Immunodiffusion assays for equine plasma IgG .....   | 99         |
| 3.3.4. Fourier-transform infrared spectroscopy for immunoglobulin isotypes and IgG<br>subclasses .....   | 100        |
| 3.3.5. Data processing and algorithm development .....   | 100        |
| 3.3.6. Statistical analysis of ELISA-derived Ig concentrations .....   | 102        |
| 3.3.7. Nanosep® centrifugal filtration device trials for the removal of albumin from<br>equine plasma samples .....  | 102        |
| 3.4. Results .....   | 103        |
| 3.5. Discussion .....  | 105        |
| 3.6. Footnotes .....   | 114        |
| 3.7. Acknowledgments .....   | 115        |
| 3.8. References .....  | 116        |
| <b>CHAPTER 4 – GENERAL DISCUSSION .....</b>  | <b>126</b> |
| 4.1. Summary of findings .....   | 127        |
| 4.2. Future directions .....   | 130        |
| 4.3. References .....  | 134        |
| <b>APPENDIX A .....</b>  | <b>136</b> |
| <b>APPENDIX B .....</b>  | <b>140</b> |

## LIST OF TABLES

|  |     |
|--|-----|
| <b>TABLE 2.1</b> - FTIR IgG false negative samples compared to IgG RID results identified within the entire data set (n =175). .....   | 85  |
| <b>TABLE 3.1</b> - Comparison of the mean ( $\pm$ SD) serum immunoglobulin concentrations (g/L) of IgGa, IgGb, IgG(T), IgM and IgA found in this study to the studies by Sheoran et al., de Camargo et al., McFarlane et al. and Holznagel et al. An (*) denotes the Ig concentration results which differed significantly from the results of this study. . | 120 |

## LIST OF FIGURES

- FIGURE 2.1** - Representative infrared spectrum of alpaca serum. The strongest features arise from proteins with relatively less abundant serum components contributing relatively weak fingerprints. The absorption at  $2062\text{ cm}^{-1}$  originates with the  $\text{KSCN}^-$  internal standard. .... 86
- FIGURE 2.2** - A scatter plot comparing the IgG concentrations obtained from RID and FTIR methods. The asterisks denote samples used in building the calibration model and the circles indicate the samples in the test set. 15 PLS factors were retained. If RID and FTIR give comparable results, the data points should distribute closely around the reference line of  $45^\circ$  ..... 87
- FIGURE 2.3** - A Bland-Altman plot of the differences in the IgG concentrations in the test set as obtained by RID and FTIR methods. The solid horizontal line represents the mean difference between RID and FTIR assays ( $-20.4\text{ mg/dl}$ ) and the dashed lines represent the 95% confidence interval. If there is no systematic bias between RID and FTIR method, the mean value of the differences should be close to zero. If the model assumption is that the errors are independent and identically distributed and follow a normal distribution, the data points should distribute around the mean of the difference randomly. Narrow dispersion of the data points means low measurement uncertainties. .... 88
- FIGURE 2.4** - Normal probability plot for the differences of the IgG concentrations in test set obtained from RID and FTIR methods. If the measurement errors follow a normal distribution, the data points should be largely located in the reference line. .... 89
- FIGURE 2.5** - Coefficient of variance plots for the RID and FTIR methods. Lower coefficient of variance means high precision of the test methods; this comparison shows that the precision of the RID and FTIR methods are roughly comparable ..... 90
- FIGURE 3.1** - Scatter plots comparing the IgGa concentrations in the training set (A) (Pearson correlation coefficient = 0.55) and test set (B) (Pearson correlation coefficient = 0.46) obtained from ELISA and FTIR methods. If ELISA and FTIR give comparable results, the data points should distribute closely around the reference line of  $45^\circ$ . .... 121
- FIGURE 3.2** - Scatter plots comparing the IgGb concentrations in the training set (A) (Pearson correlation coefficient = 0.89) and test set (B) (Pearson correlation coefficient = 0.71) obtained from ELISA and FTIR methods. If ELISA and FTIR give comparable results, the data points should distribute closely around the reference line of  $45^\circ$  ..... 122
- FIGURE 3.3** - Scatter plots comparing the IgG(T) concentrations in the training set (A) (Pearson correlation coefficient = 0.88) and test set (B) (Pearson correlation coefficient = 0.24) obtained from ELISA and FTIR methods. If ELISA and FTIR give

comparable results, the data points should distribute closely around the reference line of  $45^\circ$ . ..... 123

**FIGURE 3.4** -Scatter plots comparing the IgA concentrations in the training set (A) (Pearson correlation coefficient = 0.62) and test set (B) (Pearson correlation coefficient = 0.09) obtained from ELISA and FTIR methods. If ELISA and FTIR give comparable results, the data points should distribute closely around the reference line of  $45^\circ$ . ..... 124

**FIGURE 3.5** - Scatter plots comparing the IgM concentrations in the training set (A) (Pearson correlation coefficient = 0.66) and test set (B) (Pearson correlation coefficient = 0.27) obtained from ELISA and FTIR methods. If ELISA and FTIR give comparable results, the data points should distribute closely around the reference line of  $45^\circ$ . ..... 125

## LIST OF ABBREVIATIONS

|        |   |
|--------|---|
| AVC    | Atlantic Veterinary College               |
| BCR    | B cell receptor                           |
| BSE    | Bovine spongiform encephalopathy          |
| CVID   | Common variable immunodeficiency disorder |
| DNA-PK | Deoxyribonucleic acid-protein kinase      |
| DOC    | Depletion of albumin component            |
| ELISA  | Enzyme-linked immunosorbent assay         |
| FIS    | Foal immunodeficiency syndrome            |
| FTIR   | Fourier-transform infrared                |
| FTPI   | Failure of transfer of passive immunity   |
| GGT    | Gamma glutamyltransferase                 |
| HCAbs  | Heavy chains antibodies                   |
| HRP    | Horseradish peroxidase                    |
| Ig     | Immunoglobulin                            |
| IgA    | Immunoglobulin A                          |
| IgD    | Immunoglobulin D                          |
| IgE    | Immunoglobulin E                          |
| IgG    | Immunoglobulin G                          |
| IgM    | Immunoglobulin M                          |
| IR     | Infrared                                  |
| JLIDS  | Juvenile llama immunodeficiency syndrome  |
| MCCV   | Monte Carlo cross validation value        |
| MHC    | Major histocompatibility                  |

|       |   |
|-------|---|
| MUN   | Milk urea nitrogen                        |
| NB    | New Brunswick                             |
| OD    | Optical density                           |
| ONT   | Ontario                                   |
| PAMPs | Pathogen-associated molecular patterns    |
| PLS   | Partial-least squares                     |
| PRRs  | Pattern-recognition receptors             |
| RID   | Radial immunodiffusion assay              |
| SCID  | Severe combined immunodeficiency disorder |
| TIA   | Turbidimetric immunoassay                 |
| TMB   | Tetramethylbenzidine                      |
| TSEs  | Transmissible spongiform encephalopathies |
| TSP   | Total serum protein                       |
| UPEI  | University of Prince Edward Island        |



**CHAPTER 1**  
**GENERAL INTRODUCTION**

## **1.1. Immunology in camelid and equine species**

### **1.1.1. Protection from infectious agents**

The mammalian body is able to defend itself against invading pathogens in three main ways: anatomical barriers, the innate immune system and the adaptive immune system (1-3). Physical and chemical barriers are considered the body's first line of defence and include the skin and epithelial layers, secretions such as tears, saliva, sweat and mucous, and the normal endogenous flora and pH of the skin and urinary, respiratory and gastrointestinal tracts (4). Often these anatomical barriers are effective at protecting the body, despite a constant barrage from microorganisms within the environment. However, with enough time and persistence they can be overcome by invading pathogens, and the immune system is then activated (3-5).

In addition to anatomical barriers, the body is protected from infectious agents by a large number of effector cells and molecules which collectively form the immune system (4, 5). This system can be divided into innate and adaptive branches, each of which has their own specialized cells and mechanisms to eliminate infection (2, 4, 6).

### **1.1.2. Innate immune system**

The innate immune system is present in all multicellular organisms and is considered the next line of defence against invading pathogens after anatomical barriers are breached (4, 6, 7). It is rapid acting and possesses a variety of resistance mechanisms to block, recognize and destroy invading microorganisms as they attempt to establish infection in the body (4-7). The main elements of the innate immune system can be divided into cellular and humoral aspects (5). Cellular components include the

mononuclear (macrophages and monocytes) and polymorphonuclear (neutrophils, basophils and eosinophils) phagocytes, dendritic cells and natural killer cells; each of which plays a unique role in innate immunity (2, 3, 5, 8). For example, macrophages are well known for their ability to ingest and destroy invading microbes through the process of phagocytosis and they have a key role in cell recruitment to an infection site through the release of chemoattractant cytokines (5). On the other hand, dendritic cells are known for their ability to initiate the adaptive immune response through antigen presentation and T cell stimulation (4, 5).

Humoral components of the innate immune system include numerous antimicrobial peptides and molecules, as well as complement and acute phase proteins (1, 3, 5). As with the cellular components, each of the humoral elements of innate immunity plays a specific role in host defense (5). For instance, the enzyme lysozyme can destroy gram positive and negative bacterial cells walls through the hydrolysis of glycosidic bonds. The glycoprotein lactoferrin alters the mobility of certain bacteria, such as *Pseudomonas*, thereby decreasing their pathogenicity. C-reactive proteins will bind to the capsule of *Streptococcus* spp. to further enhance their detection and destruction by cellular components of innate immunity (4, 5). Ultimately, regardless of their classification as cellular or humoral, all cells, proteins and molecules of the innate immune system work together to initiate or participate in a variety of host defense mechanisms including pathogen recognition, phagocytosis, inflammation, complement activation, cytokine production and antigen presentation (2, 4, 5, 7, 8).

The ability of the innate immune system to identify and respond to invading microbes relies heavily on the identification of particular microbial structures which have been conserved across a broad spectrum of microorganisms (5, 7, 8). These structures, termed pathogen-associated molecular patterns (PAMPs), are a highly conserved components of the microbe not easily altered by mutation (3, 5). With time, host organisms have developed a set of pattern-recognition receptors (PRRs) on their cells (8). These PRRs are capable of identifying various PAMPs and this recognition leads to cytokine production and the activation of numerous immune responses (7). Some of the most well-known examples of PAMPs include lipopolysaccharides and techoic acids (common components of gram negative, and gram positive bacterial cell walls, respectively) and double-stranded RNA expressed by viruses (3, 4, 7). Common examples of PRRs include mannose binding lectin and toll-like receptors (of which there are numerous forms) (3, 4, 8).

This is only a brief introduction of the innate immune system, which is a large, complex and expansive subject. Full details regarding innate immunity are beyond the scope of this thesis.

### **1.1.3. Adaptive immune system**

#### **1.1.3.1. Overview**

Any invading foreign substances (e.g. bacteria, viruses, fungi, protozoa or helminths) capable of initiating an immune response are termed antigens (1). Two distinct classes of antigens capable of activating the acquired immune system have been identified. The first are microorganisms which exist extracellularly and proliferate in the

tissues and extracellular fluids. The second class includes invading organisms which have the ability to exist within the host's cells (i.e. intracellular organisms such as viruses or specific bacteria) (1, 9). Due to the immense diversity of potential antigens, the adaptive immune system is extraordinarily complex and can be divided into two major branches: cell-mediated and humoral immunity; each responsible for identifying and facilitating the destruction of specific pathogens (1, 3). Additionally, the complex nature of the adaptive immune system is governed by two main cell types, T and B lymphocytes. T lymphocytes mature in the thymus and have roles in both cellular and humoral immunity (6). Certain T lymphocytes, such as cytotoxic T cells, are responsible for cell-mediated immunity and their primary function is to kill cells infected by intracellular pathogens (4, 6). Others, like helper T cells, assist in the activation of antigen-stimulated B cells or can activate macrophages to increase their efficiency at destroying engulfed pathogens (4, 10). Finally, there are regulatory T cells which modify the immune response through suppression of other lymphocytes (4, 6). B lymphocytes mature in the bone marrow and are responsible for directing the humoral immune responses in the body (1, 4).

The adaptive immune system may take several days or weeks to become fully activated, yet is extraordinarily effective at eliminating infection (4). Adaptive immunity evolved approximately 400 million years ago and is present only in vertebrate species (6). It is characterized by the response of lymphocytes to specific antigens and the subsequent development of immunological memory (3, 4, 6). The concept of true immunological memory is an adaptive immune response intended to confer protective

immunity to the host in the event of re-exposure to an antigen (11). Following an initial response to and elimination of an infectious agent, memory B and T cells are generated in the body. Subsequent encounters with the same antigen will stimulate these memory cells, resulting in a more rapid and enhanced immunological response to a second exposure of the offending agent (3, 4, 11).

Another important feature of the adaptive immune system is the ability of immune cells to distinguish between the body's own cells and unwanted pathogens (4). Both B and T lymphocytes are able to recognize and respond to antigens due to the presence of highly specific antigen receptors on their cell surfaces (4). Each individual lymphocyte has receptors with a single antigen specificity and, collectively, the numerous lymphocytes of the body generate a large repertoire of antigen receptors which enable the immune system to identify and respond to almost any antigen it may be challenged with (3, 4).

A vast array of diverse antigen receptors are generated during B and T lymphocyte development where specific gene segments undergo irreversible DNA recombination (4, 6). Three types of gene segments are known (V, D and J) with multiple copies of each present in germline DNA. Only one of each type of gene segment is joined together during recombination to form a lymphocyte receptor specific for a particular antigen (6, 12, 13). Once a functional receptor is successfully produced during the VDJ recombination process, further rearrangement is blocked, ensuring each lymphocyte expresses only one specific antigen receptor (4). Through this process of VDJ recombination, just a few hundred gene segments are capable of combining in a

variety of ways to generate millions of different lymphocyte antigen receptors.

Junctional diversity further amplifies the lymphocyte receptor diversity through nucleotide insertions or deletions during the process of gene segment joining (4, 12). As a result, individuals encompass a large repertoire of B and T lymphocytes, each with a unique antigen binding capability (12, 13). B lymphocytes are able to recognize various conformations of antigen such as proteins, carbohydrates or simple chemical groups, whereas most T cell receptors are only capable of recognizing peptides bound to specific glycoproteins called major histocompatibility complex molecules (3, 6).

Due to the random nature of gene recombination, it is inevitable that certain self-reactive T and B lymphocytes will be generated, i.e. have receptors which respond to the body's own self-antigens (3, 14). As a result, the adaptive immune system has developed several mechanisms to identify and eliminate self-reactive lymphocytes before damage to host cells occur (4, 15). The first of these mechanisms is central tolerance. With this method, immature lymphocytes which recognize antigens in the central lymphoid organs will receive a negative signal resulting in their inactivation and/or death via apoptosis (3, 4, 14). Similar to this, but occurring in the secondary lymphoid organs (e.g. spleen, lymph nodes, etc.), is the mechanism of peripheral tolerance (3). This method relies on the co-stimulatory signals generated by the innate immune system during an infection which are essential for activation of adaptive immunity. In the absence of infection and these signals, a mature lymphocyte which encounters a self-antigen in the peripheral lymphoid organs will receive a negative, inactivating signal and mount no immune response (4). A final mechanism to assist the

immune system in discriminating between self and non-self is the tolerization of lymphocytes to self-antigens (3, 4). Many self-antigens are expressed abundantly by the cells of the body and therefore provide strong, constant signals to mature lymphocyte receptors. As a result, lymphocytes become tolerant of these antigens and do not respond by activation (4). Conversely, when a pathogen enters the body, their antigen concentration will increase rapidly as they replicate in the early stages of infection. This leads to the activation of naïve, mature lymphocytes as they respond to the sudden increase in antigen receptor signals (1, 4). Under normal physiological conditions, these mechanisms are adequate to allow lymphocytes to distinguish between self and non-self antigens, however, they are not infallible and failure to make this distinction can lead to the development of autoimmune disease (3, 4).

#### **1.1.3.2. Humoral immunity**

##### **1.1.3.2.1. Antibody overview**

Antibodies are glycoproteins, found in the tissues and fluid components of the body (4). They belong to a family of proteins called immunoglobulins (Igs) which are an essential component of the adaptive immune system. Immunoglobulins exist within the body in one of two forms: as membrane bound molecules on a B cell (B cell receptors, [BCRs]) or as soluble, secreted molecules (antibodies) (12). Each B cell has approximately 200,000 to 500,000 identical BCRs on its cell surface which allow that particular cell to respond to one specific antigen. These receptors are able to bind to an immense array of chemical structures including glycoproteins, polysaccharides, whole virus particles or bacterial cells through recognition of epitopes on the antigen's surface



(1). Certain microbial antigens are capable of directly activating B cells while others require the assistance of helper T cells for B cell activation (4).

When a B cell becomes activated, it will respond by proliferating and differentiating into either plasma B cells (also known as effector B cells) or memory B cells (3). Plasma B cells develop in the lymph nodes and spleen from where they travel via the blood stream or lymphatic system to become distributed throughout the body (16). They function to produce and secrete large amounts of antibody, up to 10,000 molecules per second, all with antigen binding specificity identical to that of the parent B cell (1, 16). Memory B cells, as previously mentioned, are one of the key components of immunological memory, capable of providing enhanced, rapid immune responses upon re-exposure to their original inciting antigen (4).

#### **1.1.3.2.2. Antibody structure**

Antibodies are Y-shaped proteins with molecular weights ranging from 160-180 kDa (1). The top portion (or 'arms') of the molecule is known as the variable region (V region) as it contains highly diverse antigen binding sites. In contrast, the area of the antibody which has a relatively unchanging amino acid sequence (the 'stem' of the Y) is known as the constant region (C region) (4, 13). The C region of an antibody molecule exists in one of five main forms, each designed to engage different effector functions of the immune system (4, 12).

Each antibody is composed of 4 peptide chains: 2 identical heavy chains (H chains) and 2 identical light chains (L chains). The light and heavy chains are linked together by disulfide bonds which also chemically bind the heavy chains to each other,

giving the antibody molecule a characteristic 'Y' shape (4, 13). The stem of the Y-shaped antibody consists only of heavy chains while the two identical arms are comprised of both heavy and light chains. The antigen binding sites are located at the tips of the arms which are joined to the stem via a flexible hinge region (4).

#### **1.1.3.2.3. Antibody classification and function**

In mammals, there are 2 distinct types of light chains, kappa (K) and lambda ( $\lambda$ ), which are differentiated by their amino acid sequences, yet are functionally identical (13). Different species of mammals have varying ratios of K and  $\lambda$  light chains, however the reason for this is unknown and no functional differences have been found between antibodies with different ratios of K and  $\lambda$  light chains (4, 13).

The C region of an Ig consists only of heavy chains and it is these chains which will determine the name and effector function of that molecule (13). In mammals, there are 5 major classes of heavy chains, denoted gamma ( $\gamma$ ), alpha ( $\alpha$ ), delta ( $\delta$ ), mu ( $\mu$ ) and epsilon ( $\epsilon$ ) (1, 13). Immunoglobulins containing  $\gamma$  chains are termed immunoglobulin G (IgG) while those with  $\alpha$  chains are immunoglobulin A (IgA),  $\mu$  chains are immunoglobulin M (IgM),  $\delta$  chains are immunoglobulin D (IgD) and  $\epsilon$  chains are immunoglobulin E (IgE) (4). Each class (or isotype) of Ig may also consist of several subtypes depending on the species (4, 17). For example, equids have 7 subclasses of IgG while cattle have three IgG subclasses and pigs have six (12, 17, 18). Early research in equine immunology categorized the IgG subclasses according to their antigenic differences and four subclasses were defined: IgGa, IgGb, IgGc and IgG(T) (18). Since then, most of the subclasses have been linked to their corresponding Ig heavy chain

constant genes. As a result, there are more IgG subclasses than originally presumed, with some authors now designating them IgG<sub>1</sub> – IgG<sub>7</sub>. What was once IgGa is now IgG<sub>1</sub> and IgG<sub>2</sub>, IgGb is now IgG<sub>4</sub>, IgGc is now IgG<sub>6</sub> and IgG<sub>7</sub> and IgG(T) is now IgG<sub>3</sub> and IgG<sub>5</sub> (18).

The main function of Ig molecules is to defend the body against a variety of invading microbes (16). As mentioned, several classes of Ig exist, each optimized to have different biological functions and act in various environments of the body such as blood, milk or mucosal surfaces (1). Immunoglobulin molecules range in size from 180-900 kDa (4). Immunoglobulin G, IgM and IgD are primarily synthesized in the spleen and lymph nodes, whereas IgE and IgA are largely synthesized in the intestinal and respiratory tracts (1, 19). Immunoglobulin G is the Ig found in highest concentration in the blood and is primarily responsible for defense against systemic pathogens. It has the smallest molecular weight of the 5 main Igs therefore allowing it to easily escape from blood vessels during periods of inflammation to participate in the defense against microorganisms in tissues and body fluids (1, 19). In most mammals, IgM has the second highest serum concentration and is the main Ig produced during a primary immune response, although it is also produced to a smaller extent in secondary immune responses (1). Immunoglobulin A is typically the Ig with the third highest concentration in the serum of most mammalian species. It is the predominant Ig in mucosal tissues and secretions and is therefore responsible for defence of the intestinal, urogenital and respiratory tracts and mammary gland (1, 4, 19). IgA is produced by plasma cells in the lamina propria underlying the mucosal epithelium and exists in one of two forms:

secretory IgA and serum IgA (19, 20). Receptors allow IgA to pass through epithelial cells into external secretions, such as saliva, intestinal fluids and milk, making it the primary Ig found in body secretions (19). Immunoglobulin E is found in very small concentrations in the serum and is responsible for mediating allergic reactions in the body and defense against parasitic infections. Finally, IgD is found on the surface of mature, naive B cells, however, its function is unknown at this time (1).

#### **1.1.3.2.4. Species-specific differences**

Although camelid species are economically important in many South American, North African and middle East countries, it was not until the mid-1990's that investigations into their immune system began (21, 22). Prior to this time, it was believed that the antibodies of all mammalian species were similar in terms of general structure, and that all antibodies in domestic mammals consisted of two identical heavy chains bound to two identical light chains (23). However in 1993, Hamers-Casterman et al. challenged this common theory with their discovery of a novel class of IgG antibodies in the serum of camelidae (24, 25). These functional antibodies were termed heavy chain antibodies (HCAbs) as they were found to be completely devoid of light chains (26). Since this discovery, it has been ascertained that in addition to conventional antibodies, the serum of not just camelids, but also nurse sharks, wobbegong sharks, and possibly ratfish all contain antibodies lacking L-chains (27, 28). Currently, three subclasses of camelid IgG have been recognized: IgG<sub>1</sub> which exhibits the conventional antibody structure, and IgG<sub>2</sub> and IgG<sub>3</sub> which do not contain associated light chains (29, 30).

Several advantages for HCAs have been identified when compared to their conventional antibody counterparts (25). For example, HCAs seem to have a higher physicochemical stability and are therefore able to remain functional at higher temperatures than regular antibodies (25, 30). Also, due to the smaller size of HCAs, they appear to have better biodistribution and tissue penetration in the body and are able to recognize antigenic sites which may not normally be recognized by conventional antibodies (25, 30).

The discovery of functional antibodies devoid of light chains has drastically altered what was perceived to be the normal rules governing antibody structure (29). As investigation of the camelid immune system is still quite recent, a finding such as this brings up many potential questions and areas for further exploration. As a result, research into HCAs is ongoing to establish the full potential and utility of such a molecule in human and veterinary medicine, as well as to clarify the roles they play in the camelid immune system (21, 26).

## **1.2. Immunodeficiency disorders**

### **1.2.1. Overview**

In large animal veterinary medicine, immunodeficiency disorders often garner attention due to their potentially life-threatening consequences (1, 4). They occur when an animal's immune system is compromised and not able to mount an appropriate immune response to ward off infectious disease (10). Frequently these disorders are classified as either primary or secondary immunodeficiencies. Occasionally though, they may also be characterized by the specific immune system component affected (such as

humoral immunodeficiencies of which selective IgM deficiency would be an example) (10, 32, 33).

Primary immunodeficiencies typically result from a defect in the animal's immune system and usually have an alleged or established genetic basis (10, 32). They occur infrequently and may be difficult to diagnose (10). The most common primary immunodeficiencies encountered in large animal veterinary medicine include severe combined immunodeficiency disorder (SCID), selective immunoglobulin M (IgM) deficiency and foal (Fell pony) immunodeficiency syndrome (FIS) (10, 32, 34). Secondary immunodeficiencies are acquired and may result from failure of transfer of passive immunity (FTPI), malnutrition, neoplasia or immunosuppression by certain microorganisms or drugs (32). Other than FTPI, acquired immunodeficiencies are uncommon in large animal veterinary medicine (35).

#### **1.2.2. Failure of transfer of passive immunity**

Newborn animals have different levels of immunologic competence at birth depending on the type of placentation found in their species, yet they all require assistance through the passive transfer of maternal Ig via the placenta or colostrum after birth (36, 37). Primates have the most intimate type of placentation, known as haemochorial, which allows for the in-utero transfer of IgG (36, 38). Dogs and cats have an endotheliochorial placenta where approximately 5-10% of IgG may be transferred to the neonate in-utero, with the remainder provided via colostrum (36). Alternately, ruminants have a syndesmochorial placenta and horses, pigs and camelids have an eplitheliochorial placenta (38, 39). Neither of these latter two forms of placentation

allow for in-utero transfer of IgG, resulting in neonates of these species essentially being born agammaglobulinemic (36-38).

Following birth, foals and crias rely solely on the passive transfer of maternal antibodies, primarily IgG, from the dam's colostrum (40, 41). Colostrum is a specialized form of milk produced in limited quantity in late gestation. It contains a variety of both cellular and soluble components, with IgG being the most significant and predominant (35, 42, 43). For approximately 24 hours following birth, a neonate's intestines are permeable to these colostral proteins which are not digested because the proteolytic activity of their gastrointestinal tract is minimal, and trypsin inhibitors present in colostrum further diminish enzymatic action (36). This decreased proteolytic activity allows colostral proteins to reach the small intestine, particularly the ileum, where they are taken up by epithelial cells and passed into the intestinal capillaries before finally reaching the systemic circulation (35, 36). Intestinal permeability is high immediately following birth but rapidly declines and by 24 hours of age, epithelial cells mature and become impermeable, and normal intestinal flora is established (36, 44).

Through passive transfer, neonates are normally able to acquire large amounts of maternal IgG to provide a protective immune response in the first few weeks of life (36, 40). When a foal or cria is unable to do this, the resulting outcome is FTPI (10). There are several potential causes of FTPI which may result from problems with the dam, the offspring, or both. Factors attributed to the mother include inadequate production of colostrum or colostral IgG, premature lactation, or rejection of offspring thus not allowing them to suckle in the immediate post-partum period (10, 35, 41, 45).

Alternately, poor intestinal absorption (due to intestinal immaturity or ileus) or failure to ingest a sufficient amount of colostrum in the post-partum period due to injury, weakness, illness or injury in the neonate will lead to FTPI in foals or crias (10, 41, 44-46).

Failure of passive transfer of IgG has been associated with increased morbidity and mortality in foals, calves, lambs and crias (47-50). It is considered the most important risk factor for the development of infections, such as septicaemia, arthritis, enteritis, pneumonia and omphalitis in the first month of life (10, 30). Septicaemia is of particular concern as it is recognized worldwide as a major cause of foal and cria morbidity and mortality and been shown to be positively correlated with FTPI (32, 35, 41, 51). The prevalence of FTPI has been reported as 20.5% in crias, up to 35% in calves and between 3 and 25% in foals (44, 48, 49, 52).

Due to the potentially devastating consequences of FTPI, early and accurate diagnosis is required to provide effective medical intervention. Accordingly, multiple testing methods for FTPI have been developed and these are discussed more in-depth later in this chapter, however, the most quantitatively accurate test currently available is the single radial immunodiffusion (RID) assay (32, 49). Typically, serum IgG concentrations are measured at 18-24 hours following birth to allow adequate time for maximum IgG absorption (35). In foals, adequate passive transfer is achieved when serum IgG concentrations are >800 mg/dL (10, 32). Foals with IgG concentrations <400 mg/dL are classified as having FTPI and foals with concentrations between 400-800 mg/dL are categorized as having partial FTPI (49). In camelids, adequate transfer of



passive immunity is considered to have been achieved when serum IgG concentrations are >1000 mg/dl (30, 48).

In cases where FTPI seems a likely outcome, preventative measures are the best option to minimize severity of disease. This may include providing an alternate high quality colostrum source, intravenous plasma transfusions, antimicrobial therapy and supportive care in a clean, low-pathogen risk environment (10, 30, 35). Ultimately, when treating patients with FTPI, clinicians must analyze each situation separately, including a thorough history, neonatal sepsis score, physical examination, complete blood count and immunoglobulin status, in order to make an appropriate treatment plan for that individual animal (10, 35).

### **1.2.3. Severe combined immunodeficiency disorder**

Severe combined immunodeficiency disorder is a fatal, inherited condition of humans, horses, dogs and mice (10, 42). It was first described in children in the 1960's but it was not until 1973 that its first spontaneous animal counterpart was reported in Arabian foals (53, 54). In horses, SCID is an autosomal recessive trait thought to be restricted to Arabian or Arabian-cross breeds. However, single cases have also been reported in a Caspian filly and a Fell pony filly (33, 53). Affected foals have been identified throughout North America, Australia and the United Kingdom (55). Among Arabian horses in the United States, the frequency of SCID gene carriers has been reported to be 8.4% (32, 55, 56).

Severe combined immunodeficiency disorder results from a 5-basepair deletion in the gene, located on chromosome 9, which encodes the catalytic subunit of the

enzyme deoxyribonucleic acid-protein kinase (DNA-PK) (10, 32, 55, 56). This enzyme is essential to gene rearrangement as it is required in the process of encoding specific antigen-receptor complexes on the surface of B and T lymphocytes (10, 53). Without a functional catalytic subunit, DNA-PK is rendered inactive and lymphocyte precursors are eliminated (53). Consequently, affected foals are born without functional T and B lymphocytes and therefore lack both cellular and antibody-mediated immunity (10, 32, 53).

Severe combined immunodeficiency disorder-affected foals appear normal at birth and may not show clinical signs until weeks or sometimes months later depending on the quantity of passive maternal antibody transferred and the extent of environmental microbial challenges encountered (10, 42, 53). As maternal immunity wanes, affected foals are unable to mount their own immune responses and become susceptible to a wide range of infections (10, 54). The respiratory tract is often the first system affected followed by gastrointestinal tract. The most common infectious agents identified in SCID foals include adenovirus, *Rhodococcus equi*, *Pneumocystis carinii* and *Cryptosporidium* spp. (10, 32, 53, 55). Initially, SCID-affected foals may respond to antimicrobial therapy, however infections continue to recur and most SCID-affected foals die in the first few months of life (10).

Definitive diagnosis of SCID is achieved through genetic testing to demonstrate the presence of the mutant SCID gene (10, 53, 55). Prior to the advent of genetic testing, diagnosis of SCID was based on the clinical presentation of an Arabian foal with recurrent infections, a severe and persistent lymphopenia (<1000 lymphocytes/ $\mu$ l), an

absence of IgM in serum collected presuckle or after 3-4 weeks of age and presence of lymphoid hypoplasia at necropsy (10, 32, 53, 55). As medical management of foals diagnosed with SCID is unrewarding, euthanasia is warranted (32, 55). Due to the devastating consequences of SCID, prevention of this disease through responsible breeding practices and genetic testing is critical in Arabian horse breeding programs (32).

#### **1.2.4. Selective immunoglobulin M deficiency**

Selective IgM deficiency is an uncommon disorder reported to occur in humans, foals and adult horses, and the pathogenesis of this condition is currently unknown (32, 57). A genetic basis for selective IgM deficiency has not been proven and the association of this disorder with neoplasia and spontaneous recovery in some patients suggests that it may represent a secondary rather than primary immunodeficiency disorder in certain cases (32). This disorder was first reported in 1977 in a group of 5 horses between the ages of 2 months to 5 years old (10, 42). While it has been known to occur in a number of breeds, Arabians and Quarter Horses appear to be over represented in case reports (10, 42).

In healthy horses, IgM accounts for approximately 10% of the total amount of circulating serum Ig (14, 15). Reference ranges of 120 (standard deviation  $\pm$  30) mg/dl have been reported for IgM concentrations in the adult horse (10, 32, 58). Originally it was proposed that to meet the criteria for a diagnosis of IgM deficiency, suspect cases must have serum IgM concentrations  $>2$  standard deviations less than age-matched horses while all other Ig classes remained within normal reference ranges (32). Based on

current reference ranges, this would equate to serum IgM concentrations <60 mg/dl being deemed deficient (10, 58). However, another report has suggested adjusting the cutoff for IgM deficiency to <23 mg/dl as a number of “normal” horses analysed in the study had IgM concentrations falling below the 60 mg/dl value (10, 58). In foals between 4 and 8 months of age, it is suggested that an IgM values <15 mg/dl, combined with normal values for all remaining Ig classes, is indicative of selective IgM deficiency (10). Due to the grave prognosis for this disorder, repeat IgM testing is warranted to confirm the diagnosis (42).

Two clinical presentations of selective IgM deficiency have been recognized with the most common being a primary immunodeficiency observed in foals between 2 and 8 months of age (42). Affected foals are typically small for their age and experience recurrent bacterial infections, often involving the respiratory tract (10, 32). Initially, they may respond well to aggressive antimicrobial therapy, only to relapse within a few weeks following the cessation of treatment (10, 42). The prognosis for selective IgM deficiency in foals is grave with the majority dying by 8 months of age (32, 59). Foals surviving beyond 1 year of age often fail to thrive and experience recurrent respiratory tract infections (10, 32, 42, 59). The second clinical presentation of selective IgM deficiency occurs in adult horses > 2 years of age (10). Originally a strong association was reported between IgM deficiency and lymphoma in adult horses (14, 15). More recently it has been recognized that this disorder may also be identified in horses diagnosed with a variety of conditions other than lymphoma (10, 32, 58). Therefore, a

true diagnosis of IgM deficiency requires the documentation of persistently low IgM concentrations (42).

As there is no specific treatment for IgM deficiency, management of affected horses can prove difficult (10, 42). Due to the short half-life of IgM, plasma transfusions are not typically regarded as beneficial, and while supportive care and antimicrobial therapy may help manage bacterial infections initially, infections often recur following the cessation of treatment (32).

#### **1.2.5. Foal immunodeficiency syndrome**

A fatal, inherited disease of severe anemia, immunodeficiency and peripheral ganglionopathy has been recognized in the Fell and Dale pony breeds native to the British Isles (34, 42, 60). This condition, previously known as Fell Pony syndrome, is now termed foal immunodeficiency syndrome (FIS). It was first reported in a Fell pony foal in the United Kingdom in 1998, and currently affects approximately 10% of Fell and 1% of Dale foals (34, 61, 62). Research suggests FIS has autosomal recessive inheritance, and a recent study identified a mutation associated with the syndrome on the sodium/myo-inositol cotransporter gene located on chromosome ECA26 (61, 62).

Affected foals appear normal at birth with clinical signs including diarrhea, cough, failure to thrive, nasal discharge, depression and hypersalivation becoming apparent by 1 month of age (32, 60, 62). These animals may initially respond to treatment but recurrent infections occur as the result of a primary B-cell deficiency with an associated decreased antibody production (60, 61). T-lymphocyte concentrations remain normal in affected foals (61). Once maternal Ig levels decline by 3-6 weeks of

age, foals become immunodeficient as they are unable to generate an adaptive immune response due to impaired antibody synthesis (61). At the same time, these foals develop a severe, non-hemolytic, non-regenerative anemia and often die or are euthanized by 3 months of age (60, 61).

#### **1.2.6. Juvenile llama immunodeficiency syndrome**

An immunodeficiency disorder characterized by ill thrift and recurrent, opportunistic infections has been described in juvenile llamas (63, 64). Termed juvenile llama immunodeficiency syndrome (JLIDS), affected animals often appear normal prior to weaning; with clinical signs typically developing between 2 to 30 months of age (63, 65). Llamas with JLIDS present for weight loss, failure to thrive and recurrent infections, with clinical signs depending on the stage of JLIDS and the site(s) of infection (65).

A complete blood count from JLIDS-affected llamas will reveal inflammation and a normocytic, normochromic, non-regenerative anemia. Measurement of serum IgG will reveal decreased concentrations (64, 66). *Eperythrozoon* organisms are commonly found in the peripheral blood smears and are considered secondary pathogens, typically only causing disease in immunocompromised hosts (66, 67). Llamas with JLIDS fail to respond to *Clostridium perfringens* C and D toxoid based on pre and post vaccination antibody titres, indicating a dysfunction in their acquired humoral immune response (64, 65). These animals will either fail to respond or respond poorly to conventional treatment of their infections and inevitably die or are euthanized due to a grave prognosis (63, 65). Necropsy findings often reveal hypoplasia or atrophy of lymphatic tissue (68).

The etiology of JLIDS is unknown but a number of genetic, infectious and environmental causes have been considered. A study by Davis et al. in 2000 found a defect in the development of B-cells in these animals and provided evidence of a genetic basis for JLIDS (63). It is unclear whether this disorder also affects alpacas. One case report in 1999 described an alpaca with clinical signs of JLIDS but no definitive diagnostic tests were performed prior to the death of the animal (63). JLIDS is diagnosed based on the aforementioned clinical signs, the results of a complete blood count and through ruling out other causes of ill-thrift and weight loss such as endoparasitism, malnutrition, dental problems, iron deficiency and congenital defects (65, 68).

#### **1.2.7. Other immunologic disorders**

Common variable immunodeficiency (CVID) is a rare disorder occurring in horses and humans (69). In horses, this disease has an unknown etiology. Cases in adults of both sexes, different breeds and geographical locations have been described (69-71). This disease is characterized by recurrent fevers and bacterial infections, particularly pneumonia, B cell lymphopenia or depletion and impaired humoral responses to protein vaccination (69-72). Hypo or agammaglobulinemia, most commonly involving IgG and IgM, is another frequent feature of this disorder (69). Cases of CVID have been reported in three adult horses with presumptive bacterial meningitis. This condition should be considered in adult horses with recurrent bacterial infections, meningitis, or both (69, 71). Confirmation of CVID is through immunological testing. The prognosis has been described as guarded to grave depending upon concurrent clinical symptoms (69, 71). Some horses have been treated with continuous or intermittent antimicrobial and

immunoglobulin therapies, however, these options are economically impractical and raise concerns regarding antibiotic resistance and opportunistic infections (69). More often, euthanasia is elected by owners due to the severity of infections such as pneumonia, meningitis or septicemia, the requirement for intensive clinical monitoring, treatment and hospitalization and the associated financial costs to do so (70, 71).

A condition characterized as agammaglobulinemia has been reported in 5 male horses between 2 and 6 months of age (10). In humans, this condition occurs due to an x-linked inherited trait caused by a mutation in the Bruton tyrosine kinase gene (32). As a result, only males are affected while female carriers appear clinically healthy (32). This disorder has currently only been reported in male horses, which is suggestive (but not indicative) of an x-linked mode of inheritance (10, 32, 59). Foals affected with agammaglobulinaemia present with signs of infectious disease, most often involving the respiratory, gastrointestinal or musculoskeletal systems (10, 73). These infections may initially respond to antimicrobial therapy but recurrence is common and most foals do not survive beyond 2 years of age (10, 32). Immunologic evaluation of foals with this condition reveals an absence of B lymphocytes with low or undetectable concentrations of immunoglobulins in the presence of normal T lymphocyte function (10, 32, 59, 73). Consequently, affected horses are unable to produce an appreciable antibody response following immunization (73). Treatment for this disorder is unrewarding and, until the specific genetic defect is identified, prevention is not possible (10).

### **1.3. Diagnostic testing methods to determine immunoglobulin status**



### **1.3.1. Introduction**

Assessing different aspects of the humoral immune system in equine and camelid species is achieved by measuring serum or plasma Ig concentrations (74). Testing is extremely important as it allows for early and accurate diagnosis of immunodeficiencies and provision of timely medical intervention if indicated (49). The consequences of immunodeficiency disorders are emotionally and financially taxing for owners, thus there is a demand for up-to-date, economic, rapid and precise diagnostic options. As a result, multiple methods for the evaluation of Ig concentrations have been developed for animals resulting in a wide range of testing options, each with advantages and disadvantages (49).

### **1.3.2. Testing methods currently available for immunoglobulin measurement in equine species**

Equine radial immunodiffusion (RID) assays are commercially available from a variety of manufacturers. They work on the principle that sample antigen (such as serum IgG) added to a RID plate well diffuses into the surrounding agarose gel which contains antiserum specific for the protein to be measured. A ring of antigen/antibody precipitate will form, which is proportional in size to the concentration of antigen in the sample. Reference sera zone diameters are measured and used to form a standard curve which is then used to determine the concentration of the protein of interest in the unknown sample (based on its measured ring diameter) (44, 52).

The RID assays are currently the gold standard for determining serum IgG concentrations in horses as they provide the most quantitatively accurate results (44,

46). Unfortunately these assays require an 18-24 hour incubation period (44, 46). This substantial delay in obtaining results is a major disadvantage as quick identification of immunological disorders in foals, especially FTPI, is essential for timely therapeutic intervention (32, 44). Other disadvantages include a requirement for enhanced technical skill by the user, potential variation in different RID assays when calibrated to different standards, increased cost when compared with other testing methods and utilization of specific reagents with a limited shelf-life (46, 49).

A number of other tests to estimate Ig concentrations in equine serum, plasma or whole blood are available (32). These include zinc sulphate turbidity, glutaraldehyde coagulation and enzyme and turbidimetric immunoassays (10, 49). In calves, total serum protein (TSP) measurement by refractometry is a quick, inexpensive and accurate screening test for FTPI (46, 75). However, research indicates this method is an unreliable predictor of FTPI in neonatal foals due to their wide range of TSP concentrations (46, 75). A latex agglutination test is also available for the detection of FTPI in foals, however, it is considered an inappropriate screening method due to poor sensitivity and specificity (10).

The glutaraldehyde coagulation test is a simple, inexpensive and rapid semiquantitative FTPI screening test which can be performed in a field setting with results in minutes (76). This test has a good sensitivity for the diagnosis of FTPI but suffers from poor specificity, especially for IgG concentrations <800 mg/dl (32, 46). As a result, the predictive value of a negative test is reliable but a positive test does not necessarily indicate FTPI in that animal and confirmatory testing is warranted (32). Two

studies comparing glutaraldehyde coagulation tests with RID assays in neonatal foals found sensitivities of 100% and 92.9% and specificities of 59% and 58.6% for the glutaraldehyde test when identifying IgG concentrations <800 mg/dl (46, 77).

The zinc sulphate turbidity test is another FTPI field screening test that is relatively cheap and rapid, providing results in approximately 1 hour (10, 32). However, similar to the glutaraldehyde coagulation test, it also suffers from poor specificity, with one study reporting a sensitivity of 81% and specificity of 56.9% for the detection of serum IgG concentrations of <800 mg/dl in foals (46). In addition, both the glutaraldehyde coagulation and zinc sulfate turbidity tests are nonspecific for IgG as they are able to detect other serum proteins which may lead to false positive test results (49, 78).

Turbidimetric immunoassay (TIA) can be used for the detection of IgG in equine serum (44). The assay provides accurate, rapid, quantitative data and can now be measured on a routine chemistry analyzer commonly found in many clinical veterinary laboratories (44, 79). Benefits of TIA over RID include complete automation and a greatly decreased turnaround time for results. In one study, TIA sensitivity and specificity were 91.5% and 70.5% for the detection of plasma IgG concentrations <800 mg/dl in foals and 92.3% and 99.1% for IgG concentrations <400 mg/dl. This study concluded that the TIA-generated values were highly correlated with the RID-generated values (79). A disadvantage of TIA is the requirement for specific reagents with a limited shelf-life (44).

A number of quantitative and semiquantitative enzyme-linked immunosorbent (ELISA) assays are commercially available for the detection of Ig in equine serum, plasma or whole blood (10). A semiquantitative stall-side ELISA (Snap Foal Test, IDEXX, Westbrook, ME) is popular among practitioners for the diagnosis of FTPI in foals due to its ease of use and rapid results (10, 75, 80). One study found sensitivity and specificity values of 81% and 94.7% for the detection of serum IgG concentrations <800 mg/dl in foals when using the SNAP test (46). Another study, looking at hospitalized foals only, found the sensitivity of the SNAP test for detecting serum IgG concentrations <800 mg/dl was 95% while the specificity was 52% (75). Disadvantages of ELISAs include the use of heat and contamination-sensitive reagents and generally a higher cost per test than other screening methods (49).

More recently, Fourier-transform infrared (FTIR) spectroscopy has been investigated as a new testing method for IgG quantitation in equine serum (49). A study by Riley et al. in 2007 measured serum IgG concentrations in foals using FTIR analysis and compared these results to RID-derived concentrations. The sensitivity, specificity and accuracy for the FTIR-based test were 92.5%, 96.8% and 95.9% for the diagnosis of FTPI in foals. As a result, the authors felt that the overall performance of the IR-based was similar to the current gold standard RID assay and an accurate means for FTPI diagnosis in foals (49).

Few testing options are available for the measurement of Ig isotypes other than IgG or for the different IgG subclasses. Past literature exploring equine immunology utilized RID assays (VMRD Laboratories Inc.) for Ig isotype quantitation, yet these are no

longer commercially available (81, 82). Currently to this authors' knowledge, only ELISAs (Bethyl Laboratories Inc.; Montgomery, TX) are available for IgM, IgA and IgG(T) quantitation (ELISAs produced by the same company for IgGb and IgGa analysis have been discontinued by the company since 2012).

### **1.3.3. Testing methods currently available for immunoglobulin measurement in camelid species**

Significant research has gone into assessing the commonly used tests available for the measurement of Ig in foals and calves. In contrast, few studies have looked at evaluating these same tests in the various camelid species (52). Methods that have been evaluated for diagnosing FPT in camelids include measurement of total serum protein, globulin and albumin, measurement of serum gamma glutamyltransferase (GGT), zinc sulphate turbidity, glutaraldehyde coagulation, sodium sulphate precipitation, TIA and RID (52, 74, 83).

Radial immunodiffusion is a testing method available in camelids which provides quantitative IgG concentrations (52, 68, 83). Currently, only one RID assay is available for commercial use (Llama IgG Test Kit, Triple J Farms, Redmond, WA) as a second RID assay (Llama VET-RID, Bethyl Laboratories, Montgomery, TX) previously available has been discontinued by manufacturer's (52, 68). One study demonstrated these two RIDs were not in agreement for the measurement of camelid IgG. The authors concluded it was not possible to determine which assay more accurately predicted the actual IgG concentration as no other gold standard method was available for measuring camelid

IgG (68). Regardless, the RID assay currently available suffers the same disadvantages as in the equine RID assays previously discussed (52).

A few studies have looked at using different components of serum, such as total protein, albumin, globulin and GGT, as aids in the diagnosis of FTPI in crias (40, 83). In one study, results revealed no significant association between GGT activity and IgG concentrations determined via RID (40, 52). A second study corroborated this finding but did indicate that TSP and globulin concentrations were significantly associated with serum IgG concentrations and therefore are potential methods for identifying suspect cases of FTPI in crias (52). This study found that using a TSP endpoint of  $\geq 5.0$  g/L, the proportion of crias correctly diagnosed with FTPI was 72% with a sensitivity of 71% and specificity of 80% when compared with RID IgG values (52). For globulins, an endpoint of  $\geq 2.5$  mg/dl led to the correct classification of 70% of crias with a sensitivity of 64% and specificity of 100% (52). Serum albumin is not considered predictive of FTPI in crias (52, 83).

One study looked at using both the zinc sulphate turbidity and the glutaraldehyde coagulation tests for estimating IgG values in crias (83). When compared to RID, the zinc sulphate turbidity test had a sensitivity of 100%, specificity of 54.3% and accuracy of 69.4%. The glutaraldehyde coagulation test had a sensitivity of 78.4%, specificity of 91.2% and accuracy of 83.5% when compared with the RID results (83). The authors cautioned against using the glutaraldehyde coagulation test for FTPI screening in crias due to its low sensitivity and concluded that the zinc sulphate turbidity test was not accurate for identifying low IgG concentrations in camelids (83).

A sodium sulphate turbidity test (Llama-S, VMRD, Pullman, WA) is commercially available for the estimation of IgG concentrations in camelid serum (52). This test provides rapid, semiquantitative results and is user-friendly and inexpensive. One study found that using an endpoint of 300 mg/dl in the commercial sodium sulphate turbidity test generated a sensitivity of 89%, specificity of 100% and accuracy of 89% when compared with the results produced by RID (52). The authors concluded it was an appropriate method for assessing FPT in crias if used at an endpoint of 300 mg/dl rather than the 600 mg/dl or 1200 mg/dl recommended manufacturer's endpoints (52).

A recent study investigated the diagnostic agreement for IgG measurement in alpaca serum between the currently available RID assay and 2 new commercially available TIA assays (84). The authors found a lack of agreement between the 3 methods with the significant differences between assay results mainly attributed to their use of different standards (84). Of the 3 assays, RID was found to be the most imprecise leading the authors to question if the RID assay should continue as the "gold standard" for camelid serum IgG quantification or whether a more automated and precise method, such as TIA, should be adopted (84).

Ultimately, it is important to take all factors, including accuracy, time requirements, ease of use and cost, into account when selecting a test for the measurement of Ig concentrations. When results are questionable, or in those tests with low specificities, confirmation of results with another testing method is recommended (10).

#### **1.4. Fourier Transform Infrared Spectroscopy of Biological Samples**

#### **1.4.1. Overview**

Discovery of the infrared (IR) region of the electromagnetic spectrum by Sir William Herschel in 1800 was the pioneering step leading to the development of IR spectroscopy (85, 86). Within 35 years of this discovery, the first mid-infrared spectrometer was constructed and in 1913 the first commercially available IR spectrometer was manufactured (85, 87). However, it was not until approximately 30 years later, during World War II, that the usefulness of IR spectroscopy was realized in both industry and medical research (87). It was during this period that the breakthrough of IR spectroscopy occurred when it was employed for various projects such as the analysis of petroleum and identifying the structure of penicillin (87). Following World War II, an increase in industrial manufacturers led to a surge in the number of IR spectrometers in the United States, most with better design and flexibility than prior models. This in turn led to a quick growth in the use of IR spectroscopy for analysis of various chemical and biological systems (87).

A significant advancement in IR spectroscopy came with the production of Fourier-transform infrared (FTIR) spectrometers (87). These machines were able to drastically improve the quality of data obtained by using an interferometer in combination with the mathematical process of Fourier transformation (88). In 1969, Digilab produced the first commercially available computer-controlled FTIR that quickly led to an increase in the use of this technology to study different types of biomolecules (87). In the past few decades, enormous advances in instrumentation and computational power have allowed for the growth, refinement and widespread



implementation of FTIR in industry and biomedical research (86, 87). Today, FTIR spectrometers are able to routinely produce large volumes of data that would have been inconceivable only a mere decade ago (86). This ability allows for the analysis of complex biological samples, yet has created the need for the development of sophisticated methods of data interpretation. As a result, biomedical spectroscopists now use chemometrics and other mathematical processing methods to gather significant amounts of information from the generated spectra (86).

#### **1.4.2. Principles of operation and use**

The electromagnetic spectrum is made up of several regions of radiation including radiowave, microwave, infrared, visible, ultraviolet, x-rays and  $\gamma$ -rays (88). The IR portion of the electromagnetic spectrum lies between the microwave and visible sections and is divided into three regions, near-IR, mid-IR and far-IR, based on their relation to the visible region of the spectrum (89). The positions of IR absorption on the spectrum are typically presented as wavenumbers ( $\text{cm}^{-1}$ ) or wavelengths ( $\mu\text{m}$ ) with wavenumber defined as the number of waves per unit length (i.e. cm). The relationship between wavenumber and wavelength ( $\lambda$ ) can be represented as  $\text{wavenumber} = 1/\text{wavelength}$  (88, 89). Information produced from the measurement of IR absorption is often presented as a spectrum with wavenumber (or wavelength) on the x-axis and absorption intensity on the y-axis (89).

As mentioned previously, the IR spectrum is divided into three subsections: the near-IR ( $14285\text{--}4000\text{ cm}^{-1}$ ), mid-IR ( $4000\text{--}400\text{ cm}^{-1}$ ) and far-IR ( $<400\text{ cm}^{-1}$ ) (88). In particular, the mid- and near-IR regions have gained specific interest in analytical

chemistry for their ability to diagnose or solve various clinical problems in human and veterinary medicine (88, 90). Factors which help the researcher decide as to the suitability of mid or near spectroscopic techniques include the disease process and type of tissue to be analysed, sample thickness and volume, and whether in-vivo or ex vivo measurements are desired (91, 92).

The basis for infrared spectroscopy is that all molecules within a sample are in continuous vibration at temperatures above absolute zero (89, 93). When IR light is transmitted through a sample in a FTIR spectrometer, molecules within that sample will absorb light when a specific vibrational frequency is matched by the frequency of the IR radiation (93). The amount of radiation absorbed at a specific wavenumber is measured by an IR spectrometer and displayed as absorption bands on an IR spectrum. The IR spectrum of a multi-component sample (such as the biological samples of interest here) will consist of numerous absorption bands at different wavenumbers; each unique chemical component contributes its own unique vibrational spectrum (absorption pattern), and the measurement thus yields a superposition of the spectra for the various different biomolecules in that sample (93, 94). Small molecules will generate simple spectra with their chemical structure reflected by well-defined absorption bands. In contrast, complex samples are composed of an increased number of biomolecules thus generating spectra with an increased number of absorbance bands, many of which will overlap (94). It is important to note that the IR spectrum of a sample depicts both the structure and abundance of the IR active components within that sample. Therefore,

changes to either of these features will result in changes in the absorbance bands of the sample's spectrum (49, 93).

The oldest, most basic form of IR spectroscopy is transmission spectroscopy whereby the absorption of IR radiation is measured as a function of wavelength when it is passed through a sample (88). Any state of sample can be analyzed using transmission spectroscopy. With aqueous samples, the strong absorptions bands produced by water within the sample may overlap with the absorption bands of interest on the spectra, thereby making it difficult to obtain meaningful results (85, 88). Two options to overcome this obstacle have been identified. These include allowing the liquid to dry (and thereby removing the water) and form a film which can then be analyzed, or using more advanced techniques such as attenuated total reflectance (85).

Following the acquisition of an IR spectrum for a given sample, the challenge is to then extract information which will provide clinically useful data (88). As modern spectroscopic equipment can now provide large volumes of data in a short period of time, it has created the need to develop sophisticated interpretative methods for data analysis. As mentioned earlier, the use of chemometrics and other mathematical processing techniques has aided in this process, providing new solutions for data acquisition that were previously not available (86). These chemometric techniques provide the basis to develop either quantitative analytical methods or classification methods (e.g. "healthy" vs. "diseased") that provide the basis for categorical diagnostic tests (86, 95, 96).

To optimise the accuracy of the analytical method, the spectra are often preprocessed with the aim of amplifying useful information latent within them, and suppressing irrelevant features and noise. Some of the techniques commonly employed for this purpose, and utilized in this research project, include spectral smoothing of data, standard normal variate transformation of spectra and partial least squares regression (97-99). The premise behind smoothing of the spectral data is that the information output from an experiment will contain both the measurements of interest as well as random errors superimposed upon and indistinguishable from these measurements (these errors are commonly referred to as noise) (99). As a result, the Savitzky-Golay method was developed with the intent of removing as much of this noise as possible while maintaining the integrity of the underlying measurements (99).

Processing of IR spectra via standard normal variate transformation is often performed with the intent to remove the interference of radiation scatter within an individual spectrum (97). Subsequently, it is useful to reduce within-set-sample variation among the spectra and generate a more uniform, manageable set of data (97).

Once the spectral preprocessing is complete, partial least squares (PLS) regression is utilized as the basis to develop a quantitative analytical method. To begin, the method explores the relationship between IR spectra generated for each sample of interest and their corresponding “true” reference standard concentration values (i.e. RID or ELISA-derived Ig concentrations in this project) (100). This process yields a “calibration model” that is capable of converting spectroscopic data into useful quantitative analytical data (49). The accuracy of this provisional analytical method (the

PLS algorithm that takes a spectrum as input and provides concentration value as output) is then verified by using it as the basis to predict concentrations for “unknown” validation, or test samples. This provides an estimate of the predictive accuracy of the method in clinical use (49).

#### **1.4.3. Advantages of Fourier-transform infrared spectroscopy**

There are numerous advantages to the use of FTIR spectroscopy for the quantitative and qualitative characterization of biological samples. Perhaps one of the most distinguishing features is that no reagents are required as the spectra generated are the direct result of IR-active components within the sample of interest (90). Due to this, there is no requirement for chemical modification of the sample or comparative substances or standards (49, 90, 91). An additional advantage of this approach is that it is an economical testing modality with a low per-sample cost and inexpensive repeat testing (49). Another benefit with FTIR spectroscopy is that results can be available within minutes. This advantage, combined with no reagent requirements, make IR based testing methods well suited for point-of-care use in diagnostic laboratories, operating theatres, emergency rooms or veterinary clinics (49, 101).

An important feature of FTIR spectroscopy is that almost any form of a sample, including gas, solid or liquid, can be successfully analyzed, often with only a small sample volume required. For instance, mid-IR spectroscopic analysis can be performed on using  $\leq 10$   $\mu\text{l}$  of sample volume while near-IR typically requires only 0.1-0.2 ml of sample (89, 91). Modern FTIR-based analytical methods are also amenable to automation (91).

An attractive feature of FTIR spectroscopy is its ability to identify spectral “signatures” or “fingerprints” of disease due to its sensitivity in identifying changes at a molecular level in cells and tissues (49, 102). In theory, the IR spectrum obtained from a fluid or tissue will depict the absorptions from all major biomolecules present within that sample, with the relative absorbance intensity of each correlating to its relative concentration (103). Therefore, the IR spectrum from a specific type of tissue or fluid may be considered characteristic. Consequently, if a disease process changes the composition of a fluid or tissue, it will alter the molecular fingerprint of that sample which should be diagnostic (103). As a result, spectral differences have been found between normal and diseased tissues or fluids, aiding in the detection and classification of numerous diseases (90, 93, 104).

As demonstrated below, many studies have proven FTIR-based analytical methods to have excellent accuracy and sensitivity in the screening, diagnosis and classification of disease (49, 94, 104-106). These results, combined with the numerous aforementioned advantages, make FTIR spectroscopy a promising technique in the future of human and veterinary health care.

#### **1.4.4. Practical applications of infrared spectroscopy in human medicine**

##### **1.4.4.1. Overview**

Infrared spectroscopy has emerged as a powerful diagnostic tool in analytical chemistry for the quantitative and qualitative analysis of biological fluids in both human and veterinary medicine (85, 90). It has promise in the development of more practical,

accurate biomedical tests and current research demonstrates its potential in the study of pathological disease processes (85, 90).

#### **1.4.4.2. Infrared Clinical Chemistry**

Infrared clinical chemistry is the quantitative determination of analytes of interest in biological fluids through analysis with IR spectroscopy (85). Significant research has been undertaken in this field to investigate the use of IR spectroscopy in multiple areas including serum and urine component quantitation, assessment of fetal lung maturity, saliva component quantitation and the diagnosis and classification of arthritis through synovial fluid analysis (85, 103).

A number of studies have demonstrated the potential for FTIR in a clinical chemistry laboratory setting (96, 101). Whole blood, plasma, serum and urine samples are all composed of a variety of different components, such as proteins, clotting factors, Igs, etc., each of which have their own unique IR absorption pattern (91, 96, 101, 107). This unique IR pattern provides the basis to distinguish among the different sample constituents and separately quantify them, thus providing a multitude of useful clinical data from a single sample (91). Multiple analytes of importance in both veterinary and human medicine have proven suitable for FTIR based analysis in prior studies. These include total protein, albumin, glucose, triglycerides, urea, creatinine, lactate, fibrinogen and cholesterol (91, 96, 101, 107). As a result, it may be possible for FTIR spectrometers to become a part of routine analytical methods in diagnostic chemistry laboratories in the future.

In humans, there are a number of diseases that can significantly affect joint mobility and potentially progress to disability and joint deformities. These include osteoarthritis, rheumatoid arthritis and spondyloarthropathy (95, 103). Diagnosis of these diseases is typically through a combination of clinical history and physical examination with other diagnostic methods (such as radiology, magnetic resonance imaging and laboratory tests) used to verify clinical suspicions. However, obtaining a diagnosis through such methods can often be labor intensive, costly and time consuming. Additionally, in some cases a diagnosis may not be reached for several months if clinical symptoms are not significant enough to be diagnostically definitive and by that time irreversible damage to the joint may have occurred (103). Recently, IR spectroscopy has been investigated for its use in the diagnosis of arthritis via synovial fluid analysis (95, 103).

Two studies measured the IR spectra of synovial fluid and combined these with linear discriminant analysis to categorize the type of disease present in a given joint (either as osteoarthritis, rheumatoid arthritis or spondyloarthropathy) (95, 103). They hypothesized that the different disease processes would each alter the composition of synovial fluid in the associated joints and that this alteration would create a diagnostic molecular fingerprint on IR spectra (103). Results confirmed that the IR spectrum of synovial fluid from each of the three types of diseased joints differed significantly from each other, thus allowing for disease classification based on the different synovial fluid spectra (95, 103). This work indicates that IR spectroscopy may be useful as an aid in the



diagnosis of arthritic conditions through the analysis of synovial fluid from affected joints.

#### **1.4.4.3. Infrared Pathology**

The term infrared pathology refers to the analysis of excised tissues or isolated cells by IR spectroscopy to further investigate disease processes within the body (85). In the past few decades, this concept has gained notice in the field of oncology with numerous studies indicating the potential for FTIR spectroscopy in the screening, diagnosis or characterization of cancerous cells and tissues (92, 105, 108). Results of these studies indicate IR spectroscopy is able to reliably detect changes in the biochemical composition of cells at a molecular level and as a result, its use has been investigated in a variety of cancers including cervical, esophageal, breast, gastric, colorectal and certain leukemias (85, 93, 106, 109-111).

Worldwide, cervical cancer is the second leading cause of cancer-related death in females, with more than half a million cases diagnosed yearly (112). The introduction of cervical cancer screening methods by Papanicalou in the 1960s and 1970s led to a decrease in the prevalence of cervical cancer by 75% between 1955 and 1992 yet despite this, incidence rates of cervical cancer are still high, particularly in under-developed countries where screening programs are lacking (112, 113). Currently, cervical cancer screening is done via a pap smear where exfoliated cervical cells are collected and undergo cytologic examination, yet this method is widely recognized as having a low accuracy due to the occurrence of false negative results (113). As a result, alternate methods for cervical cancer screening are under investigation with numerous

publications found in recent literature assessing the use of IR spectroscopy for this purpose (104, 109, 113-116).

Earlier research investigating the use of IR spectroscopy for cervical cancer screening focused on detecting changes at the molecular level in diseased cells (104, 114). One study by Wong et al. was able to determine that the infrared spectra obtained from normal cervical cells were significantly different than the spectra obtained from abnormal cells (those with either cervical cancer or dysplasia) due to alterations in the intensity of various bands in different spectral regions. They concluded that the spectral changes found in dysplastic cells were the same as those in cancerous cells, just to a lesser magnitude (114).

More recently, studies have focused on the application of IR spectroscopy in a clinical setting for the detection of cervical cancer in comparison with the current standard screening method (pap smear) (109, 116). One study compared FTIR spectroscopy screening of exfoliated cervical cells to pap smear cytology screening in 301 samples using colposcopic biopsy as the gold standard for cervical cancer diagnosis (109). Results of this study generated a sensitivity and specificity of 98.6% and 98.8% for FTIR and 86.6% and 90.5% for pap smears. The false negative rates differed significantly between the two testing methods in favor of FTIR (1.4% for FTIR versus 13.4% for pap smears). Based on these promising results, further investigation into the role of IR spectroscopy in the screening of cervical cancer is warranted (109).

Significant research efforts have been employed in the fields of gastric and colon cancer detection through use of IR spectroscopy (102, 106, 108, 110, 117, 118). Similar

to with other forms of cancer, IR spectroscopy has been used to successfully identify alterations in the spectrum generated from malignant gastric and colon tissues when compared to normal tissues (108, 118). In one study, 10 bands in the region of 925-1660  $\text{cm}^{-1}$  were identified as having significantly greater absorptions in the malignant gastric tissues than in normal tissues. By using these absorption bands and linear discriminant analysis, 22 out of 23 gastric cancer samples and 9 out of 12 normal gastric tissue samples were correctly categorized yielding an accuracy of 88.6% (with a sensitivity of 96% and sensitivity of 75%) for the classification of gastric tissue samples in this study. The high sensitivity in this study, comparable to or better than certain other current methods of gastric cancer screening, depicts FTIR spectroscopy as a promising technique for the differentiation between normal and malignant gastric tissues (108).

Breast cancer is one of the most commonly diagnosed and significant forms of cancer in woman worldwide, with a rapidly increasing incidence and a mortality of up to 40% (119). As a result, rapid, accurate techniques for early screening of breast cancer are required. Mammography is currently the most common screening tool for breast cancer, but has various limitations including a high degree of false positive results (due to its poor ability to identify cancerous lesions in radiologically dense breast tissue) (119). Therefore, considerable research efforts have focussed on determining whether IR spectroscopy may be a clinically useful tool in screening, characterization and staging of breast cancer (85, 119).

Use of IR spectroscopy in the analysis of breast tissue can be more difficult than with other forms of tissue due to the complex matrix of adipose tissue and collagen

which anchors the epithelial cells of the breast (85). There exists a large variation in normal breast tissue composition, which in turn generates numerous variations in the spectral characteristics of breast tissue in almost all regions of the spectrum. Due to this variation, less pronounced changes in the spectrum, such as those relating to progression of the disease within the epithelial cells, may be more difficult to identify (85).

Despite this inherent complexity of breast tissue, one study was able to illustrate that a large amount of clinically relevant information may still be obtained from the spectra of breast tissue samples using appropriate pattern recognition methods (85). In this study, a linear discriminant algorithm was used to identify spectral features that were considered characteristic of high, intermediate and low grade breast tumors. The accuracy of the algorithm to correctly classify high, intermediate and low grade breast tumors was 100%, 76.5% and 90.5% respectively (85).

#### **1.4.4.4. Other applications in human medicine**

The aforementioned fields of medicine are just a portion of those where the use of IR spectroscopy is currently being explored for its application in the screening, diagnosis or classification of disease. Other areas where researchers are delving into the use of IR spectroscopy for medical purposes include characterizing Alzheimer's disease tissue and the non-invasive measurement of tissue perfusion and haemoglobin oxygen saturation (85). IR spectroscopy is also under investigation for its use as a non-invasive screening tool in various dermatological and arthritic disease processes as well as for its

application in the determination of fetal lung maturity through amniotic fluid analysis (92, 120-123).

#### **1.4.5. Practical applications of infrared spectroscopy in veterinary medicine**

##### **1.4.5.1. Overview**

Following the success of IR spectroscopy in various aspects of human medicine, research has emerged exhibiting its promise in the field of veterinary medicine. As a logical next step, many of the concepts and techniques of IR spectroscopy that were developed for use in human medicine, have been utilized to screen, diagnose or solve similar clinical problems in animals (94, 124).

##### **1.4.5.2. Arthrology**

Musculoskeletal disorders are common in equine athletes and can have significant effects on the animal's well-being and performance ability. Osteoarthritis is one such disease which involves the synovial joints and is characterized by cartilage degeneration, osteophyte formation, subchondral bone sclerosis and inflammation of synovial structures (125). The incidence of osteoarthritis-induced lameness in performance horses is quite high with one study implicating it in 54% of lameness cases admitted to one veterinary teaching hospital (125). Another important musculoskeletal disorder in horses is osteochondrosis. Osteochondrosis is considered a developmental orthopedic disease characterized by failure of endochondral ossification leading to articular cartilage damage and subchondral bone defects in affected joints. It has a reported prevalence in the literature ranging from 10% - 31.5% making it another significant cause of lameness and poor performance in equine athletes (90).

Numerous diagnostic modalities are available for the identification of osteoarthritis and osteochondrosis in horses. Recent studies performed at the Atlantic Veterinary College (AVC) investigated the potential for IR spectroscopy in this area (90, 94). One study hypothesized that osteochondrosis in an equine joint may alter its synovial fluid composition thereby creating different IR absorption patterns in synovial fluid samples obtained from affected joints (90). This study compared the IR spectra generated from synovial fluid samples of joints with osteochondrosis to those of normal joints and found significant features in the IR absorption pattern of samples taken from osteochondrosis-affected joints (90). The classification success rate for this study was promising at 77% but the authors noted that a larger sample size in future FTIR-based studies of osteochondrosis would be ideal to improve the accuracy and range of applicability to a larger, more diverse diseased population (90).

A similar study looking at traumatic arthritis rather than osteochondrosis in horses was also performed at the AVC (94). The hypothesis was similar in that the authors believed traumatic arthritis in an equine joint would lead to changes in the synovial fluid composition of that joint which could be detected by alterations in the IR absorption patterns when compared to control samples. A classification model was developed, from a calibration dataset, with its performance determined by the use of two validation datasets. The model was able to classify spectra from the calibration dataset with an overall accuracy of 97%, sensitivity of 93% and specificity of 100% and yielded an overall accuracy of 89% and 100% for the validation datasets (94). These results show that alterations in the IR spectroscopic absorption patterns of synovial fluid

obtained from traumatic arthritis-affected joints may be used with an appropriate classification algorithm for the diagnosis of this equine joint disease (94).

#### **1.4.5.3. Transmissible spongiform encephalopathies**

Infrared spectroscopy has been studied for its feasibility in the screening and detection of infectious diseases such as transmissible spongiform encephalopathies (TSEs) (124, 126-129). This family of diseases, which includes scrapie in sheep, bovine spongiform encephalopathy (BSE) in cattle, chronic wasting disease in deer, transmissible mink encephalopathy in mink and Creutzfeldt-Jakob disease in humans, is a group of fatal neurodegenerative diseases resulting from changes to the prion proteins in brain tissue (124, 126). Due to the severe public health and economic concerns these diseases generate, research in the past few years has focused on the development of rapid, reliable diagnostic tests for TSEs (124).

In recent years, IR spectroscopy has been used to analyse the blood and tissues from TSE-affected animals (124, 126-129). Kniepp et al. examined brain tissue harvested from both scrapie-infected and non-infected hamsters in attempts to identify preclinical and clinical pathological changes in the brain specimens from diseased hamsters (128, 129). Through comparison of the IR spectra of the scrapie-infected and control brains, consistent alterations in both protein composition and carbohydrate and nucleic acid components were identified within the scrapie-infected brains. These results show IR spectroscopy is able to detect certain molecular changes which allow for spectral discrimination between normal hamster brain tissue and the brain tissue from hamsters with preclinical, clinical and terminal-stage scrapie (128, 129).

More recently, studies have looked at using IR spectroscopy for the antemortem diagnosis of BSE in cattle serum (124, 126, 130). Researchers found that the composition of serum samples from BSE-affected animals was slightly, but characteristically, altered thereby providing “signatures” specific to BSE on their associated IR spectra (124, 126). These results display a method for antemortem BSE diagnosis via serum, but further work is required to determine whether these same BSE-specific “signatures” can also be identified in animals prior to the onset of clinical signs of disease (126).

#### **1.4.5.4. Dairy herd health management**

Large scale dairy herd operations are common practice in North America and other parts of the world with producers continuously looking for ways to improve cow health and increase their quality and quantity of milk production. Infrared spectroscopy, often in combination with chemometrics, has been investigated for these purposes with success in various aspects of herd health management (131-134).

Primary ketosis in dairy cattle occurs in the postpartum period due to insufficient energy intake. This metabolic disorder is associated with lower milk yield, increased time to first ovulation and lower fertility in affected cattle (131, 132). Measurement of acetone concentration in milk is one method for ketosis diagnosis in dairy cattle with recent research looking into the use of IR spectroscopy for this purpose (131, 132). Typically, the concentration of acetone in milk ranges between 0-2 mM with concentrations <0.7 mM indicating the cow is healthy, 0.7-1.4 mM indicating potential subclinical ketosis and >1.4 indicating ketosis (132).



Two independent studies were both able to determine that acetone can be found at two locations in the mid-infrared spectral region:  $1370\text{ cm}^{-1}$  and  $1239\text{ cm}^{-1}$ . Based on this information, one study reduced the spectrum of analysis for acetone (from  $3000\text{-}1000\text{ cm}^{-1}$  to  $1450\text{-}1200\text{ cm}^{-1}$ ) and combined FTIR spectroscopy with partial least squares regression to successfully identify subclinical ketosis in cattle (131). Using this method and a threshold of 0.4-1.0 mM for subclinical ketosis, the study was able to develop an accurate testing method for subclinical ketosis with a sensitivity of 95-100% and specificity of 96-100% (131).

Other studies have investigated the reliability of IR spectroscopy as a diagnostic tool for the measurement of milk components such as somatic cell count and milk urea nitrogen (MUN) (133, 134). As machines are now commercially available which utilize FTIR spectroscopy for milk sample analysis, research is necessary to determine whether this new technology is able to consistently produces results comparable to or better than the historically accepted methods of analysis (133). One study, performed at the AVC, found no significant differences between an IR-based method of MUN measurement and the current gold standard enzymatic testing method (133).

#### **1.4.5.5. Urolithiasis**

Urolithiasis is a disorder most commonly treated in felids, canids, small ruminants and equids although it has been identified in a variety of other species including pigs, cattle, birds and turtles (135). The treatment and prevention of urolithiasis requires an in depth knowledge of both the composition and structure of the urinary calculi (136). As a result, various modalities, including IR spectroscopy, have

been utilized in recent years to better identify and study urinary calculi in canine, feline and equine species (136-139).

Urinary calculi are composed of a variety of constituents, such as calcium carbonate, calcium oxalate, struvites, ammonium urate, etc., each of which can be differentiated by their distinctive absorption band within an IR spectra (137, 139). For example, research using IR spectroscopy to identify equine urinary calculi found characteristic bands for calcium carbonate at the 1500-1400  $\text{cm}^{-1}$  region (138). As well, research looking at calculi in humans and dogs found calcium oxalate uroliths may be identified by the presence of strong absorption bands at 1320  $\text{cm}^{-1}$  in the IR spectrum (137). These and other previous studies demonstrate the potential for IR spectroscopy to be used in a basic clinical setting to assist in the prevention and treatment of urinary calculi in companion animals and equids (136-138).

#### **1.4.6. Application of infrared spectroscopy in immunoglobulin quantification**

Recently, FTIR spectroscopy has been investigated for its ability to quantify immunoglobulins in the blood of both humans and horses (49, 140). To date, only two studies have used FTIR spectroscopy to measure IgG, IgA and IgM in human plasma, each with a different technique for Ig quantitation (107, 140). Of these studies, only one was fully validated and able to prove the reproducibility of its technique (140). In this study, IR spectroscopy was combined with partial least square regression to build and calibrate a model to predict the IgG, IgA and IgM concentrations from the spectra obtained from 90 samples of human plasma. Nephelometry was used as the gold standard reference method. Results demonstrated significant correlation between the

IR-predicted Ig concentrations and those obtained by nephelometry with  $R^2 = 0.98$  for IgA,  $R^2 = 0.98$  for IgG and  $R^2 = 0.78$  for IgM (140). Using various statistical methods, the authors were able to validate and prove the reproducibility of their IR-based technique for Ig quantitation as well as demonstrate the interchangeability of the FTIR and nephelometry techniques (140).

A study evaluating the use of FTIR spectroscopy for the measurement of IgG concentrations in horses was also recently published (49). Similar to the aforementioned paper, partial least squares was used to successfully build an algorithm for the prediction of IgG concentrations from the IR spectra derived from equine serum samples. Validation of the algorithm was achieved through its ability to predict IgG concentrations based on the spectra produced from independent test sets of samples (49).

### **1.5. Objectives of current study**

Based on the above proof of concept studies, it is hypothesized that FTIR spectroscopy may be a clinically useful tool for the measurement of IgG concentrations in camelid serum and Ig isotypes and subclasses in equine serum. More specifically, the objectives of the current research project include:

- 1) to develop an FTIR based assay for the measurement of IgG concentrations in alpaca serum and compare its performance to that of the current gold standard RID assay, and

- 2) to develop FTIR based assays for the measurement of equine serum IgG(a), IgG(b), IgA, IgM and IgG(t) concentrations and compare their performance to that of the ELISA assay.

## 1.6. References

1. Tizard IR. Veterinary Immunology :An Introduction. 8th ed. St. Louis, Mo.: Saunders Elsevier, 2009:574.
2. Shi F, Ljunggren H, Sarvetnick N. Innate immunity and autoimmunity: From self-protection to self-destruction. Trends Immunol. 2001;22:97-101.
3. Kennedy MA. A brief review of the basics of immunology: The innate and adaptive response. Veterinary Clinics of North America, Small Animal Practice. 2010;40:369-379.
4. Janeway C, Murphy KP, Travers P, Walport M. Janeway's Immunobiology. 7th ed. New York, NY: Garland Science, 2008:887.
5. Beutler B. Innate immunity: An overview. Mol Immunol. 2004;40:845-859.
6. Fearon DT, Locksley RM. The instructive role of innate immunity in the acquired immune response. Science. 1996;272:50-54.
7. Medzhitov R, Janeway Jr CA. Innate immunity: Impact on the adaptive immune response. Curr Opin Immunol. 1997;9:4-9.
8. Coffman RL, Sher A, Seder RA. Vaccine adjuvants: Putting innate immunity to work. Immunity. 2010;33:492-503. 9. Reed SM, Bayly WM, Sellon DC. Equine Internal Medicine. 3rd ed. St. Louis, MO: Saunders Elsevier, 2010:32-43.
10. Crisman MV, Scarratt WK. Immunodeficiency disorders in horses. Veterinary Clinics of North America, Equine Practice. 2008;24:299-310.
11. Ahmed R, Gray D. Immunological memory and protective immunity: Understanding their relation. Science. 1996;272:54-60.
12. Yi S, ZhanCai L, LiMing R, et al. Immunoglobulin genes and diversity: What we have learned from domestic animals. *Journal of Animal Science and Biotechnology*. London; UK: BioMed Central Ltd; 2012;3.
13. Yi S, ZhiGuo W, Ning L, YaoFeng Z. A comparative overview of immunoglobulin genes and the generation of their diversity in tetrapods. *Dev Comp Immunol*. Oxford; UK: Elsevier Ltd; 2013;39:103-109.
14. Hartley SB, Cooke MP, Fulcher DA, et al. Elimination of self-reactive B lymphocytes proceeds in two stages: Arrested development and cell death. Cell (Cambridge). 1993;72:325-335.

15. Kouskoff V, Lacaud G, Pape K, Retter M, Nemazee D. B cell receptor expression level determines the fate of developing B lymphocytes: Receptor editing versus selection. *Proc Natl Acad Sci U S A*. 2000;97:7435-7439.
16. Manz RA, Arce S, Cassese G, Hauser AE, Hiepe F, Radbruch A. Humoral immunity and long-lived plasma cells. *Curr Opin Immunol*. 2002;14:517-521.
17. Wagner B, Miller DC, Lear TL, Antczak DF. The complete map of the ig heavy chain constant gene region reveals evidence for seven IgG isotypes and for IgD in the horse. *Journal of Immunology*. Bethesda; USA: American Association of Immunologists; 2004;173:3230-3242.
18. Wagner B. Immunoglobulins and immunoglobulin genes of the horse. *Dev Comp Immunol*. 2006;30:155-164.
19. Lamm ME. Interaction of antigens and antibodies at mucosal surfaces. *Annu Rev Microbiol*. 1997;51:311-340.
20. Brandtzaeg P. Induction of secretory immunity and memory at mucosal surfaces. *Vaccine*. 2007;25:5467-5484.
21. De Genst E, Saerens D, Muyldermans S, Conrath K. Antibody repertoire development in camelids. *Dev Comp Immunol*. 2006;30:187-198.
22. Dawson DR, DeFrancisco RJ, Stokol T. Reference intervals for hematologic and coagulation tests in adult alpacas (*vicugna pacos*). *Vet Clin Pathol*. 2011;40:504-512.
23. Nguyen VK, Su C, Muyldermans S, van der Loo W. Heavy-chain antibodies in camelidae; a case of evolutionary innovation. *Immunogenetics*. 2002;54:39-47.
24. De Simone EA, Saccodossi N, Ferrari A, Leoni J. Development of ELISAs for the measurement of IgM and IgG subclasses in sera from llamas (*lama glama*) and assessment of the humoral immune response against different antigens. *Vet Immunol Immunopathol*. 2008;126:64-73.
25. Harmsen MM, De Haard HJ. Properties, production, and applications of camelid single-domain antibody fragments. *Appl Microbiol Biotechnol*. 2007;77:13-22.
26. De Simone E, Saccodossi N, Ferrari A, Leoni L, Leoni J. Immunochemical analysis of IgG subclasses and IgM in south american camelids. *Small Ruminant Research*. 2006;64:2-9.
27. Conrath KE, Wernery U, Muyldermans S, Nguyen VK. Emergence and evolution of functional heavy-chain antibodies in camelidae. *Dev Comp Immunol*. 2003;27:87-103.

28. Wesolowski J, Alzogaray V, Reyelt J, et al. Single domain antibodies: Promising experimental and therapeutic tools in infection and immunity. *Med Microbiol Immunol*. 2009;198:157-174.
29. Daley LP, Gagliardo LF, Duffy MS, Smith MC, Appleton JA. Application of monoclonal antibodies in functional and comparative investigations of heavy-chain immunoglobulins in new world camelids. *Clin Diagn Lab Immunol*. 2005;12:380-386.
30. Wernery U. Camelid immunoglobulins and their importance for the new-born--a review. *J Vet Med B Infect Dis Vet Public Health*. 2001;48:561-568.
31. Muyldermans S, Baral TN, Retamozzo VC, et al. Camelid immunoglobulins and nanobody technology. *Vet Immunol Immunopathol*. 2009;128:178-183.
32. Giguere S, Polkes AC. Immunologic disorders in neonatal foals. *Vet Clin North Am Equine Pract*. 2005;21:241-72, v.
33. Jelinek F, Faldyna M, Jasurkova-Mikutova G. Severe combined immunodeficiency in a fell pony foal. *J Vet Med A Physiol Pathol Clin Med*. 2006;53:69-73.
34. Fox-Clipsham LY, Brown EE, Carter SD, Swinburne JE. Population screening of endangered horse breeds for the foal immunodeficiency syndrome mutation. *Vet Rec*. 2011;169:655.
35. Sellon DC. Secondary immunodeficiencies of horses. *Vet Clin North Am Equine Pract*. 2000;16:117-130.
36. Chappuis G. Neonatal immunity and immunisation in early age: Lessons from veterinary medicine. *Vaccine*. 1998;16:1468-1472.
37. Bravo P, Garnica J, Fowler M. Immunoglobulin G concentrations in periparturient llamas, alpacas and their crias. *Small Ruminant Research*. 1997;26:145-149.
38. Senger PL. *Pathways to Pregnancy and Parturition*. 2nd ed. Pullman, Washington: Current Conceptions Inc., 2003:305-313.
39. Weaver DM, Tyler JW, VanMetre DC, Hostetler DE, Barrington GM. Passive transfer of colostral immunoglobulins in calves. *J Vet Intern Med*. 2000;14:569-577.
40. Johnston NA, Parish SM, Tyler JW, Tillman CB. Evaluation of serum gamma-glutamyltransferase activity as a predictor of passive transfer status in crias. *J Am Vet Med Assoc*. 1997;211:1165-1166.

41. McClure JT, DeLuca JL, Lunn DP, Miller J. Evaluation of IgG concentration and IgG subisotypes in foals with complete or partial failure of passive transfer after administration of intravenous serum or plasma. *Equine Vet J.* 2001;33:681-686.
42. Perryman LE. Primary immunodeficiencies of horses. *Vet Clin North Am Equine Pract.* 2000;16:105-16.
43. El-Hatmi H, Levieux A, Levieux D. Camel (*camelus dromedarius*) immunoglobulin G,  $\alpha$ -lactalbumin, serum albumin and lactoferrin in colostrum and milk during the early post partum period. *J Dairy Res.* 2006;73:288-293.
44. Davis DG, Schaefer DM, Hinchcliff KW, Wellman ML, Willet VE, Fletcher JM. Measurement of serum IgG in foals by radial immunodiffusion and automated turbidimetric immunoassay. *J Vet Intern Med.* 2005;19:93-96.
45. LeBlanc MM, Tran T, Baldwin JL, Pritchard EL. Factors that influence passive transfer of immunoglobulins in foals. *J Am Vet Med Assoc.* 1992;200:179-183.
46. Davis R, Giguere S. Evaluation of five commercially available assays and measurement of serum total protein concentration via refractometry for the diagnosis of failure of passive transfer of immunity in foals. *J Am Vet Med Assoc.* 2005;227:1640-1645.
47. Garmendia AE, Palmer GH, DeMartini JC, McGuire TC. Failure of passive immunoglobulin transfer: A major determinant of mortality in newborn alpacas (*lama pacos*). *Am J Vet Res.* 1987;48:1472-1476.
48. Weaver DM, Tyler JW, Scott MA, Wallace LM, Marion RS, Holle JM. Passive transfer of colostral immunoglobulin G in neonatal llamas and alpacas. *Am J Vet Res.* 2000;61:738-741.
49. Riley CB, McClure JT, Low-Ying S, Shaw RA. Use of fourier-transform infrared spectroscopy for the diagnosis of failure of transfer of passive immunity and measurement of immunoglobulin concentrations in horses. *J Vet Intern Med.* 2007;21:828-834.
50. Clabough DL, Levine JF, Grant GL, Conboy HS. Factors associated with failure of passive transfer of colostral antibodies in standardbred foals. *J Vet Intern Med.* 1991;5:335-340.
51. Robinson JA, Allen GK, Green EM, Fales WH, Loch WE, Wilkerson CG. A prospective study of septicaemia in colostrum-deprived foals. *Equine Vet J.* 1993;25:214-219.



52. Weaver DM, Tyler JW, Marion RS, Wallace LM, Nagy JK, Holle JM. Evaluation of assays for determination of passive transfer status in neonatal llamas and alpacas. *J Am Vet Med Assoc.* 2000;216:559-563.
53. Larson J, Buechner-Maxwell V, Crisman MV, LeRoith T, Witonsky S. Severe combined immunodeficiency in a caspian filly. *J Vet Intern Med.* 2011;25:954-958.
54. Perryman LE. Molecular pathology of severe combined immunodeficiency in mice, horses, and dogs. *Vet Pathol.* 2004;41:95-100. doi:10.1354/vp.41-2-95.
55. Finno CJ, Spier SJ, Valberg SJ. Equine diseases caused by known genetic mutations. *Vet J.* 2009;179:336-347.
56. Bernoco D, Bailey E. Frequency of the SCID gene among arabian horses in the USA. *Anim Genet.* 1998;29:41-42.
57. Weldon AD, Zhang C, Antczak DF, Rebhun WC. Selective IgM deficiency and abnormal B-cell response in a foal. *J Am Vet Med Assoc.* 1992;201:1396-1398.
58. Perkins GA, Nydam DV, Flaminio MJ, Ainsworth DM. Serum IgM concentrations in normal, fit horses and horses with lymphoma or other medical conditions. *J Vet Intern Med.* 2003;17:337-342.
59. Perryman LE, McGuire TC. Evaluation for immune system failures in horses and ponies. *J Am Vet Med Assoc.* 1980;176:1374-1377.
60. Thomas GW, Bell SC, Carter SD. Immunoglobulin and peripheral B-lymphocyte concentrations in fell pony foal syndrome. *Equine Vet J.* 2005;37:48-52.
61. Fox-Clipsham LY, Carter SD, Goodhead I, et al. Identification of a mutation associated with fatal foal immunodeficiency syndrome in the fell and dales pony. *PLoS Genet.* 2011;7:e1002133.
62. Tallmadge RL, Stokol T, Gould-Earley MJ, et al. Fell pony syndrome: Characterization of developmental hematopoiesis failure and associated gene expression profiles. *Clin Vaccine Immunol.* 2012;19:1054-1064.
63. Davis WC, Heirman LR, Hamilton MJ, et al. Flow cytometric analysis of an immunodeficiency disorder affecting juvenile llamas. *Vet Immunol Immunopathol.* 2000;74:103-120.
64. Hutchison JM, Garry FB, Belknap EB, et al. Prospective characterization of the clinicopathologic and immunologic features of an immunodeficiency syndrome affecting juvenile llamas. *Vet Immunol Immunopathol.* 1995;49:209-227.

65. Hutchison JM, Garry F. Ill thrift and juvenile llama immunodeficiency syndrome. *Veterinary Clinics of North America, Food Animal Practice*. 1994;10:331-343.
66. Hutchison JM, Garry FB, Johnson LW, et al. Immunodeficiency syndrome associated with wasting and opportunistic infection in juvenile llamas: 12 cases (1988-1990). *J Am Vet Med Assoc*. 1992;201:1070-1076.
67. Sivasankar M. Immunodeficiency syndrome in a 3-year-old llama. *The Canadian veterinary journal. La revue veterinaire canadienne* JID - 0004653. 0607.
68. Hutchison JM, Salman MD, Garry FB, Johnson LW, Collins JK, Keefe TJ. Comparison of two commercially available single radial immunodiffusion kits for quantitation of llama immunoglobulin G. *J Vet Diagn Invest*. 1995;7:515-519.
69. Pellegrini-Masini A, Bentz AI, Johns IC, et al. Common variable immunodeficiency in three horses with presumptive bacterial meningitis. *J Am Vet Med Assoc*. 2005;227:114-22, 87.
70. Tallmadge RL, Such KA, Miller KC, Matychak MB, Felipe MJ. Expression of essential B cell development genes in horses with common variable immunodeficiency. *Mol Immunol*. 2012;51:169-176.
71. Flaminio MJ, Tallmadge RL, Salles-Gomes CO, Matychak MB. Common variable immunodeficiency in horses is characterized by B cell depletion in primary and secondary lymphoid tissues. *J Clin Immunol*. 2009;29:107-116.
72. Flaminio MJ, LaCombe V, Kohn CW, Antczak DF. Common variable immunodeficiency in a horse. *J Am Vet Med Assoc*. 2002;221:1296-302, 1267.
73. Perryman LE, McGuire TC, Banks KL. Animal model of human disease. infantile X-linked agammaglobulinemia. agammaglobulinemia in horses. *Am J Pathol*. 1983;111:125-127.
74. Hutchison JM, Salman MD, Garry FB, Johnson LW, Keefe TJ. Characterization of plasma immunoglobulin G concentrations of llamas. *Am J Vet Res*. 1998;59:406-409.
75. Metzger N, Hinchcliff KW, Hardy J, Schwarzwald CC, Wittum T. Usefulness of a commercial equine IgG test and serum protein concentration as indicators of failure of transfer of passive immunity in hospitalized foals. *J Vet Intern Med*. 2006;20:382-387.
76. Beetson SA, Hilbert BJ, Mills JN. The use of the glutaraldehyde coagulation test for detection of hypogammaglobulinaemia in neonatal foals. *Aust Vet J*. 1985;62:279-281.

77. McClure JT, DeLuca JL, Miller J. Comparison of five screening tests for detection of failure of passive transfer in foals. Presented at: ACVIM forum Proceedings. Dallas, TX, May 29, 2002.
78. Clabough DL, Conboy HS, Roberts MC. Comparison of four screening techniques for the diagnosis of equine neonatal hypogammaglobulinemia. *J Am Vet Med Assoc.* 1989;194:1717-1720.
79. McCue PM. Evaluation of a turbidimetric immunoassay for measurement of plasma IgG concentration in foals. *Am J Vet Res.* 2007;68:1005-1009.
80. Pusterla N, Pusterla JB, Spier SJ, Puget B, Watson JL. Evaluation of the SNAP foal IgG test for the semiquantitative measurement of immunoglobulin G in foals. *Vet Rec.* 2002;151:258-260.
81. McFarlane D, Sellon DC, Gibbs SA. Age-related quantitative alterations in lymphocyte subsets and immunoglobulin isotypes in healthy horses. *Am J Vet Res.* 2001;62:1413-1417.
82. de Camargo MM, Kuribayashi JS, Bombardieri CR, Hoge A. Normal distribution of immunoglobulin isotypes in adult horses. *Vet J.* 2009;182:359-361.
83. Drew ML, Fowler ME. Comparison of methods for measuring serum immunoglobulin concentrations in neonatal llamas. *J Am Vet Med Assoc.* 1995;206:1374-1380.
84. Pinn TL, Gagliardo LF, Purdy SR, Appleton JA, Stokol T. Comparison of three immunoglobulin G assays for the diagnosis of failure of passive transfer of immunity in neonatal alpacas. *Journal of Veterinary Diagnostic Investigation.* 2013;25:91-98.
85. Jackson M, Sowa MG, Mantsch HH. Infrared spectroscopy: A new frontier in medicine. *Biophys Chem.* 1997;68:109-125.
86. Dubois J, Shaw RA. IR spectroscopy in clinical and diagnostic applications. *Anal Chem.* 2004;76:361A-367A.
87. Barth A, Haris PI. *Biological and Biomedical Infrared Spectroscopy.* IOS Press, 2009.
88. Stuart B, ed. *Biological Applications of Infrared Spectroscopy.* Rexdale, Ontario: John Wiley & Sons, Ltd., 1997:1-33.
89. Hsu C. Infrared spectroscopy. In: Settle F, ed. *Handbook of Instrumental Techniques for Analytical Chemistry.* New Jersey: Prentice Hall, 1997:247-283.

90. Vijarnsorn M, Riley CB, Ryan DAJ, Rose PL, Shaw RA. Identification of infrared absorption spectral characteristics of synovial fluid of horses with osteochondrosis of the tarsocrural joint. *Am J Vet Res.* 2007;68:517-523.
91. Shaw RA, Low-Ying S, Leroux M, Mantsch HH. Toward reagent-free clinical analysis: Quantitation of urine urea, creatinine, and total protein from the mid-infrared spectra of dried urine films. *Clin Chem.* 2000;46:1493-1495.
92. McIntosh LM, Summers R, Jackson M, et al. Towards non-invasive screening of skin lesions by near-infrared spectroscopy. *J Invest Dermatol.* 2001;116:175-181.
93. Maziak DE, Do MT, Shamji FM, Sundaresan SR, Perkins DG, Wong PTT. Fourier-transform infrared spectroscopic study of characteristic molecular structure in cancer cells of esophagus: An exploratory study. *Cancer Detect Prev.* 2007;31:244-253.
94. Vijarnsorn M, Riley CB, Shaw RA, et al. Use of infrared spectroscopy for diagnosis of traumatic arthritis in horses. *Am J Vet Res.* 2006;67:1286-1292.
95. Shaw RA, Kotowich S, Eysel HH, Jackson M, Thomson GT, Mantsch HH. Arthritis diagnosis based upon the near-infrared spectrum of synovial fluid. *Rheumatol Int.* 1995;15:159-165.
96. Shaw R, Kotowich S, Mantsch H, Leroux M. Quantitation of protein, creatinine, and urea in urine by near-infrared spectroscopy. *Clinical biochemistry JID - 0133660.* 0403.
97. Barnes RJ, Dhanoa MS, Lister SJ. Standard normal variate transformation and de-trending of near-infrared diffuse reflectance spectra. *Appl Spectrosc.* 1989;43:772-777.
98. Rajalahti T, Kvalheim OM. Multivariate data analysis in pharmaceuticals: A tutorial review. *Int J Pharm.* 2011;417:280-290.
99. Savitzky A, Golay MJE. Smoothing and differentiation of data by simplified least squares procedures. *Anal Chem.* 1964;36:1627-1639.
100. Geladi P, Kowalski B. Partial least-squares regression: A tutorial. *Analytica Chimica Acta.* 1986;185:1-17.
101. Low-Ying S, Shaw RA, Leroux M, Mantsch HH. Quantitation of glucose and urea in whole blood by mid-infrared spectroscopy of dry films. *Vibrational Spectroscopy.* 2002;28:111-116.
102. Kallenbach-Thieltges A, Grosseruschkamp F, Mosig A, Diem M, Tannapfel A, Gerwert K. Immunohistochemistry, histopathology and infrared spectral histopathology of colon cancer tissue sections. *J Biophotonics.* 2013;6:88-100.

103. Eysel HH, Jackson M, Nikulin A, Somorjai RL, Thomson GTD, Mantsch HH. A novel diagnostic test for arthritis: Multivariate analysis of infrared spectra of synovial fluid. *Biospectroscopy*. 1997;3:161-176.
104. Yazdi HM, Bertrand MA, Wong PT. Detecting structural changes at the molecular level with fourier transform infrared spectroscopy. A potential tool for prescreening preinvasive lesions of the cervix. *Acta Cytol*. 1996;40:664-668.
105. Schultz CP, Liu K, Johnston JB, Mantsch HH. Study of chronic lymphocytic leukemia cells by FT-IR spectroscopy and cluster analysis. *Leuk Res*. 1996;20:649-655.
106. Li QB, Sun XJ, Xu YZ, et al. Diagnosis of gastric inflammation and malignancy in endoscopic biopsies based on fourier transform infrared spectroscopy. *Clin Chem*. 2005;51:346-350.
107. Petibois C, Cazorla G, Cassaigne A, Deleris G. Plasma protein contents determined by fourier-transform infrared spectrometry. *Clin Chem*. 2001;47:730-738.
108. Fujioka N, Morimoto Y, Arai T, Kikuchi M. Discrimination between normal and malignant human gastric tissues by fourier transform infrared spectroscopy. *Cancer Detect Prev*. 2004;28:32-36.
109. Fung Kee Fung M, Senterman M, Eid P, Faught W, Mikhael NZ, Wong PT. Comparison of fourier-transform infrared spectroscopic screening of exfoliated cervical cells with standard papanicolaou screening. *Gynecol Oncol*. 1997;66:10-15.
110. Li X, Li QB, Zhang GJ, et al. Identification of colitis and cancer in colon biopsies by fourier transform infrared spectroscopy and chemometrics. *ScientificWorldJournal*. 2012;2012:936149.
111. Babrah J, McCarthy K, Lush RJ, Rye AD, Bessant C, Stone N. Fourier transform infrared spectroscopic studies of T-cell lymphoma, B-cell lymphoid and myeloid leukaemia cell lines. *Analyst*. 2009;134:763-768.
112. Kamemoto LE, Misra AK, Sharma SK, et al. Near-infrared micro-raman spectroscopy for in vitro detection of cervical cancer. *Appl Spectrosc*. 2010;64:255-261.
113. Schubert JM, Bird B, Papamarkakis K, et al. Spectral cytopathology of cervical samples: Detecting cellular abnormalities in cytologically normal cells. *Laboratory Investigation*. 2010;90:1068-1077.
114. Wong PT, Wong RK, Caputo TA, Godwin TA, Rigas B. Infrared spectroscopy of exfoliated human cervical cells: Evidence of extensive structural changes during carcinogenesis. *Proc Natl Acad Sci U S A*. 1991;88:10988-10992.

115. El-Tawil S, Adnan R, Muhamed ZN, Nor HO. Comparative study between pap smear cytology and FTIR spectroscopy: A new tool for screening for cervical cancer. *Pathology*. 2008;40:600-603.
116. Chiriboga L, Xie P, Vigorita V, Zarou D, Zakim D, Diem M. Infrared spectroscopy of human tissue. II. A comparative study of spectra of biopsies of cervical squamous epithelium and of exfoliated cervical cells. *Biospectroscopy*. 1998;4:55-59. doi:2-R.
117. Li Q, Wang W, Ling X, Wu JG. Detection of gastric cancer with fourier transform infrared spectroscopy and support vector machine classification. *Biomed Res Int*. 2013;2013:942427.
118. Rigas B, Morgello S, Goldman IS, Wong PT. Human colorectal cancers display abnormal fourier-transform infrared spectra. *Proc Natl Acad Sci U S A*. 1990;87:8140-8144.
119. Zhang Y, Chen Y, Yu Y, Xue X, Tuchin VV, Zhu D. Visible and near-infrared spectroscopy for distinguishing malignant tumor tissue from benign tumor and normal breast tissues in vitro. *J Biomed Opt*. 2013;18:077003.
120. Canvin JM, Bernatsky S, Hitchon CA, et al. Infrared spectroscopy: Shedding light on synovitis in patients with rheumatoid arthritis. *Rheumatology (Oxford)*. 2003;42:76-82.
121. McIntosh LM, Jackson M, Mantsch HH, Mansfield JR, Crowson AN, Toole JWP. Near-infrared spectroscopy for dermatological applications. *Vibrational Spectroscopy*. 2002;28:53-58.
122. Liu KZ, Dembinski TC, Mantsch HH. Rapid determination of fetal lung maturity from infrared spectra of amniotic fluid. *Am J Obstet Gynecol*. 1998;178:234-241.
123. Liu KZ, Shaw RA, Dembinski TC, Reid GJ, Ying SL, Mantsch HH. Comparison of infrared spectroscopic and fluorescence depolarization assays for fetal lung maturity. *Am J Obstet Gynecol*. 2000;183:181-187.
124. Lasch P, Schmitt J, Beekes M, et al. Antemortem identification of bovine spongiform encephalopathy from serum using infrared spectroscopy. *Anal Chem*. 2003;75:6673-6678.
125. Kidd JA, Fuller C, Barr ARS. Osteoarthritis in the horse. *Equine Veterinary Education*. 2001;13:160-168.
126. Martin TC, Moecks J, Belouossov A, et al. Classification of signatures of bovine spongiform encephalopathy in serum using infrared spectroscopy. *Analyst*. 2004;129:897-901.

127. Lasch P, Beekes M, Schmitt J, Naumann D. Detection of preclinical scrapie from serum by infrared spectroscopy and chemometrics. *Analytical and Bioanalytical Chemistry*. 2007;387:1791-1800.
128. Kneipp J, Beekes M, Lasch P, Naumann D. Molecular changes of preclinical scrapie can be detected by infrared spectroscopy. *Journal of Neuroscience*. 2002;22:2989-2997.
129. Kneipp J, Lasch P, Baldauf E, Beekes M, Naumann D. Detection of pathological molecular alterations in scrapie-infected hamster brain by fourier transform infrared (FT-IR) spectroscopy. *Biochimica et Biophysica Acta, Molecular Basis of Disease*. 2000;1501:189-199.
130. Menze BH, Petrich W, Hamprecht FA. Multivariate feature selection and hierarchical classification for infrared spectroscopy: Serum-based detection of bovine spongiform encephalopathy. *Anal Bioanal Chem*. 2007;387:1801-1807.
131. Heuer C, Luinge HJ, Lutz ET, et al. Determination of acetone in cow milk by fourier transform infrared spectroscopy for the detection of subclinical ketosis. *J Dairy Sci*. 2001;84:575-582.
132. Hansen PW. Screening of dairy cows for ketosis by use of infrared spectroscopy and multivariate calibration. *J Dairy Sci*. 1999;82:2005-2010.
133. Arunvipas P, VanLeeuwen JA, Dohoo IR, Keefe GP. Evaluation of the reliability and repeatability of automated milk urea nitrogen testing. *Can J Vet Res*. 2003;67:60-63.
134. Tsenkova R, Atanassova S, Kawano S, Toyoda K. Somatic cell count determination in cow's milk by near-infrared spectroscopy: A new diagnostic tool. *J Anim Sci*. 2001;79:2550-2557.
135. Robinson MR, Norris RD, Sur RL, Preminger GM. Urolithiasis: Not just a 2-legged animal disease. *J Urol*. 2008;179:46-52. doi:10.1016/j.juro.2007.08.123.
136. Escolar E, Bellanato J. Analysis of feline urinary calculi and urethral plugs by infrared spectroscopy and scanning electron microscopy. *Vet Rec*. 2003;152:625-628.
137. Escolar E, Bellanato J. Spectroscopic and ultrastructural comparative study of cystine calculi in humans and dogs. *Biospectroscopy*. 1999;5:237-242. doi:2-E.
138. Diaz-Espineira M, Escolar E, Bellanato J, De La Fuente MA. Infrared and atomic spectrometry analysis of the mineral composition of a series of equine sabulous material samples and urinary calculi. *Res Vet Sci*. 1997;63:93-95.

139. Diaz-Espiñeira M, Escolar E, Bellanato J, Rodriguez M. Structure and composition of equine uroliths. *Journal of Equine Veterinary Science*. 1995;15:27-34.
140. Benzeddine-Boussaidi L, Cazorla G, Melin AM. Validation for quantification of immunoglobulins by fourier transform infrared spectrometry. *Clin Chem Lab Med*. 2009;47:83-90.



**CHAPTER 2**

**USE OF FOURIER-TRANSFORM INFRARED SPECTROSCOPY TO QUANTIFY**

**IMMUNOGLOBULIN G CONCENTRATIONS IN ALPACA SERUM**

Jennifer J. Burns, Siyuan Hou, Christopher B. Riley, R. Anthony Shaw, Nicole Jewett and J  
T. McClure

Published in Journal of Veterinary Internal Medicine  
Year: 2014, Volume: 28, Issue: 2, pages: 639-645

## 2.1. Abstract

**Background:** Rapid, economical and quantitative assays for measurement of camelid serum immunoglobulin G (IgG) are limited. In camelids, failure of transfer of maternal immunoglobulins has a reported prevalence of up to 20.5%. An accurate method for quantifying serum IgG concentrations is required.

**Objectives:** To develop an infrared (IR) spectroscopy-based assay for measurement of alpaca serum IgG and compare its performance to the reference standard radial immunodiffusion (RID) assay.

**Animals:** One hundred and seventy-five privately-owned, healthy alpacas.

**Methods:** Serum IgG concentrations were determined by RID assays and mid-IR spectra were collected for each sample. Fifty samples were set aside as the test set and the remaining 125 training samples were employed to build a calibration model using partial least squares (PLS) regression. The predictive performance of the calibration model was evaluated by the test set.

**Results:** Correlation coefficients for the IR-based assay were 0.93 and 0.87, respectively, for the entire data set and test set. Sensitivity in the diagnosis of failure of transfer of passive immunity (FTPI) ( $[IgG] < 1000 \text{ mg/dl}$ ) was 71.4% and specificity was 100% for the IR-based method (test set) as gauged relative to the RID reference method assay.

**Conclusions and clinical importance:** This study indicates that IR spectroscopy, in combination with chemometrics, is an effective method for IgG measurement in alpaca serum.

## 2.2. Introduction

Pregnant camelids have an epitheliochorial form of placentation that unlike humans, does not allow for the in-utero transfer of immunoglobulins (Igs) (1). Consequently, newborn crias are born agammaglobulinemic and rely upon the transfer of maternal antibodies from the dam's colostrum to acquire protective passive immunity for the first few weeks of life (2, 3). In the newborn cria, transfer of Igs is considered successful when immunoglobulin G (IgG) concentration in the serum is  $\geq 1000\text{mg/dl}$  (4). Failure to absorb sufficient amounts of Igs in the immediate post-partum period leads to a condition known as failure of transfer of passive immunity (FTPI) (1). FTPI has a reported prevalence between 9% and 20.5% in camelids and is recognized as an important disorder that might lead to an increased susceptibility to infectious organisms (4-7).

The most common clinical reason for measuring camelid Igs is suspicion of FTPI, therefore early and accurate diagnosis is required to provide timely medical intervention (7). Testing methods available for use in camelids includes total serum protein and globulin concentration measurements, zinc sulphate turbidity, glutaraldehyde coagulation, sodium sulphate precipitation, immunoturbidimetric assay (TIA) and radial immunodiffusion (RID) (3, 4, 6, 8-11). Of these, RID provides quantitative data and is currently considered the reference method test for IgG quantification in various species (7). Notwithstanding the benefit of providing quantitative data, RID has a number of disadvantages including a substantial turnaround time of 18-24 hours for results, a requirement for enhanced technical skill by the user, high cost compared with

other testing methods and a requirement for specific reagents with a limited shelf-life (7, 9, 12). An accurate, more rapid and economic IgG assay for quantifying serum IgG is desirable for camelids.

Fourier-transform infrared spectroscopy (FTIR) has emerged as a powerful diagnostic tool for quantitative and qualitative characterization of biological samples in human and veterinary medicine (13-15). The basis for this technique is that infrared radiation passing through a sample of interest is absorbed by that sample more or less strongly as a function of wavelength across the infrared spectral region. The resultant infrared absorption spectrum uniquely characterizes that sample, with the absorbance of radiation measured as a function of wavelength ( $\mu\text{m}$ ) or wavenumber ( $\text{cm}^{-1}$ ), translating to absorption bands across the infrared spectrum (7, 14, 15). The infrared absorption patterns reflect the molecular composition of the sample (7). To the extent that molecular composition is characteristically affected by disease, the absorption patterns for biomedical specimens (biofluids and tissues) might be equated to biochemical “fingerprints”. These “fingerprints” then have the potential to correlate directly with the presence or absence of disease or provide the basis to quantify diagnostically pertinent biological fluid analytes (7). Thus, infrared spectroscopy could serve as a robust, reagent-free method to quantify certain biofluid components of diagnostic interest (7, 13, 14). If it were to prove sufficiently accurate, the ease of use and low cost per sample may make FTIR a desirable testing method for determining serum IgG concentrations.

The objective of this study was to develop a FTIR based assay for the measurement of IgG concentrations in alpaca serum and to compare its performance to that of the RID assay.

### **2.3. Materials and Methods**

#### **2.3.1. Experimental animals**

Serum samples collected from privately owned alpacas (n=175) between 2009 and 2011 were used for this study. Eighty-two alpaca samples were from multiple farms located in Ontario and New Brunswick, Canada, while the remaining 93 were from properties in the Adelaide Hills region of South Australia. All alpacas were considered healthy based on general physical examination and no observable signs of disease. Age and gender was collected for 129 of the alpacas.

#### **2.3.2. Serum sampling protocol**

Blood samples were collected via jugular venipuncture in accordance with the University of Prince Edward Island's Animal Care Committee animal utilization protocol and the Animal Ethics Committee of the University of Adelaide. Following collection, blood samples from Canada were centrifuged and the serum collected into a cryovial and frozen at -20°C until transported on ice by overnight courier to the Atlantic Veterinary College (AVC) where they were stored at -80°C prior to use. Blood samples collected in Australia were taken directly to a diagnostic laboratory for hematological analysis as part of a separate study. These samples were centrifuged and the serum collected and refrigerated at 4°C for 24-48 hours until biochemical analysis was

performed. The remaining serum was then stored frozen at  $-80^{\circ}\text{C}$  prior to being couriered on ice to the AVC.

### **2.3.3. Radial Immunodiffusion assay for immunoglobulin G antibodies**

Commercial RID assays (Triple J Farms; Bellingham, WA) were used as the reference method for determining IgG serum concentrations. RID assays were performed according to manufacturer's instructions. The zones of precipitation diameters were read at 22-24 hours by the same individual to the nearest tenth of a millimetre using a handheld calliper. Samples exceeding the manufacturer's stated upper testing limit (3000 mg/dL) were diluted with 0.85% saline and rerun. Each sample and standard was tested in replicates of five (one replicate per RID plate). The average of the 5 replicates of the assay standards were fitted by linear regression, and that equation was used to determine the concentration of IgG for the unknown serum samples. Regression equations for  $R^2 > 0.9$  were accepted for analysis. The average of the 5 replicate results for each sample was used to determine the IgG concentration of that sample.

### **2.3.4. Fourier-transform Infrared spectroscopy for immunoglobulin G antibodies**

Thawed serum samples were diluted 1:1 with a 4 g/L potassium thiocyanate solution. Following dilution, six replicate dry films were made for each serum sample by evenly spreading 12 $\mu\text{l}$  aliquots of diluted sample onto 5-mm wells within a custom-made, adhesive-masked, 96-well silicon microplate.<sup>(7)</sup> Each loaded microplate was allowed to dry at room temperature before being loaded into a multisampler<sup>a</sup>

interfaced with a FTIR spectrometer<sup>b</sup> and controlled with proprietary software<sup>c</sup>.

Absorbance spectra in the IR range of 400-4000  $\text{cm}^{-1}$  were recorded (resolution 4  $\text{cm}^{-1}$ , 512 scans) for each replicate of each sample, using the single beam spectrum of an empty well as the background.

#### **2.3.5. Data processing**

Absorbance spectra were converted into printable format by GRAMS software package<sup>d</sup>, then imported into MATLAB<sup>®e</sup> for further analysis. Calculations were performed using scripts written by the authors.

A total of 1050 (175 samples x 6 replicates/sample) spectra were smoothed using the Savitzky-Golay method and processed by the standard normal variate transformation (16). This was followed by spectrum region selection chosen as 3700-2600  $\text{cm}^{-1}$  and 1800-1300  $\text{cm}^{-1}$  (based on previous work for FTIR IgG analysis in horses and further refined to specific areas within those regions that exhibited strong signals) (7). With six replicate spectra per serum sample, spectrum outlier detection was carried out by using Dixon's Q-test at each wavenumber with a confidence level set as 95% (18, 19). Those spectra with over 50% of the absorbance values detected as outliers were excluded from further analysis. Outlier detection was performed for all the 175 serum samples. The spectra for each sample were then averaged and used for succeeding analysis.

#### **2.3.6. Calibration model development and assay validation**

A test set of spectra from serum samples (N=50) was randomly drawn from the pool of 175 samples and set aside for the purpose of later testing the predictive

performance of the calibration model. Spectra from the remaining samples (N=125) were again randomly split into a training set (N=75) and a validation set (N=50). Partial least squares (PLS) regression was applied to the training set to develop calibration models with the number of PLS factors ranging from 1 up to 50. This procedure (with new random training/validation splits for each trial, and the same test set throughout) was repeated 5000 times and the Monte Carlo Cross validation value (MCCV) was calculated by the equation

$$\text{MCCV} = \frac{1}{Nn_v} \sum_{i=1}^N \|\mathbf{y}_i - \hat{\mathbf{y}}_i\|^2$$

where  $N$  denotes the number of repeated procedures ( $N=5000$ ),  $n_v$  is the number of samples in the validation set ( $n_v=50$ ), and  $\mathbf{y}_i$  and  $\hat{\mathbf{y}}_i$  represent the IgG concentrations for the samples, in the validation set, obtained from RID experiments and predicted from the IR spectroscopic data, respectively (20, 21). The number of PLS factors that gave the lowest MCCV value was chosen as the optimal value. Once the optimal number of PLS factors was determined, the training and validation sets were combined and the combined set was used to build a new calibration model. The predictive performance of the new calibration model was then evaluated by the test set that had been set aside in advance. The agreement among the RID and FTIR values for both the test set and combined data set was assessed by scatter plot, the Pearson correlation coefficient, and the concordance correlation coefficient. The differences between the RID and FTIR values for the test set was further characterized by the Bland-Altman plot and the



normal probability plot to further evaluate the model assumptions and performance (22).

#### **2.3.7. Precision of Fourier-transform infrared spectroscopic analyses**

With replicate spectra collected in this study, the precision of the FTIR method was evaluated based on the concentrations predicted for the test set samples/spectra. To that end, individual replicate spectra (not the averaged spectra) were used to calculate the IgG concentrations and the relative standard deviations (also called coefficient of variation) were used as the criteria to evaluate precision. For comparison, the relative standard deviation was also calculated for the individual replicate RID assays.

#### **2.3.8. Diagnostic sensitivity and specificity**

To assess potential applicability in the clinical diagnosis of FTPI (7), the diagnostic sensitivity and specificity of FTIR were calculated for the test set and entire data set using IgG <1000 mg/dl (based on RID) as the cut-off for a positive test for FTPI.

### **2.4. Results**

#### **2.4.1. Demographic data and RID-derived IgG concentration results**

Of the 129 alpacas for which signalment data were available, 81 were female and 48 were male. Four alpacas were <2 months of age, 5 were 2-3 months of age, 15 were 3-6 months of age, 12 were between 6 months and 1 year of age and 93 were > 1 year of age. Demographic data were unavailable for the remaining 46 alpacas.

The RID IgG concentrations for the 175 serum samples ranged from 394 mg/dL to 6327 mg/dl. Twenty-one samples had IgG concentrations below the 1000 mg/dl cut-

off typically used to define FTPI in camelid neonates. Of the remaining 154 samples, 89 had IgG concentrations between 1000 mg/dL and 3000 mg/dl and 65 had IgG concentrations >3000 mg/dL.

#### **2.4.2. Analysis of agreement between FTIR and RID IgG quantitation methods**

The overall patterns for blood/serum/plasma infrared spectra are characterized by strong absorptions in two regions ( $3600\text{--}2750\text{ cm}^{-1}$  and  $1800\text{--}400\text{ cm}^{-1}$ ), the former corresponding to stretching vibrations of the X-H moieties (X=C, N, O), and the latter corresponding to bending vibrations and stretching modes involving heavier atoms (e.g. the C=O stretch cited above) (Figure 2.1, page 86) (7). Within each spectrum, the most intense features result from proteins (the absorptions centering around  $3300\text{ cm}^{-1}$  are attributed to N-H stretching and those around  $1650\text{ cm}^{-1}$  correlate with C=O stretching of backbone protein amide linkages) (7).

As a first step toward development of the IR-based analytical method, ten spectra were identified as outliers (using the method described above) and removed from further analysis. The PLS regression trials yielded an optimal model (based on the lowest MCCV) with 15 PLS factors. A scatter plot (Figure 2.2, page 87) demonstrates the level of agreement between IgG concentrations obtained via RID and FTIR. The Pearson correlation coefficients for the combined set (training and validation sets) and test set were 0.93 and 0.87, respectively. The concordance correlation coefficients were 0.93 and 0.86, respectively (23, 24). Both correlation coefficients indicated that the FTIR predicted IgG concentrations had good to excellent correlation with RID determined IgG concentrations.

The mean value of the differences (FTIR – RID) is -20.4 mg/dl, which is small compared to the IgG concentration values, indicating no significant systematic difference (bias) between the two methods (Figure 2.3, page 88). However, the 95% confidence intervals on the Bland-Altman plot indicated a high variability (standard deviation  $\cong$  600 mg/dl) between FTIR and RID methods. A normal probability plot for the differences (Figure 2.4, page 89) demonstrates the majority of data points are distributed closely around the reference line. No obvious non-normality was observed in the error distribution, indicating the model assumption was not violated and further validating the developed model.

#### **2.4.3. Precision of the FTIR Spectroscopic Analyses**

The relative standard deviations for the RID did not show an obvious correlation with the IgG concentration but the relative standard deviations for the FTIR method decreased with an increase of IgG concentration (Figure 2.5, page 90). The relative standard deviations for the RID and FTIR methods overlapped when the IgG concentration was high, but when the IgG concentration was low, the FTIR method had larger relative standard deviations.

#### **2.4.4. Diagnostic Sensitivity and Specificity**

For the test set (n=50), 7 samples had IgG concentrations below the 1000 mg/dl diagnostic cut-off value generating a FTPI prevalence of 14% in the test set. Sensitivity for this data set was 71.4% (95% confidence interval (95%CI) = 30.3-94.9) and specificity was 100% (95% CI = 89.8-100). Using the entire data set (n=175; 21 samples with IgG concentrations below 1000 mg/dl), sensitivity was 81% (95% CI = 57.4-93.7) and

specificity was 100% (95% CI = 97-100). Within the entire data set, there were no false positives and 4 false negatives identified (Table 2.1, page 85).

## **2.5. Discussion**

This study showed that infrared spectroscopy, in combination with a quantification algorithm developed using PLS regression, is a promising technique for the measurement of IgG concentrations in camelid serum. This method was validated by its ability to accurately quantify IgG concentrations in an independent test set of samples.

Within this study the specificity was excellent but the sensitivity of the FTIR method was slightly lower than desired for diagnosis of FTPI in neonates. However, when compared with reported data for other methods available to quantify camelid serum IgG concentrations, these results are equivalent to or better than most (3, 6). One study looked at using a commercially available sodium sulphate turbidity test for the diagnosis of FTPI in crias. The authors found that when compared with RID and used according to manufacturer's instructions, the sensitivity for this test was only 36% and specificity was 100% (6). However, they also noted that by lowering the test's endpoint, the performance of the test could be significantly improved (6). The same study also found that serum total protein concentration, at an endpoint of 5.0 g/dl, yielded a sensitivity of 71% and specificity of 80% and that serum globulin concentration, at an endpoint of 2.5 g/dl, produced a sensitivity of 64% and specificity of 100% when compared with RID (6). The authors concluded that measurement of serum albumin, total solids or gamma-glutamyltransferase activity were not predictive of FTPI in crias

(6). Other researchers have found that total serum protein measurement, at an endpoint of 5.15 g/dl, had a sensitivity of 87.5% and specificity of 87.9% when compared with RID (3). Serum globulin concentration, at an endpoint of 1.6 g/dl, had a test sensitivity of 96.1% and specificity of 91.2% when compared with RID (3). This study also compared zinc sulphate turbidity and 10% glutaraldehyde coagulation tests with RID and found sensitivities of 100% and 78.4%, respectively, and specificities of 54.3% and 91.2% for these testing methods (3).

A recent study of the diagnostic agreement between the currently available camelid RID kit and 2 new commercially available turbidimetric immunoassay (TIA) assays found a lack of agreement between the 3 methods with the significant differences between assay results mainly attributed to their use of different standards (11). Of the 3 assays, RID was found to be the most imprecise leading the authors to question if the RID assay should continue as the “gold standard” for camelid serum IgG quantification or whether a more automated and precise method, such as TIA, should be adopted (11). These considerations raise an important question relevant to the present study: Might the accuracy of the FTIR-based assay be improved if a TIA assay was used as the reference standard rather than the RID assay? This issue is potentially worth exploring in future studies. However it must be emphasized that imprecision does not equate with inaccuracy and that the above referenced study did not determine the accuracy of the RID and TIA assays - only their precision and agreement.

Overestimation of IgG concentrations (false negatives) is a problem sometimes encountered with testing methods such as the zinc sulphate turbidity or the

glutaraldehyde coagulation test (25). With these tests, chemical interference from other proteins, such as albumin or hemoglobin, may occur resulting in inaccurate results (7). These erroneous test results can have clinical consequences for the neonate in question, including an increased risk of pneumonia, septicaemia, enteritis, omphalitis and death, if no medical treatment is provided due to a false negative test result (4). With FTIR the possibility for chemical interference can be reduced by ensuring that potential interferants are accounted for within the spectral data set used to develop the diagnostic algorithms (7). Within the test set of this study, 4 false negatives were identified. Upon gross examination of the serum samples, no hemolysis or lipemia was noted indicating interference from these components was not a major factor with these samples.

For the 4 false negatives within our data set, the RID-derived IgG concentrations were >700 mg/dL indicating only partial FTPI in these cases. Studies have shown that foals with serum IgG concentrations <400 mg/dl (complete FTPI) are at a significantly greater risk of developing septicaemia and other debilitating diseases, however, no similar association has been shown in foals with partial FTPI (serum IgG concentrations between 400-800 mg/dL) (26-28). While comparable studies have not been performed in camelid species, it is reasonable to assume that those crias with very low or complete FTPI may have an increased risk of morbidity and mortality when compared to crias with only partial FTPI. Accordingly, while the false negatives in this FTIR study are an issue, the partial FTPI concentrations were less likely to result in serious clinical consequences. We also note that discrepancies between concentrations determined by IR spectroscopy

and RID may arise from errors in the RID method; it is possible that better reference measurements would resolve the apparent discrepancies and reduce the apparent false negative rate accordingly.

A drawback of this study is the relatively small number of serum samples with low IgG concentrations in the data set. This limitation led to only 21 of the 175 samples, a 12% prevalence, having a serum IgG concentration below the 1000 mg/dl cut-off with only 7 of those 21 randomly assigned into the test set. As a result, the small number of samples with IgG concentrations <1000 mg/dl may affect the algorithm's accuracy in predicting IgG values at lower concentrations as algorithm development was weighted toward higher IgG concentrations. In future studies, it would be desirable to obtain another data set with a higher proportion of samples with IgG concentrations <1000 mg/dl, which would allow further modification of the algorithm and possibly better performance at lower IgG concentrations.

A variety of previous studies have demonstrated the potential for FTIR in a clinical laboratory setting (29, 30). The unique absorption pattern displayed for each unique analyte allows for the possibility to distinguish among different sample components and separately quantify them, thus providing additional useful clinical data (29, 30). For example, at least six serum constituents of importance in both veterinary and human medicine have been proven suitable for FTIR based analysis in prior studies. These include total protein, albumin, glucose, triglycerides, urea and cholesterol (29, 30). Consequently, it might be possible to acquire extra clinical pathological data from each spectrum without further time requirements or additional costs (7). In addition to

diagnosing FPT or measuring serum constituents, FTIR may also prove useful in both a clinic or laboratory setting to quantify IgG in adult camelid plasma donors.

In conclusion, Fourier-transform infrared spectroscopy is a promising technique to rapidly quantify IgG concentrations in alpaca serum. Further studies with a larger data set of low IgG serum concentrations are warranted to further refine the algorithm for screening cria's with FTPI.



## 2.6. Footnotes

<sup>a</sup> HTS-XT autosampler, Bruker Optics<sup>®</sup>, Milton, ON, Canada

<sup>b</sup> Tensor 37, Bruker Optics<sup>®</sup>, Milton, ON, Canada

<sup>c</sup> OPUS<sup>®</sup> ver. 6.5, Bruker Optics<sup>®</sup>, Milton, ON, Canada

<sup>d</sup> GRAMS software ver. 7.02, Thermo Fisher Scientific Inc, Waltham, MA, USA

<sup>e</sup> MATLAB MathWorks R2011b, Natick, MA, USA

## **2.7. Acknowledgments**

The authors would like to gratefully acknowledge Cynthia Mitchell for her technical assistance and Professor Michael Reichel for providing some of the samples used in this study.

Funding for this project was supported by the Atlantic Canada Opportunities Agency and the Atlantic Veterinary College Research Fund.

## 2.8. References

1. Chappuis G. Neonatal immunity and immunisation in early age: Lessons from veterinary medicine. *Vaccine*. 1998;16:1468-1472.
2. Garmendia AE, Palmer GH, DeMartini JC, McGuire TC. Failure of passive immunoglobulin transfer: A major determinant of mortality in newborn alpacas (lma pacos). *Am J Vet Res*. 1987;48:1472-1476.
3. Drew ML, Fowler ME. Comparison of methods for measuring serum immunoglobulin concentrations in neonatal llamas. *J Am Vet Med Assoc*. 1995;206:1374-1380.
4. Wernery U. Camelid immunoglobulins and their importance for the new-born--a review. *J Vet Med B Infect Dis Vet Public Health*. 2001;48:561-568.
5. Weaver DM, Tyler JW, Scott MA, Wallace LM, Marion RS, Holle JM. Passive transfer of colostral immunoglobulin G in neonatal llamas and alpacas. *Am J Vet Res*. 2000;61:738-741.
6. Weaver DM, Tyler JW, Marion RS, Wallace LM, Nagy JK, Holle JM. Evaluation of assays for determination of passive transfer status in neonatal llamas and alpacas. *J Am Vet Med Assoc*. 2000;216:559-563.
7. Riley CB, McClure JT, Low-Ying S, Shaw RA. Use of fourier-transform infrared spectroscopy for the diagnosis of failure of transfer of passive immunity and measurement of immunoglobulin concentrations in horses. *J Vet Intern Med*. 2007;21:828-834.
8. Bravo P, Garnica J, Fowler M. Immunoglobulin G concentrations in periparturient llamas, alpacas and their crias. *Small Ruminant Research*. 1997;26:145-149.
9. Hutchison JM, Salman MD, Garry FB, Johnson LW, Collins JK, Keefe TJ. Comparison of two commercially available single radial immunodiffusion kits for quantitation of llama immunoglobulin G. *J Vet Diagn Invest*. 1995;7:515-519.
10. Johnston NA, Parish SM, Tyler JW, Tillman CB. Evaluation of serum gamma-glutamyltransferase activity as a predictor of passive transfer status in crias. *J Am Vet Med Assoc*. 1997;211:1165-1166.
11. Pinn TL, Gagliardo LF, Purdy SR, Appleton JA, Stokol T. Comparison of three immunoglobulin G assays for the diagnosis of failure of passive transfer of immunity in neonatal alpacas. *Journal of Veterinary Diagnostic Investigation*. 2013;25:91-98.
12. Davis R, Giguere S. Evaluation of five commercially available assays and measurement of serum total protein concentration via refractometry for the diagnosis of failure of passive transfer of immunity in foals. *J Am Vet Med Assoc*. 2005;227:1640-1645.

13. Benezzeddine-Boussaidi L, Cazorla G, Melin AM. Validation for quantification of immunoglobulins by fourier transform infrared spectrometry. *Clin Chem Lab Med*. 2009;47:83-90.
14. Vijarnsorn M, Riley CB, Shaw RA, et al. Use of infrared spectroscopy for diagnosis of traumatic arthritis in horses. *Am J Vet Res*. 2006;67:1286-1292.
15. Vijarnsorn M, Riley CB, Ryan DAJ, Rose PL, Shaw RA. Identification of infrared absorption spectral characteristics of synovial fluid of horses with osteochondrosis of the tarsocrural joint. *Am J Vet Res*. 2007;68:517-523.
16. Savitzky A, Golay MJE. Smoothing and differentiation of data by simplified least squares procedures. *Anal Chem*. 1964;36:1627-1639.
17. Barnes RJ, Dhanoa MS, Lister SJ. Standard normal variate transformation and de-trending of near-infrared diffuse reflectance spectra. *Appl Spectrosc*. 1989;43:772-777.
18. Dean RB, Dixon WJ. Simplified statistics for small numbers of observations. *Anal Chem*. 1951;23:636-638.
19. Rorabacher DB. A statistical treatment for rejection of deviant values: Critical values of dixon's "Q" parameter and related subrange ratios at the 95% confidence level. *Anal Chem*. 1991;63:139-146.
20. Picard RR, Cook RD. Cross -validation of regression models. *J Amer Statist Assn*. 1984;79:575-583.
21. Xu QS, Liang YZ. Monte carlo cross validation. *Chemom Intell Lab Syst*. 2001;56:1-11.
22. Altman DG, Bland JM. Measurement in medicine: The analysis of method comparison studies. *Statistician*. 1983;32:307-317.
23. Lin LI. A concordance correlation coefficient to evaluation reproducibility. *Biometrics*. 1989;45:255-268.
24. Steichen TJ, Cox NJ. A note on the concordance correlation coefficient. *Stata J*. 2002;2:183-189.
25. Clabough DL, Conboy HS, Roberts MC. Comparison of four screening techniques for the diagnosis of equine neonatal hypogammaglobulinemia. *J Am Vet Med Assoc*. 1989;194:1717-1720.
26. Clabough DL, Levine JF, Grant GL, Conboy HS. Factors associated with failure of passive transfer of colostral antibodies in standardbred foals. *J Vet Intern Med*. 1991;5:335-340.
27. LeBlanc MM, Tran T, Baldwin JL, Pritchard EL. Factors that influence passive transfer of immunoglobulins in foals. *J Am Vet Med Assoc*. 1992;200:179-183.

28. McClure JT, DeLuca JL, Lunn DP, Miller J. Evaluation of IgG concentration and IgG subisotypes in foals with complete or partial failure of passive transfer after administration of intravenous serum or plasma. *Equine Vet J*. 2001;33:681-686.
29. Shaw RA, Low-Ying S, Leroux M, Mantsch HH. Toward reagent-free clinical analysis: Quantitation of urine urea, creatinine, and total protein from the mid-infrared spectra of dried urine films. *Clin Chem*. 2000;46:1493-1495.
30. Low-Ying S, Shaw RA, Leroux M, Mantsch HH. Quantitation of glucose and urea in whole blood by mid-infrared spectroscopy of dry films. *Vibrational Spectroscopy*. 2002;28:111-116.

**Table 2.1**

FTIR IgG false negative samples compared to IgG RID results identified within the entire data set (n =175).

| <b>Sample</b> | <b>Data Set</b> | <b>FTIR IgG Value (mg/dL)</b> | <b>RID IgG Value (mg/dL)</b> |
|---------------|-----------------|-------------------------------|------------------------------|
| A             | Calibration     | 1075                          | 719                          |
| B             | Calibration     | 1192                          | 773                          |
| C             | Test            | 1602                          | 861                          |
| D             | Test            | 1307                          | 822                          |

**Figure 2.1** Representative infrared spectrum of alpaca serum. The strongest features arise from proteins with relatively less abundant serum components contributing relatively weak fingerprints. The absorption at  $2062\text{ cm}^{-1}$  originates with the  $\text{KSCN}^-$  internal standard.

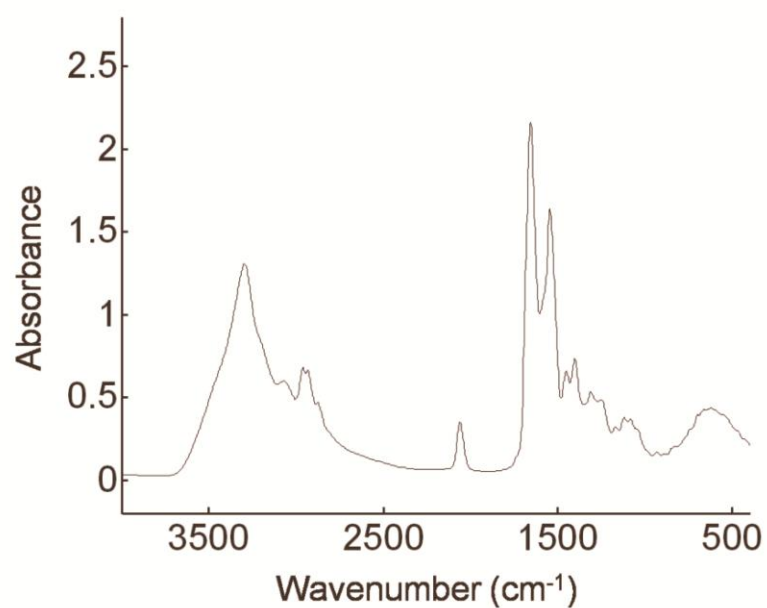


**Figure 2.2** A scatter plot comparing the IgG concentrations obtained from RID and FTIR methods. The asterisks denote samples used in building the calibration model and the circles indicate the samples in the test set. If RID and FTIR give comparable results, the data points should distribute closely around the reference line of 45°.

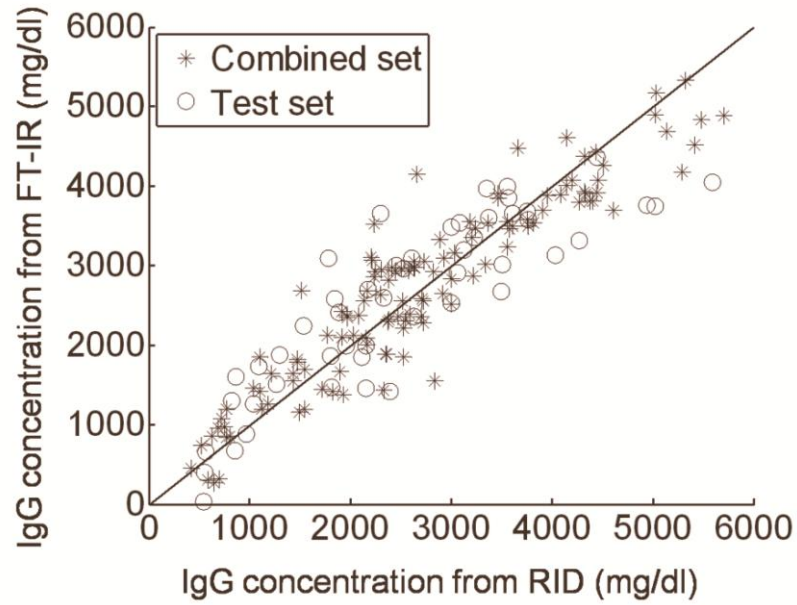




**Figure 2.3** A Bland-Altman plot of the differences in the IgG concentrations in the test set as obtained by RID and FTIR methods. The solid horizontal line represents the mean difference between RID and FTIR assays (-20.4 mg/dl) and the dashed lines represent the 95% confidence interval. If there is no systematic bias between RID and FTIR method, the mean value of the differences should be close to zero.

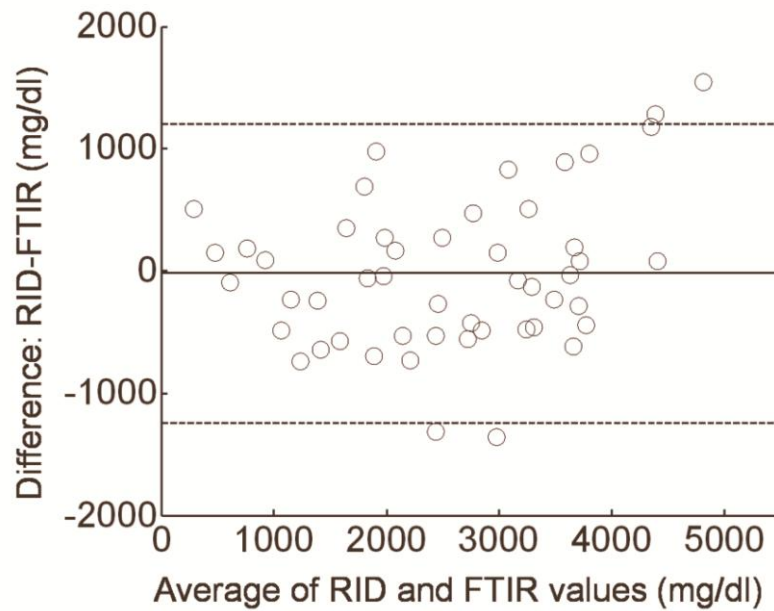


**Figure 2.4** Normal probability plot for the differences of the IgG concentrations in test set obtained from RID and FTIR methods. If the measurement errors follow a normal distribution, the data points should be largely located in the reference line.

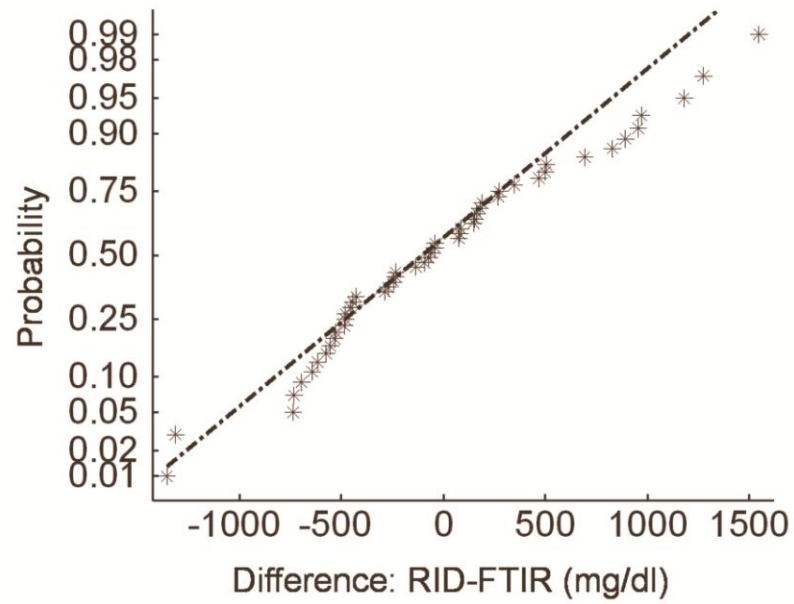
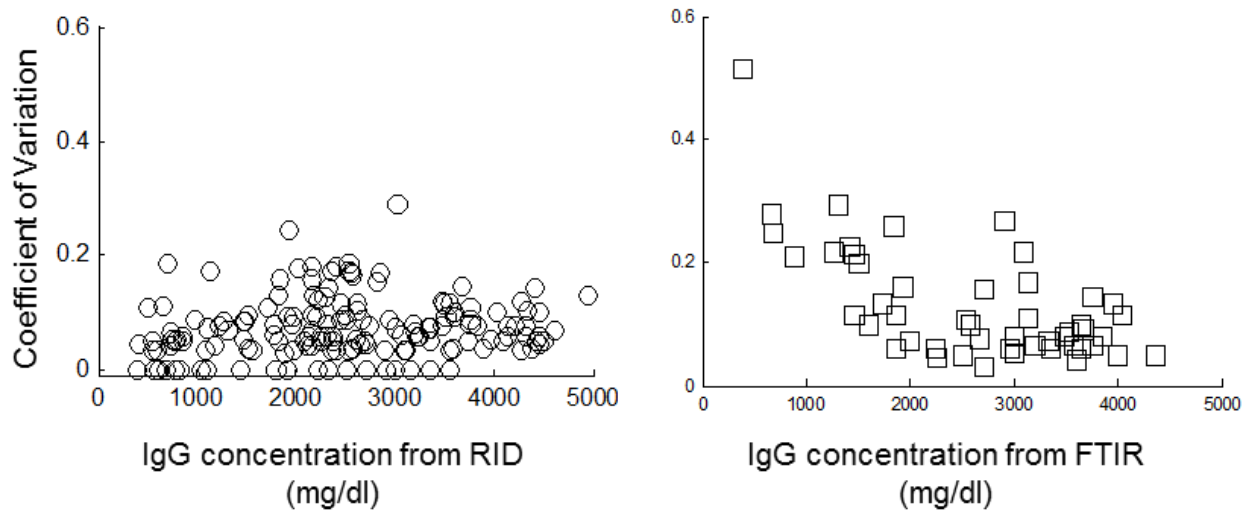


**Figure 2.5** Coefficient of variance plots for the RID and FTIR methods. Lower coefficient of variance means high precision of the test methods; this comparison shows that the precision of the RID and FTIR methods are roughly comparable.



## **CHAPTER 3**

### **EXPLORATORY STUDY EVALUATING THE USE OF FOURIER TRANSFORM INFRARED SPECTROSCOPY FOR THE QUANTITATION OF IMMUNOGLOBULIN ISOTYPES IgA and IgM AND IgG SUBCLASSES (IgGa, IgGb, IgG(T)) IN EQUINE PLASMA**

### 3.1. Abstract

Studies investigating the measurement of immunoglobulin G (IgG) subclasses (IgGa, IgGb, IgG(T)), immunoglobulin A (IgA) and immunoglobulin M (IgM) in adult equine plasma are scarce in current literature, and poor agreement is noted among the results of published studies. Previous studies have shown that Fourier-transform infrared (FTIR) spectroscopy can be used to measure IgG concentrations in horse plasma. Therefore, FTIR spectroscopy may be a promising new method for the quantification of Ig isotypes and IgG subclasses in equine plasma. The first objective of this study was to determine adult equine plasma IgGa, IgGb, IgG(T), IgA, and IgM concentrations using an enzyme-linked immunosorbent (ELISA) assay and to compare the results to previous studies. The second objective was to develop FTIR based assays for the measurement IgGa, IgGb, IgG(T), IgA, and IgM in equine plasma using the ELISA results as the reference test.

Immunoglobulin Ga, IgGb, IgG(T), IgA, and IgM concentrations were determined by ELISA assays and mid-infrared spectra were collected for 100 equine plasma samples. After preliminary assessment 99 spectra met the criteria for use in model building and were randomly divided into a training set (N=60 sera) and prediction set (N=39 sera). The training set was used to build a calibration model for each Ig isotype or subclass using partial least squares (PLS) regression. The 39 samples in the prediction set were then used to test the predictive performance of the developed models.

Mean serum concentrations ( $\pm$  standard deviation, g/L) determined via ELISA assay were  $2.72 \pm 0.77$  for IgGa,  $9.21 \pm 2.47$  for IgGb,  $4.96 \pm 2.35$  for IgG(T),  $1.01 \pm 0.76$

for IgA and  $0.79 \pm 0.31$  for IgM. Pearson correlation coefficients and scatter plots displayed moderate to good agreement between FTIR and ELISA IgGb results in the training and prediction data sets. For IgGa, IgG(T) IgA and IgM, Pearson correlation coefficients and scatter plots displayed moderate to extremely poor agreement between FTIR and ELISA results in the training and prediction data sets.

In this study an infrared spectroscopic assay was not an accurate technique for the measurement of Ig isotypes in equine plasma. Significant differences were noted between the results of this study and each of the reviewed studies from the published literature. Further work is required to establish normal reference ranges for Ig isotypes and subclasses in adult equine plasma.

### **3.2. Introduction**

Primary immunodeficiency disorders in equids, although uncommon, can be difficult to identify and often result in unfavorable outcomes (1). Recognised primary immunodeficiency syndromes in horses include severe combined immunodeficiency disorder (SCID), selective immunoglobulin M (IgM) deficiency, foal immunodeficiency syndrome (FIS) and agammaglobulinemia (1-3). Due to the potentially life-threatening consequences of these disorders, researchers have studied their pathogenesis, diagnosis, treatment and prognosis (4, 5). For many of these equine immunodeficiencies, diagnosis is based in part, or entirely, on the measurement of specific immunoglobulin (Ig) concentrations in serum (6). As a result, numerous testing methods have been developed for the rapid quantification of Igs in equine serum, with the majority focusing on the measurement of immunoglobulin G (IgG) (7-12).

Studies investigating the measurement of Ig isotypes (other than IgG) or IgG subclasses in adult horses are scarce in current literature (13). Most studies investigating the equine humoral immune response have concentrated on the pre- and post-parturient period in mares and foals (13, 14). As a result, secondary immunodeficiencies such as failure of transfer of passive immunity (FTPI) are easily recognized and treated, with various methods for IgG measurement readily available to aid in diagnosis (1). However, as certain primary immunodeficiencies result either entirely or in part from an Ig deficiency other than IgG, methods to quantify other Ig isotypes are required (15).

The most abundant Ig found in equine plasma is IgG (16). Currently, seven well-characterized IgG subclasses have been identified in equine plasma, including IgGa (IgG<sub>1</sub> and IgG<sub>2</sub>), IgGb (IgG<sub>4</sub>), IgGc (IgG<sub>6</sub> and IgG<sub>7</sub>) and IgG(T) (IgG<sub>3</sub> and IgG<sub>5</sub>) (17, 18). In addition to IgG, other isotypes that participate in equine immunity include immunoglobulin A (IgA), immunoglobulin M (IgM), immunoglobulin D (IgD) and immunoglobulin E (IgE) (4). Research investigating the measurement of these Ig isotypes and IgG subclasses in adult horse plasma is scarce. A review of current literature identified only a handful of studies where the primary objective was to establish normal ranges for IgM, IgA or IgG subclasses in adult horse serum using either radial immunodiffusion (RID) or enzyme-linked immunosorbent (ELISA) assays (13, 19-21). These papers represent the majority of recent work investigating the measurement of Ig isotypes (other than IgG) or IgG subclasses in adult horses, however, significant discrepancies were noted among their

results. Therefore, further studies are required to establish normal reference ranges for Ig isotypes and IgG subclasses in adult plasma (13, 19-21).

At present, RID assays are no longer commercially available for equine Ig isotype quantitation other than IgG or IgM. As a result, ELISA assays are one of the only remaining commercial methods for this purpose. However, ELISAs suffer from a number of disadvantages including the use of temperature and contamination sensitive reagents and a higher cost per test than other screening methods, particularly when only a few samples are assayed at one time (5). Therefore, a rapid, accurate and cost-effective assay is required for the measurement of Ig isotypes and IgG subclasses in equine serum.

In the past decade, Fourier-transform infrared (FTIR) spectroscopy has emerged as a powerful diagnostic tool for the quantitative characterization of biological fluids in both human and veterinary medicine (5, 22-24). In particular, FTIR spectroscopy has proven to be an accurate, economical and reagent-free method for equine IgG quantitation in foal serum and adult equine plasma samples (5, 25). Based on these successful proof-of-concept studies for IgG measurement in equids, it would seem plausible that infrared spectroscopy may also serve as a promising new method for the quantification of other Ig isotypes and IgG subclasses in equine plasma.

The first objective of this study was to determine adult equine plasma IgGa, IgGb, IgG(T), IgA, and IgM concentrations using an ELISA assay and to compare these results to previous studies using the ELISA assay, as well as to compare the sum of IgGa, IgGb, and IgG(T) results to the total IgG concentrations found in horses included in the



study. The second objective was to develop FTIR based assays for the measurement IgGa, IgGb, IgG(T), IgA, and IgM for equine plasma using the ELISA results as the reference test.

### **3.3. Materials and methods**

#### **3.3.1. Experimental animals & sample collection**

This study was carried out in accordance with the University of Prince Edward Island's Animal Care Committee animal utilization protocol. Plasma samples were collected from 100 healthy adult horses. All horses were a part of a closed herd that was privately owned by a commercial equine plasma company (Lake Immunogenics Inc., located in Ontario, New York, USA). Blood samples were collected by company employees from donor horses via jugular venipuncture using sodium citrate as the anticoagulant. Samples were collected in compliance with a New York State permit for the use of living animals and a United States Department of Agriculture research license. Samples were frozen and shipped on dry ice to the Atlantic Veterinary College (AVC) where they were stored at -80°C. All samples were used in a separate study at the AVC prior to use in the current study and were stored at -80°C for the duration between studies (25).

#### **3.3.2. Enzyme-linked immunosorbant assays for equine plasma IgG subclasses, IgM and IgA**

##### **3.3.2.1. Plasma sample dilutions**

To ensure plasma sample concentrations fell within a specific range, as per the manufacturer's instructions, plasma samples were diluted prior to their use in the

commercial ELISA kits (Bethyl Laboratories Inc.; Montgomery, TX). Dilution factors were determined using the expected concentrations of the immunoglobulin isotype to be measured (obtained from the literature) (13, 21) and the manufacture stated concentration range limits of the different ELISA kits (200 – 3.12 ng/ml for IgGa and IgGb and 1000 – 15.6 ng/ml for the IgG(T), IgM and IgA kits). The dilution factor that would theoretically allow the results to best fall within the middle of the concentration range for each ELISA kit was employed. For example, the IgGb concentration range in the literature is  $7.8 - 35.5 \times 10^6$  ng/ml (21). Using  $20 \times 10^6$  ng/ml as the median expected IgGb concentration to be measured, it was calculated that a dilution factor of 1:200,000 would allow the sample results to fall within the centre (i.e., 100 ng/ml) of our standard curve. Using the same calculation method for the other isotypes or IgG subclasses, dilution factors of 1:40,000 for IgGa, 1:8,000 for IgG(T), 1:3,000 for IgA and 1:2,000 for IgM were obtained. These dilutions were adequate for IgGa, IgGb, IgA and IgM. However, IgG(T) required further dilution to 1:15,000 to allow all serum samples to fall within the standard range of the test kit.

#### **3.3.2.2. Standard dilutions**

A set of eight standards were prepared in accordance with the manufacturer's instructions for each ELISA kit (see APPENDIX A, section 1 for details). The eight standard concentrations varied depending on the specificity of each ELISA. For the IgG(T), IgA and IgM ELISA quantitation kits, the standard concentrations were 1,000 ng/ml, 500 ng/ml, 250 ng/ml, 125 ng/ml, 62.5 ng/ml, 31.25 ng/ml, 15.6 ng/ml and 0 ng/ml. For the IgGa and IgGb ELISA quantitation kits, the standard concentrations were

200 ng/ml, 100 ng/ml, 50 ng/ml, 25 ng/ml, 12.5 ng/ml, 6.25 ng/ml, 3.12 ng/ml and 0 ng/ml.

#### **3.3.2.3. Detection antibody dilutions**

The manufacturer-supplied detection antibody was a horseradish peroxidase (HRP) conjugated polyclonal immunoglobulin (specific to each kit). Detection antibody dilutions were prepared for use in the individual ELISAs as per manufacturer's instructions (see APPENDIX A, section 2 for details). Recommended starting dilutions were provided for each kit with instructions to increase or decrease the detection antibody dilution if the optical density (OD) value for the highest standard was above or below the required range of 1.8-2.2. Recommended starting dilutions were 1:75,000 for IgG(T), 1:60,000 for IgGb, 1:35,000 for IgGa, 1:35,000 for IgM and 1:100,000 for IgA. With the exception of IgG(T) and IgA, these recommended starting dilutions were inadequate to maintain the OD value of the highest standard within the required 1.8-2.2 range. To resolve this issue, multiple trials investigating different detection antibody dilutions were performed for IgGa, IgGb and IgM to identify the optimal detection antibody concentration for each of these three Ig isotypes/subclasses (see APPENDIX A, section 3 for details). Final dilutions of 1:42,000 for IgGa, 1:65,000 for IgGb and 1:45,000 for IgM were used in this study.

#### **3.3.2.4. Procedure overview**

For each isotype or IgG subclass, all 100 samples were run simultaneously by a single operator. Using the previously determined serum, standard and detection antibody dilutions for each antibody isotype or subclass, commercially available ELISA

kits were used according to the manufacturer's instructions (Bethyl Laboratories Inc.; Montgomery, TX). Briefly, 100µl of diluted coating antibody was added to each well of a 96-well microplate and incubated at room temperature (20-25°C) for one hour. After incubation, plates were washed five times (with a Tris-saline wash buffer containing 0.05% Tween) using an automated washer<sup>d</sup>. All wells were then blocked with 200ul/well of blocking solution containing the basic wash solution (without Tween) plus 1% BSA for 30 minutes at room temperature. Plates were washed five times. Next, 100µl of diluted sample (n=100) or standard were added to duplicate wells and allowed to incubate at room temperature for one hour. Following incubation, plates were washed five times and 100µl of diluted HRP conjugated detection antibody was added to each well and allowed to incubate at room temperature for one hour. Plates were then washed five times and 100µl of tetramethylbenzidine (TMB) substrate solution was added to each well and incubated for 15 minutes at room temperature in the dark. The reaction was stopped by adding 100µl of stop solution (0.18M H<sub>2</sub>SO<sub>4</sub>) to each well. The absorbance of each well was measured on an ELISA microplate reader<sup>e</sup> at a wavelength of 450 nm. The microplate reader was interfaced with a software program<sup>f</sup> that created a standard curve for each plate from which the serum Ig isotypes or subclasses concentrations were derived.

### **3.3.3. Radial immunodiffusion assays for equine plasma IgG**

Commercial RID assays (Triple J Farms; Bellingham, WA) were used as the reference method for determining total IgG plasma concentrations. RID assays were performed according to manufacturer's instructions and all samples were diluted 1:1

with sterile saline. The zones of precipitation diameters were read at 22-24 hours by a single operator to the nearest tenth of a millimetre using a handheld calliper. Each sample and standard was tested in replicates of five. The average of the 5 replicates of the assay standards were fitted by linear regression, and that equation was used to determine the concentration of IgG for the unknown serum samples. The average of the 5 replicate results for each sample was used to determine the IgG concentration of that sample.

#### **3.3.4. Fourier-transform infrared spectroscopy for immunoglobulin isotypes and IgG subclasses**

Thawed plasma samples were diluted 1:1 with a 4 g/L potassium thiocyanate solution. Following dilution, dry films were made for each serum sample by evenly spreading 8 $\mu$ l aliquots of diluted sample onto 5-mm wells within a custom-made, adhesive-masked, 96-well silicon microplate.<sup>(5)</sup> Twelve sample replicates were made for sample 1 – 63, while 6 sample replicates were made for samples 64 – 100. Each loaded microplate was allowed to dry at room temperature before being loaded into a multisampler<sup>a</sup> interfaced with a FTIR spectrometer<sup>b</sup> and controlled with proprietary software<sup>c</sup>. Absorbance spectra in the infrared (IR) range of 400-4000  $\text{cm}^{-1}$  were recorded (resolution 4  $\text{cm}^{-1}$ , 512 scans) for each replicate of each sample, using the single beam spectrum of an empty well as the background. These spectral parameters were utilized in a previous study (25).

#### **3.3.5. Data processing and algorithm development**

The data set for each Ig isotype (IgGa, IgGb, IgG(T), IgA and IgM) was processed and analysed separately using the same methods as outlined below. For each of the 100 serum samples, absorbance spectra in the IR range of 400-4000  $\text{cm}^{-1}$  were converted into printable format by GRAMS software package<sup>g</sup>, then imported into MATLAB<sup>®h</sup> for further analysis.

A total of 978 spectra (63 samples x 12 replicates + 37 samples x 6 replicates) were processed using the Savitzky-Golay method to smooth the spectra and standard normal variate transformation to reduce the effect of light scattering and baseline variations (26, 27). Spectrum region selections at 3700-2600  $\text{cm}^{-1}$  and 1800-1300 $\text{cm}^{-1}$  were chosen based on earlier work at the using FTIR spectroscopy for IgG analysis in horses (5). The spectra for each sample were then averaged and used for succeeding analysis.

Using Dixon's Q-test, one sample was identified and removed as an outlier, leading to spectra from 99 samples used in further analysis (28). For each of the five isotype data sets, the spectra were divided into a training set (N=60 sera) and prediction set (N=39 sera). Partial least squares (PLS) regression was employed to build the calibration model (29). To determine the number of PLS factors in PLS regression, the training set was further randomly split into two sets of equal size (N=30 each). The first set was used to build a model with the number of PLS factors chosen from 1 to 30 and the second set was used to calculate the sum of squares of the difference between the Ig values from FTIR and ELISA. This procedure was repeated 5,000 times. The number of PLS factors was chosen as the one giving the lowest Monte Carlo cross validation value

(see equation in Chapter 2, page 72). Once the number of PLS factors were determined, the whole training set was used to develop a calibration model for each Ig isotype or subclass. Then 39 samples in the prediction set were used to test the predictive performance of the developed models.

### **3.3.6. Statistical analysis of ELISA-derived Ig concentrations**

Agreement between the ELISA and FTIR generated Ig concentrations for each isotype in the training and prediction sets was assessed by scatter plot and the Pearson correlation coefficient.

Descriptive statistics (mean + standard deviation [SD]) for each data set were calculated using a computer-based statistical software program<sup>i</sup>. Comparisons between ELISA Ig isotype concentration results in this study and those in current literature were performed using two-sample t-tests. Results with  $p \leq 0.05$  were considered significant. For comparison with the present study, standard deviations were calculated for results in the literature which only provided the standard margin of error (SEM) using the equation  $SD = \sqrt{n} * SEM$ , where  $n$  = sample size.

The mean RID IgG concentration for the 100 equine plasma samples was compared to the mean ELISA total IgG concentration (obtained by summing the IgGa, IgGb and IgG(T) concentrations for each sample then acquiring the mean of these results) using a two-sample t-test ( $p \leq 0.05$ ).

### **3.3.7 Nanosep® centrifugal filtration device trials for the removal of albumin from equine plasma samples**

Following the above procedures, trials were conducted using Nanosep® 100K centrifugal filter devices (Pall Life Sciences; Ann Arbor, MI) in an attempt to increase the relative concentration of Ig isotypes and subclasses in equine plasma by removing albumin from the sample. Full details of these trials are outlined in APPENDIX B. In brief, multiple trials were performed according to the manufacturer's instructions using various plasma starting volumes, plasma dilutions and filter washing techniques. Visual examination of the resulting spectra, and comparison of these to the original un-filtered spectra, was used to determine whether albumin was successfully removed from the plasma samples. Visual examination of the filtrate spectra was also performed to identify whether albumin had in fact passed through the membrane into the filtrate.

### **3.4. Results**

Serum concentrations (g/L) ranged from 1.31 – 5.05 for IgGa, 5.45 – 19.85 for IgGb, 1.59 – 16.69 for IgG(T), 0.18 – 7.04 for IgA and 0.25 – 1.65 for IgM. Table 3.1 (page 120) displays the mean serum immunoglobulin concentrations of IgGa, IgGb, IgG(T), IgA and IgM found in this study, as well as those from previously published studies for comparison (13, 19-21). No significant differences were noted between the IgG(T) and IgM results in this study and those of de Camargo et al., yet significant differences were observed between IgA concentrations (13). The IgGa and IgG(T) concentration results of Sheoran et al. were similar to those calculated in this study, yet their IgGb and IgA concentrations differed significantly (21). Results of this study were all significantly different from those found in the studies by McFarlane et. al. and Holznagel et al. (19, 20).



The RID IgG concentrations for the 100 plasma samples ranged from 17.98 g/L to 53.14 g/L with a mean and standard deviation [SD] of  $30.98 \pm 8.25$  g/L. The sum of the IgGa, IgGb and IgG(T) ELISA concentrations for the 100 plasma samples ranged from 11.65 g/L to 28.56 g/L with a mean ( $\pm$  SD) of  $16.90 \pm 3.54$  g/L. T-test results indicate the two data sets are statistically different ( $p=0.000$ ) from one another.

The PLS regression trials yielded a model with 20 PLS factors for each of the Ig isotypes. In the training data sets, the Pearson correlation coefficients comparing the ELISA and FTIR-derived IgGa, IgGb, IgG(T), IgM and IgA concentrations were 0.55, 0.89, 0.88, 0.66 and 0.62, respectively. These results indicate that the FTIR predicted IgGb and IgG(T) concentrations in the training set had good correlation with their ELISA determined counterparts. The FTIR predicted IgGa, IgM and IgA concentrations in the training set exhibited poor correlation with their corresponding IgGa, IGM and IgA ELISA-determined concentrations.

In the prediction data sets, the Pearson correlation coefficients for the IgGa, IgGb, IgG(T), IgM and IgA results were 0.46, 0.71, 0.24, 0.27 and 0.09, respectively. These findings reveal that the FTIR predicted concentration values for each of the Ig isotypes in the prediction set had poor correlation with their corresponding ELISA-determined concentrations, with the exception of IgGb, which demonstrated moderate correlation. Scatter plots (Figures 3.1-3.5, pages 121-125) further show the findings of the Pearson correlation coefficients.

The full details of the results for the filtration trials are outlined in APPENDIX B. However, the key finding was that upon visual examination of the spectra obtained from

the fluid remaining in the sample reservoir, and comparison of these spectra to the original un-filtered spectra, large amounts of albumin were still present within the samples. The spectra obtained from the fluid remaining in the sample reservoir were very similar in appearance to the non-filtered whole serum spectra, almost displaying identical FTIR spectroscopy signals in most cases. Spectra obtained from the filtrate fluids displayed very weak signals, indicating albumin was not effectively removed from the plasma samples.

### **3.5. Discussion**

Within the limited sample size used, this study was unable to develop an infrared spectroscopic assay as an accurate technique for the measurement of Ig isotypes in equine plasma. It is possible that the Ig isotype concentrations evaluated were too low, and cover such a narrow range of values, that their identification via IR spectroscopy is more difficult than for previously published techniques for total equine plasma and serum IgG (5, 25).

For this study, IgGb showed the strongest level of agreement between FTIR and ELISA results, with correlation coefficients of 0.89 and 0.71 for the training and prediction sets, respectively. This is likely due to the fact that IgGb is the predominant IgG subclass found in equine serum, accounting for >60% of the total serum IgG concentration, which itself is the most abundant isotype in body fluids, typically having concentration values 10 to 100 times greater than IgA or IgM (13, 19-21, 30). As a result, IgGb is the predominant Ig constituent in equine plasma and this fact, combined with the results of this study, support the theory that it is less difficult to develop a successful

FTIR quantitation algorithm when the Ig to be measured is in higher concentrations.

Further work is required to identify methods which may improve algorithm development for the measurement of lower-concentration Ig's in equine plasma.

A potential reason for the disagreement noted in this study between FTIR and ELISA generated results may in part be due to other confounding plasma constituents which overshadow the lower-concentration Ig's in equine plasma. Plasma is a complex biological fluid consisting of numerous proteins, peptides, glycosaminoglycans, and exogenous substances (4, 31). Proteins normally found in equine plasma include albumin, Ig's, fibrinogen,  $\alpha_1$ -antitrypsin, transferrin and many others (31). Within this large repertoire of equine plasma proteins, albumin and Ig's (predominately IgG) are often the most abundant proteins measured (31). In particular, plasma albumin is considered the most abundant protein of the mammalian circulatory system and has a molecular weight ranging between 65-68kDa (32, 33).

Due to its abundance, it was hypothesized that the absorption bands produced by albumin within a plasma sample may overlap the IR bands of interest (such as those for the Ig isotypes). For this reason, a trial using Nanosep® 100K filter devices was performed in an attempt to remove albumin from the equine plasma samples and allow other constituents (such as the immunoglobulin isotypes and subclasses) with smaller concentrations to feature more prominently in the resulting IR spectra (31).

Unfortunately, in this study the Nanosep® filtration devices failed to effectively remove enough albumin from our equine plasma samples to obtain meaningful results.

Consequently, a potential area for further research may be to identify different methods

of albumin removal in an attempt to enhance the detection of equine Ig isotypes on resulting IR spectra.

Over the past two decades, increasing interest in the proteome of human serum and plasma has resulted in a large amount of research dedicated solely to the specific removal of albumin from these biofluids, in order to discover and/or detect proteins existing in lower concentrations (34-36). Authors of these studies believe that many of these lower-abundance proteins may provide useful clinical data on the physiological or clinical status of patients or serve as biomarkers of various disease conditions (34, 35). Several techniques have been proposed for the removal of albumin from human plasma and serum samples (34, 37). Similar to our study, methods attempting to remove plasma albumin by molecular weight separation via centrifugal filtration have proven unsuccessful in human research (37). Other methods relying on the affinity of albumin for certain blue textile dyes have proven effective at removing albumin from serum, yet these methods lack specificity as various other serum proteins also bind to the dye-based resins (34-36). Chen et al. described a method of precipitating albumin out of human serum using a trichloroacetic acid/acetone combination (35). With this method, they were able to remove 60% of albumin from their serum samples, with Ig's becoming the predominant proteins found in the resulting precipitate (35). In another study investigating the use of antibodies against human serum albumin, the authors were able to develop an immunoaffinity resin capable of removing albumin from serum (34). This method proved more efficient and specific than dye-based methods of albumin removal, however, the quantity of antibody required proved both problematic and

costly (34). Finally, a depletion of albumin component (DOC) protocol was developed which utilized a chemical based extraction method for the removal of albumin from human serum (36). This DOC protocol was able to effectively and specifically remove albumin from serum samples, thereby facilitating the detection and identification of many less abundant proteins within the samples (36). These studies in human literature provide useful insight into possible future directions for albumin depletion in equine serum.

Another potential limitation in this study was the use of ELISA assays as the reference standard to which to compare our FTIR algorithm-derived Ig results. In particular, the ELISA assays used for this study had considerable potential for human error with requirements for both high plasma and detection antibody dilutions. For example, with the IgGb assay, a plasma dilution of 1:200,000 and a detection antibody dilution of 1:65,000 were required. This resulted in only a few microliters of plasma or detection antibody being diluted in a large volume of diluent, thus allowing for possible errors in calculating, measuring or performing the dilutions. Any such error could then have the potential to significantly alter or skew the ELISA results in this study.

During the study, another technical difficulty encountered with the ELISA assays was the inability to consistently have the OD value for the highest standard of a particular kit to fall within the manufacturer's required range of 1.8 – 2.2. As an example, when initially using the IgGb assay, the OD value for the highest standard was > 2.2 on the first day, then fell within or below the range the next day, despite using the same procedure, materials and detection antibody dilution. This problem also occurred

with the IgG<sub>a</sub> and IgM and ELISA assays. In order to deal with this issue, multiple trials were performed to determine the most appropriate detection antibody dilution for each of the Ig isotype ELISA assays. The dilution of detection antibody which best allowed for the highest standard of that specific assay kit to fall within the range of  $1.8 \times 10^{-2}$  was chosen. Once this was determined, all 100 serum samples were run with that particular Ig ELISA assay kit by a single individual at the same time using the pre-determined detection antibody dilution. By doing this, it also allowed the same batch of coating antibody, wash solution, diluent and TMB substrate solution to be used for all 100 samples run, thereby increasing the consistency among the 100 sample results for each Ig isotype or subclass.

Due to the difficulties experienced with the ELISA assays in this project, it is reasonable to assume that other laboratories may have experienced similar problems. If so, what was perceived as significant differences between the results of this study and those previously mentioned, may be more attributable to interlab variation when running the ELISA assays. Not only were significant differences noted between our ELISA Ig concentration results and those found in the previously published studies, but one of the published papers also identified poor levels of agreement among some of the results found in current literature (13, 19-21). These findings indicate that there are currently no consistent published data regarding the normal concentration ranges of Ig isotypes in equine plasma using the ELISA assay. Further work, with larger data sets, is needed to establish universal reference ranges for Ig isotypes and subclasses in adult and foal plasma.

The mean IgG concentration determined by RID assay was found to be statistically different than the ELISA determined total IgG concentrations for the 100 equine plasma samples. In horses, IgGb is the predominant equine IgG subclass (constituting > 60%), followed by IgG(T), then IgGa and finally IgGc (which normally accounts for < 1% of the total IgG concentration) (30). In this study, the ELISA total IgG concentrations were obtained by summing IgGa, IgGb and IgG(T), which left IgGc as the only IgG subclass not accounted for. When comparing the data, it is evident that the ELISA total IgG concentrations were underestimated as 74% were more than 10 g/L lower than their corresponding RID values. Based on these results, the absence of IgGc from our ELISA total IgG concentrations cannot account for such a sizable difference as to do so would require the plasma IgGc concentrations to be higher than the IgGb values (which is highly improbable). Therefore, it is logical to assume that the ELISA determined IgG subclass concentrations, IgGb in particular, in this study were underestimated by the ELISA assays.

Only two of the previous studies reviewed attempted to quantify IgGa, IgGb and IgG(T) in equine serum (19, 21). These studies each used an ELISA assay for IgG subclass quantification and their IgGb results displayed no statistical difference from one another (21). In contrast, our mean ELISA IgGb concentration (9.21 g/L) was significantly different than the mean IgGb concentrations (19.60 g/L for Sheoran et al. and 16.87 g/L for Holznagel et al.) found in each the aforementioned studies (19, 21). These findings further highlight the likelihood that the ELISA assay used in this study underestimated the equine plasma IgGb concentrations which in turn led to the low total IgG values

calculated. Since completion of this project, the commercial IgGb ELISA assay used for this study has been discontinued by the manufacturers; making repeat testing of the samples with the ELISA impossible.

An additional source for potential error within this study could relate to the age and prior usage of the equine plasma samples themselves. The samples were over 5 years old at their time of use in this study and consequently had been exposed to multiple freeze-thaw cycles. This may have resulted in some degree of degradation of constituents, despite reasonable precautions being taken with respect to sample refrigeration. Although it is possible the protein composition of the samples may have changed with time, current literature indicates this is an unlikely cause of the discrepancies noted between FTIR and ELISA generated Ig concentrations in this study (38).

A study evaluating the stability of select proteins in human serum concluded that long term storage (>25 years at -20°C) of serum did not significantly alter the concentrations of certain proteins within that sample (38). In particular, this study evaluated serum albumin, IgE and IgG and concluded that it is possible to obtain reliable concentration results for these proteins, even in samples which have been undergone long term storage (38). Another study was able to demonstrate the long term stability of IgE within human serum samples stored long term (32-37 years) at -20°C (39). The authors were able to conclude that it is possible to reliably measure IgE concentrations in serum samples which have been stored long term (>30 years at -20°C) (39). While these studies investigated the effects of long term storage on human serum, they still



provide circumstantial evidence that the Ig concentrations in our equine plasma samples should be relatively stable and reliable, despite their longer storage time at -80°C.

Studies in both human and veterinary literature have investigated the effects of storage temperature and freeze-thaw cycles on different biochemical constituents of both serum and plasma samples (40-43). Human, canine and rat serum has been reported to be most stable, and therefore having the fewest changes in analyte levels, when stored long term at a temperature of -70°C (40). As well, a study assessing the effects of various freeze-thaw cycles on 13 canine plasma components (including total protein) found no significant differences between the original component concentrations and those concentrations calculated after one, two and three freeze-thaw cycles (42). These studies lend additional evidence that the storage time, temperature and freeze-thaw cycles of our equine plasma samples, while still potentially having mild changes in the protein concentrations within those samples, are not likely important factors in this study.

In conclusion, significant discrepancies were noted between the ELISA Ig isotype concentrations found in this study and those reported in the literature. It is unknown whether these differences are the result of interlab variability between testing methods or true differences among study groups. Regardless, further work is required to establish normal reference ranges for Ig isotypes and subclasses in adult plasma using an alternative analytical method. Additionally, further research is needed to identify the potential uses of Fourier-transform infrared spectroscopy in the quantification of Ig

isotypes in equine plasma. Studies using albumin-depleted plasma may be useful to better identify Ig isotypes within resulting IR spectra. If successful, these studies may provide valuable data to further enhance and refine the calibration model and algorithm development for the measurement of Ig isotypes in equine plasma.

### 3.6. Footnotes

- <sup>a</sup> HTS-XT autosampler, Bruker Optics<sup>®</sup>, Milton, ON, Canada
- <sup>b</sup> Tensor 37, Bruker Optics<sup>®</sup>, Milton, ON, Canada
- <sup>c</sup> OPUS<sup>®</sup> ver. 6.5, Bruker Optics<sup>®</sup>, Milton, ON, Canada
- <sup>d</sup> Microplate reader, Tecan Group Ltd., Markham, ON, Canada
- <sup>e</sup> Spectra Max Plus 384, Molecular Devices, Sunnyvale, CA, USA
- <sup>f</sup> SoftMax Pro 5 software, Molecular Devices, Sunnyvale, CA, USA
- <sup>g</sup> GRAMS software ver. 7.02, Thermo Fisher Scientific Inc, Waltham, MA, USA
- <sup>h</sup> MATLAB MathWorks R2011b, Natick, MA, USA
- <sup>i</sup> Minitab 16.0, Minitab Inc.<sup>®</sup>, State College, PA, USA
- <sup>j</sup> Cary 630 FTIR spectrometer, Agilent Technologies Canada Inc., Mississauga, ON
- <sup>k</sup> MicroLab FTIR software, Agilent Technologies Canada Inc., Mississauga, ON

### **3.7. Acknowledgements**

The authors would like to gratefully acknowledge Cynthia Mitchell and Judy Sheppard for their technical assistance with this project.

Funding for this project was supported by the Atlantic Canada Opportunities Agency and the Atlantic Veterinary College Research Fund.

### 3.8. References

1. Crisman MV, Scarratt WK. Immunodeficiency disorders in horses. *Veterinary Clinics of North America, Equine Practice*. 2008;24:299-310.
2. Leber R, Wiler R, Perryman LE, Meek K. Equine SCID: Mechanistic analysis and comparison with murine SCID. *Vet Immunol Immunopathol*. 1998;65:1-9.
3. Perkins GA, Nydam DV, Flaminio MJ, Ainsworth DM. Serum IgM concentrations in normal, fit horses and horses with lymphoma or other medical conditions. *J Vet Intern Med*. 2003;17:337-342.
4. Reed SM, Bayly WM, Sellon DC. *Equine Internal Medicine*. 3rd ed. St. Louis, MO: Saunders Elsevier, 2010:32-43.
5. Riley CB, McClure JT, Low-Ying S, Shaw RA. Use of fourier-transform infrared spectroscopy for the diagnosis of failure of transfer of passive immunity and measurement of immunoglobulin concentrations in horses. *J Vet Intern Med*. 2007;21:828-834.
6. Giguere S, Polkes AC. Immunologic disorders in neonatal foals. *Vet Clin North Am Equine Pract*. 2005;21:241-72, v. doi:10.1016/j.cveq.2005.04.004.
7. Davis R, Giguere S. Evaluation of five commercially available assays and measurement of serum total protein concentration via refractometry for the diagnosis of failure of passive transfer of immunity in foals. *J Am Vet Med Assoc*. 2005;227:1640-1645.
8. Clabough DL, Conboy HS, Roberts MC. Comparison of four screening techniques for the diagnosis of equine neonatal hypogammaglobulinemia. *J Am Vet Med Assoc*. 1989;194:1717-1720.
9. Pusterla N, Pusterla JB, Spier SJ, Puget B, Watson JL. Evaluation of the SNAP foal IgG test for the semiquantitative measurement of immunoglobulin G in foals. *Vet Rec*. 2002;151:258-260.
10. McCue PM. Evaluation of a turbidimetric immunoassay for measurement of plasma IgG concentration in foals. *Am J Vet Res*. 2007;68:1005-1009.
11. Davis DG, Schaefer DM, Hinchcliff KW, Wellman ML, Willet VE, Fletcher JM. Measurement of serum IgG in foals by radial immunodiffusion and automated turbidimetric immunoassay. *J Vet Intern Med*. 2005;19:93-96.

12. Metzger N, Hinchcliff KW, Hardy J, Schwarzwald CC, Wittum T. Usefulness of a commercial equine IgG test and serum protein concentration as indicators of failure of transfer of passive immunity in hospitalized foals. *J Vet Intern Med.* 2006;20:382-387.
13. de Camargo MM, Kuribayashi JS, Bombardieri CR, Hoge A. Normal distribution of immunoglobulin isotypes in adult horses. *Vet J.* 2009;182:359-361.  
doi:10.1016/j.tvjl.2008.05.014.
14. Riley CB, McClure JT, Low-Ying S, Dolenko BK, Somorjai RL, Shaw RA. Feasibility of infrared spectroscopy with pattern recognition techniques to identify a subpopulation of mares at risk of producing foals diagnosed with failure of transfer of passive immunity. *Aust Vet J.* 2012;90:387-391.
15. Perryman LE. Primary immunodeficiencies of horses. *Vet Clin North Am Equine Pract.* 2000;16:105-16, vii.
16. Tizard IR. *Veterinary Immunology :An Introduction.* 8th ed. St. Louis, Mo.: Saunders Elsevier, 2009:574.
17. Wagner B. Immunoglobulins and immunoglobulin genes of the horse. *Dev Comp Immunol.* 2006;30:155-164.
18. Wagner B, Miller DC, Lear TL, Antczak DF. The complete map of the ig heavy chain constant gene region reveals evidence for seven IgG isotypes and for IgD in the horse. *Journal of Immunology.* Bethesda; USA: American Association of Immunologists; 2004;173:3230-3242.
19. Holznagel DL, Hussey S, Mihalyi JE, Wilson WD, Lunn DP. Onset of immunoglobulin production in foals. *Equine Vet J.* 2003;35:620-622.
20. McFarlane D, Sellon DC, Gibbs SA. Age-related quantitative alterations in lymphocyte subsets and immunoglobulin isotypes in healthy horses. *Am J Vet Res.* 2001;62:1413-1417.
21. Sheoran AS, Timoney JF, Holmes MA, Karzenski SS, Crisman MV. Immunoglobulin isotypes in sera and nasal mucosal secretions and their neonatal transfer and distribution in horses. *Am J Vet Res.* 2000;61:1099-1105.
22. Shaw RA, Low-Ying S, Leroux M, Mantsch HH. Toward reagent-free clinical analysis: Quantitation of urine urea, creatinine, and total protein from the mid-infrared spectra of dried urine films. *Clin Chem.* 2000;46:1493-1495.

23. Low-Ying S, Shaw RA, Leroux M, Mantsch HH. Quantitation of glucose and urea in whole blood by mid-infrared spectroscopy of dry films. *Vibrational Spectroscopy*. 2002;28:111-116. doi:10.1016/S0924-2031(01)00150-3.
24. Dubois J, Shaw RA. IR spectroscopy in clinical and diagnostic applications. *Anal Chem*. 2004;76:361A-367A.
25. Hou S, McClure JT, Shaw RA, Riley CB. Immunoglobulin G measurement in blood plasma using infrared spectroscopy. *J of Applied Spectroscopy*. Accepted November 2013 with anticipated publication in April 2014.
26. Savitzky A, Golay MJE. Smoothing and differentiation of data by simplified least squares procedures. *Anal Chem*. 1964;36:1627-1639.
27. Barnes RJ, Dhanoa MS, Lister SJ. Standard normal variate transformation and de-trending of near-infrared diffuse reflectance spectra. *Appl Spectrosc*. 1989;43:772-777.
28. Rorabacher DB. A statistical treatment for rejection of deviant values: Critical values of dixon's "Q" parameter and related subrange ratios at the 95% confidence level. *Anal Chem*. 1991;63:139-146.
29. Beebe KR, Kowalski BR. An introduction to multivariate calibration and analysis. *Anal Chem*. 1987;59:1007A-1017A.
30. Lewis MJ, Wagner B, Woof JM. The different effector function capabilities of the seven equine IgG subclasses have implications for vaccine strategies. *Mol Immunol*. 2008;45:818-827.
31. Miller I, Friedlein A, Tsangaris G, Maris A, Fountoulakis M, Gemeiner M. The serum proteome of equus caballus. *Proteomics*. 2004;4:3227-3234.
32. Bujacz A. Structures of bovine, equine and leporine serum albumin. *Acta Crystallogr D Biol Crystallogr*. 2012;68:1278-1289. doi:10.1107/S0907444912027047.
33. Ho JX, Holowachuk EW, Norton EJ, Twigg PD, Carter DC. X-ray and primary structure of horse serum albumin (equus caballus) at 0.27-nm resolution. *Eur J Biochem*. 1993;215:205-212.
34. Steel LF, Trotter MG, Nakajima PB, Mattu TS, Gonye G, Block T. Efficient and specific removal of albumin from human serum samples. *Mol Cell Proteomics*. 2003;2:262-270.
35. Chen YY, Lin SY, Yeh YY, et al. A modified protein precipitation procedure for efficient removal of albumin from serum. *Electrophoresis*. 2005;26:2117-2127.

36. Colantonio DA, Dunkinson C, Bovenkamp DE, Van Eyk JE. Effective removal of albumin from serum. *Proteomics*. 2005;5:3831-3835.
37. Georgiou HM, Rice GE, Baker MS. Proteomic analysis of human plasma: Failure of centrifugal ultrafiltration to remove albumin and other high molecular weight proteins. *Proteomics*. 2001;1:1503-1506.
38. Gislefoss RE, Grimsrud TK, Morkrid L. Stability of selected serum proteins after long-term storage in the janus serum bank. *Clin Chem Lab Med*. 2009;47:596-603.
39. Henderson CE, Ownby D, Klebanoff M, Levine RJ. Stability of immunoglobulin E (IgE) in stored obstetric sera. *J Immunol Methods*. 1998;213:99-101.
40. Cray C, Rodriguez M, Zaias J, Altman NH. Effects of storage temperature and time on clinical biochemical parameters from rat serum. *J Am Assoc Lab Anim Sci*. 2009;48:202-204.
41. Cuhadar S, Koseoglu M, Atay A, Dirican A. The effect of storage time and freeze-thaw cycles on the stability of serum samples. *Biochemia Medica*. 2013;23:70-77. doi:10.11613/BM.2013.009.
42. Reynolds B, Taillade B, Medaille C, Palenche F, Trumel C, Lefebvre HP. Effect of repeated freeze-thaw cycles on routine plasma biochemical constituents in canine plasma. *Vet Clin Pathol*. 2006;35:339-340.
43. Thoresen SI, Tverdal A, Havre G, Morberg H. Effects of storage time and freezing temperature on clinical chemical parameters from canine serum and heparinized plasma. *Vet Clin Pathol*. 1995;24:129-133.



**Table 3.1.** Comparison of the mean ( $\pm$ SD) serum immunoglobulin concentrations (g/L) of IgGa, IgGb, IgG(T), IgM and IgA found in this study to the studies by Sheoran et al., de Camargo et al., McFarlane et al. and Holznagel et al. (13, 19-21). An (\*) denotes the Ig concentration results which differed significantly from the results of this study.

|               | Burns<br>(n=100) |       | Sheoran<br>(n=27) |     | deCamargo<br>(n=44 for<br>IgG(T), n=19<br>for IgA, n=47<br>for IgM) |      | McFarlane<br>(n=30) |      | Holznagel<br>(n=5) |      |
|---------------|------------------|-------|-------------------|-----|---|------|---------------------|------|--------------------|------|
|               | ELISA assays     |       | ELISA assays      |     | RID assays  |      | RID assays          |      | ELISA assays       |      |
|               | Mean             | SD    | Mean              | SD  | Mean  | SD   | Mean                | SD   | Mean               | SD   |
| <b>IgGa</b>   | 2.718            | 0.767 | 3.4               | 2.0 | ---   | ---  | ---                 | ---  | 3.68*              | 0.62 |
| <b>IgGb</b>   | 9.207            | 2.465 | 19.6*             | 6.5 | ---   | ---  | ---                 | ---  | 16.87*             | 1.96 |
| <b>IgG(T)</b> | 4.964            | 2.350 | 4.0               | 2.5 | 4.19  | 2.20 | 6.89*               | 1.85 | 8.36*              | 1.79 |
| <b>IgA</b>    | 1.013            | 0.760 | 0.4*              | 0.3 | 1.96*   | 0.73 | 2.99*               | 0.46 | 0.58*              | 0.21 |
| <b>IgM</b>    | 0.789            | 0.313 | ---               | --- | 0.70  | 0.30 | 1.91*               | 0.73 | ---                | ---  |

**Figure 3.1** Scatter plots comparing the IgGa concentrations in the training set (A) (Pearson correlation coefficient = 0.55) and test set (B) (Pearson correlation coefficient = 0.46) obtained from ELISA and FTIR methods. If ELISA and FTIR give comparable results, the data points should distribute closely around the reference line of  $45^\circ$ .

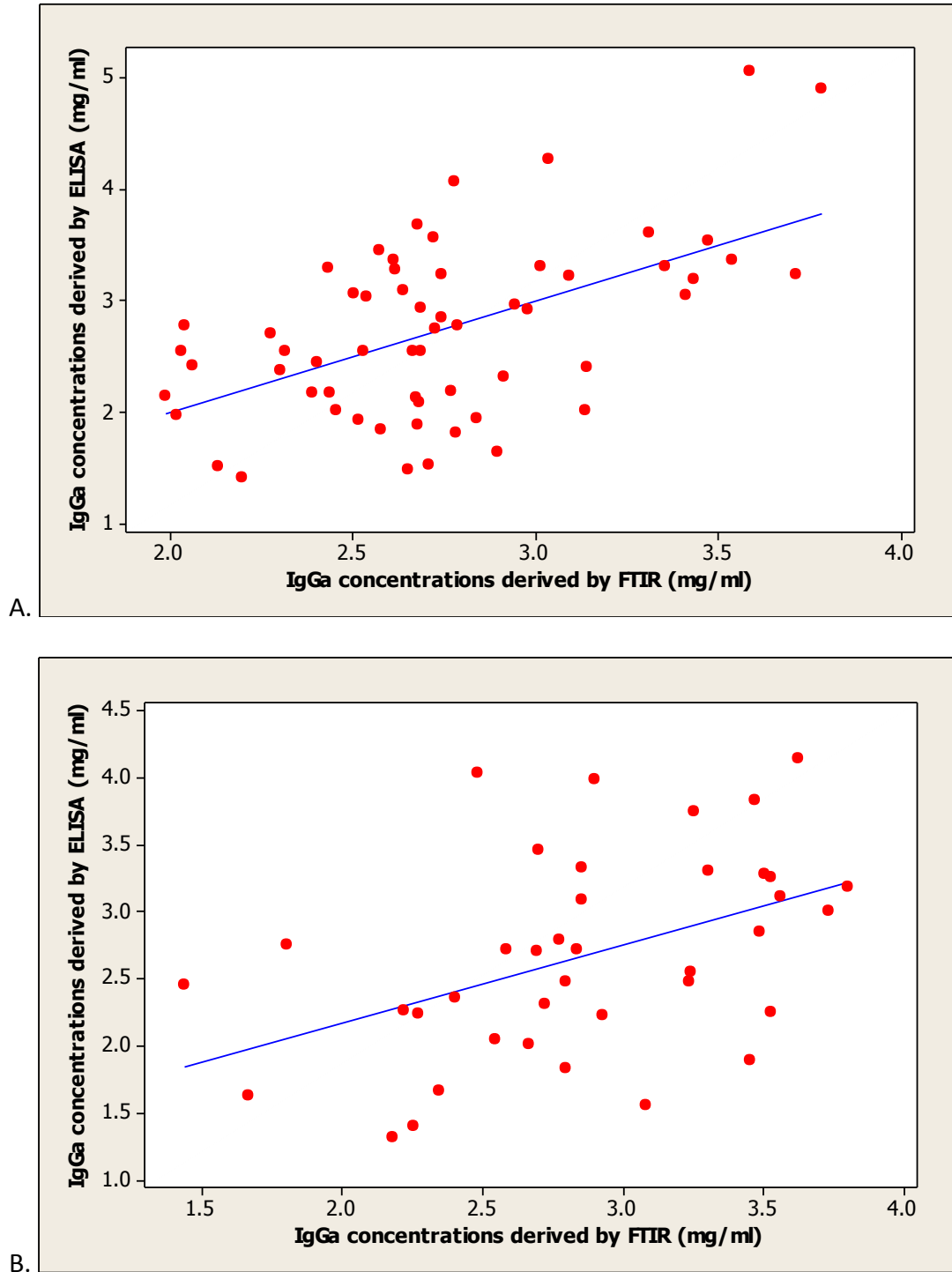


**Figure 3.2** Scatter plots comparing the IgGb concentrations in the training set (A) (Pearson correlation coefficient = 0.89) and test set (B) (Pearson correlation coefficient = 0.71) obtained from ELISA and FTIR methods. If ELISA and FTIR give comparable results, the data points should distribute closely around the reference line of 45°.

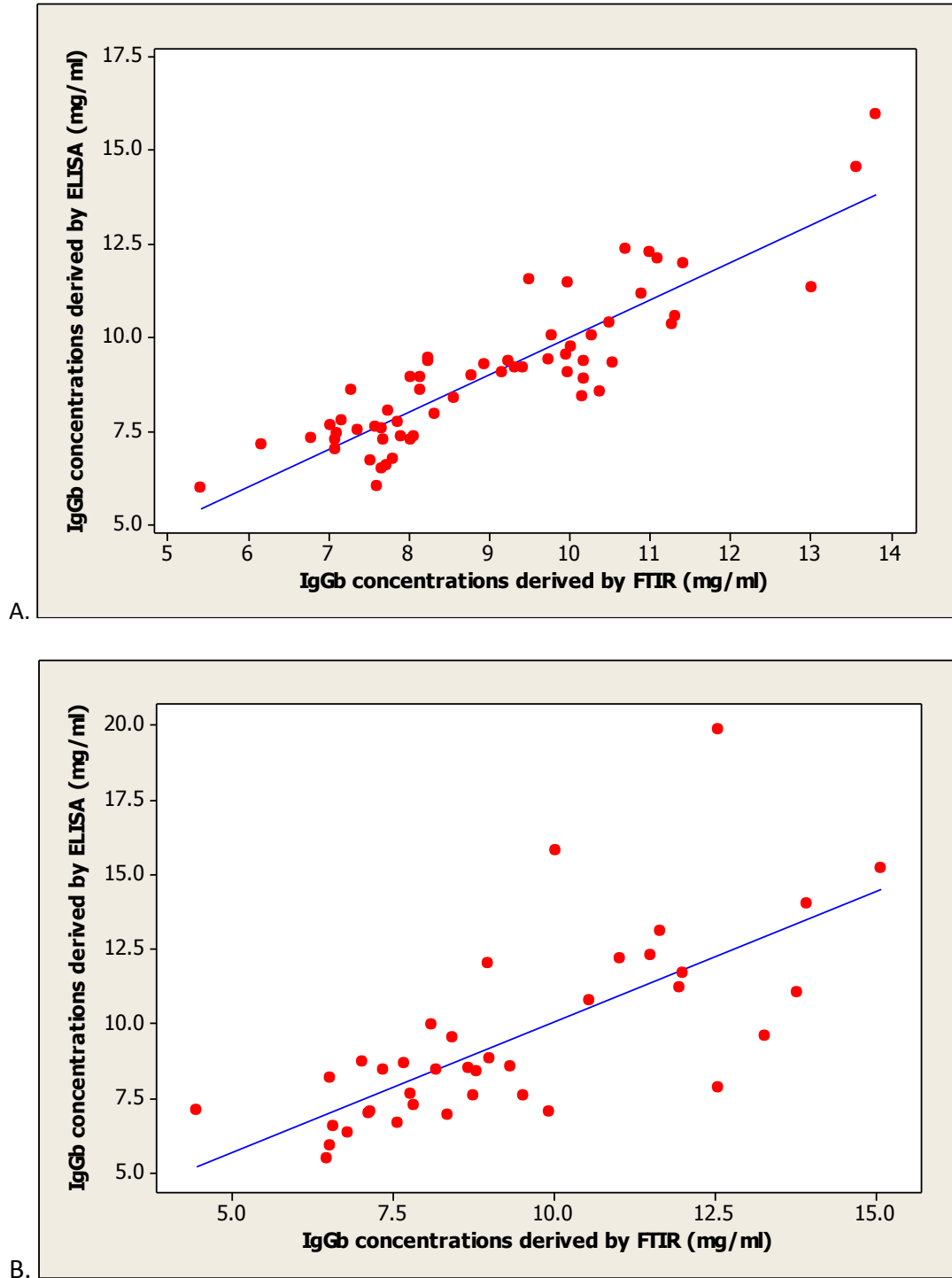


**Figure 3.3** Scatter plots comparing the IgG(T) concentrations in the training set (A) (Pearson correlation coefficient = 0.88) and test set (B) (Pearson correlation coefficient = 0.24) obtained from ELISA and FTIR methods. If ELISA and FTIR give comparable results, the data points should distribute closely around the reference line of 45°.

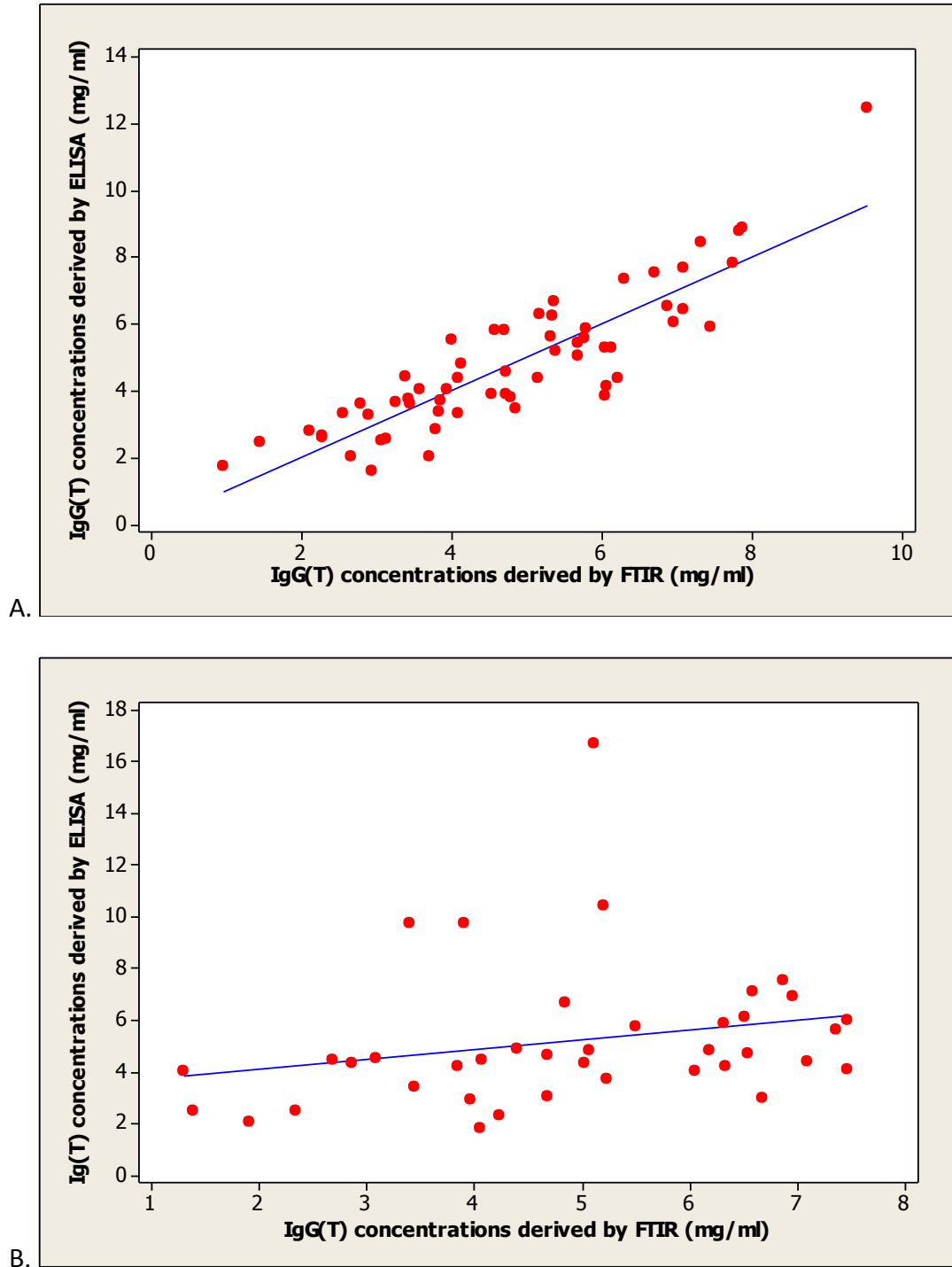


**Figure 3.4** Scatter plots comparing the IgA concentrations in the training set (A) (Pearson correlation coefficient = 0.62) and test set (B) (Pearson correlation coefficient = 0.09) obtained from ELISA and FTIR methods. If ELISA and FTIR give comparable results, the data points should distribute closely around the reference line of 45°.

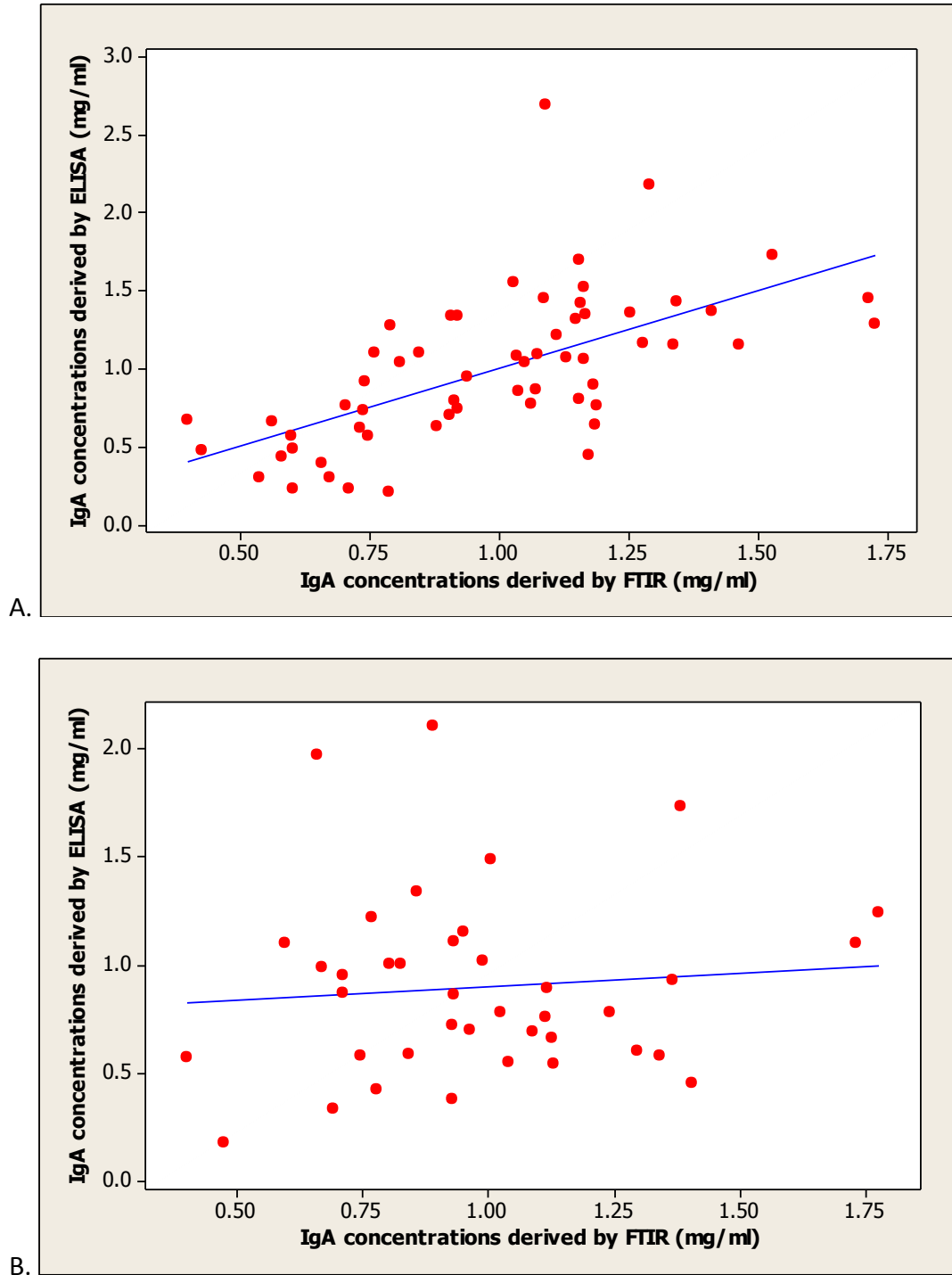
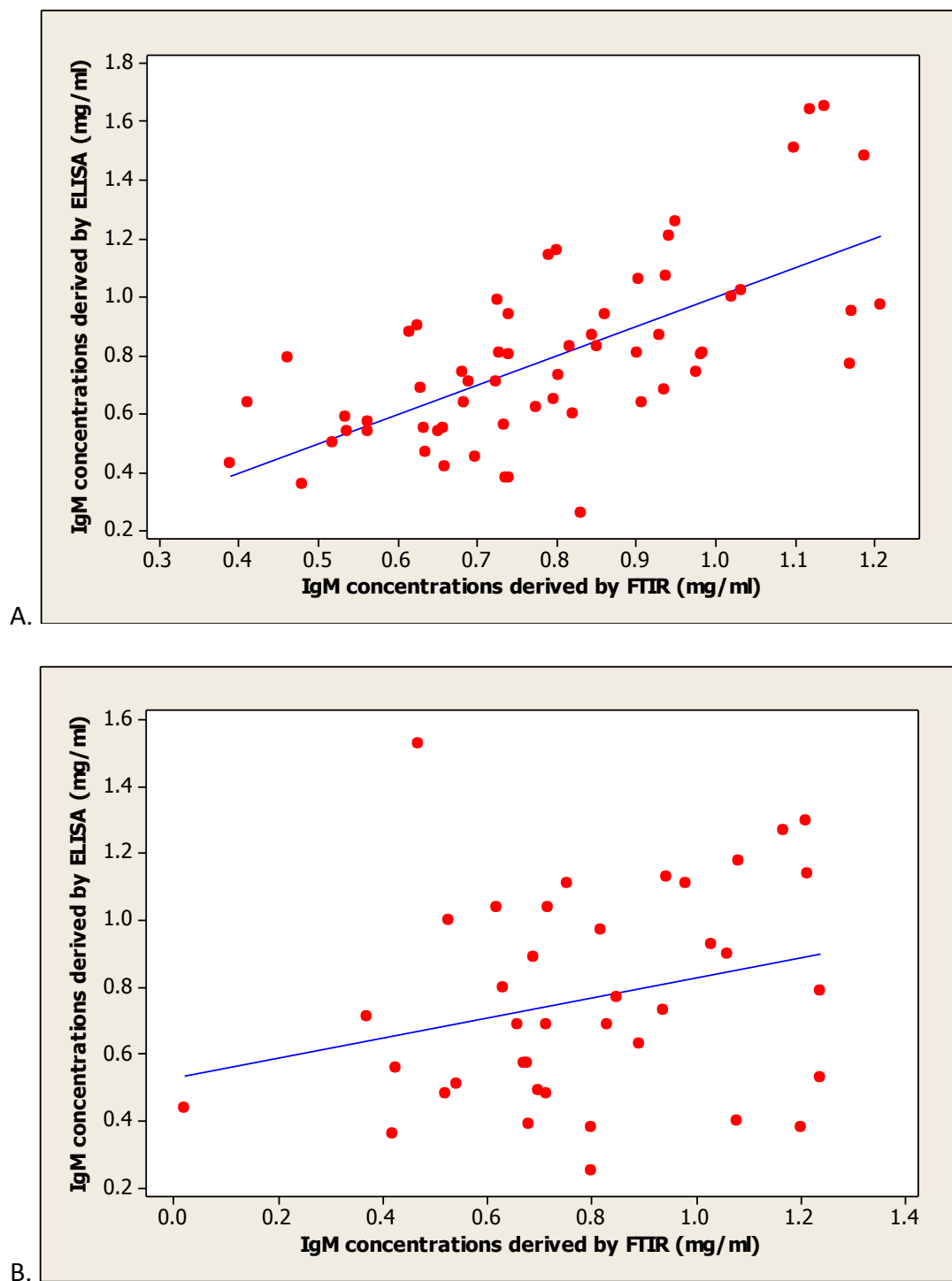


**Figure 3.5** Scatter plots comparing the IgM concentrations in the training set (A) (Pearson correlation coefficient = 0.66) and test set (B) (Pearson correlation coefficient = 0.27) obtained from ELISA and FTIR methods. If ELISA and FTIR give comparable results, the data points should distribute closely around the reference line of 45°.



**CHAPTER 4**  
**GENERAL DISCUSSION**

#### **4.1. Summary of findings**

The primary objective of this project was to investigate the use of Fourier-transform infrared (FTIR) spectroscopy for the quantification of specific immunoglobulin (Ig) isotypes and subclasses in equine and camelid serum. In the first chapter of this thesis, a detailed review of relevant current literature identified important factors which provided evidence for pursuing this research. First and foremost, chapter 1 highlighted the need for improved testing methods to aid in the diagnosis of immunodeficiency disorders in camelid and equine species. More specifically, it emphasized the demand for an accurate, rapid and economical assay to quantify immunoglobulin G (IgG) in camelid serum. It also outlined the current lack of specific and sensitive testing options available for the measurement of Ig isotypes (other than IgG) or IgG subclasses in equine serum.

The first chapter also introduced the background and methodologies relating to infrared spectroscopy, as well as its current applications in both human and veterinary medicine. Considerable research has shown FTIR-based analytical methods to have excellent accuracy for the screening, diagnosis or classification of various diseases in both human and animal species (1-4). However, despite this success, limited research to date has focused on the use of FTIR spectroscopy for the measurement of Ig concentrations in human or animal serum (5, 6). Prior to this study, only two publications were found detailing the use of infrared spectroscopy for the quantification of serum or plasma Ig's in an animal species ( both of which were performed at the Atlantic Veterinary College [AVC]) (5, 7). As a result, this present study is the first to



report the use of FTIR spectroscopy for the measurement of IgG in camelid serum. This study also examined the potential of FTIR spectroscopy for the measurement of equine Ig isotypes (other than IgG) and IgG subclasses, building on of previous research at the AVC where total IgG concentrations were effectively measured in equine serum (5).

The second chapter of this thesis specifically examined the ability of FTIR spectroscopy to measure alpaca serum IgG concentrations. To do this, serum from 175 privately-owned, healthy alpacas was analysed by radial immunodiffusion (RID) assay and FTIR spectroscopy. An algorithm for an infrared based assay was built using partial least squares regression to convert the spectroscopic data into quantitative values which were then compared with their RID-derived counterparts. Scatter plots and Pearson correlation coefficients indicated that the FTIR predicted IgG concentrations had good to excellent correlation with RID determined IgG concentrations. As a result, this study confirmed that FTIR spectroscopy, in combination with chemometrics, is a promising technique for the measurement of IgG concentrations in camelid serum. This data is believed to be the first published work outlining the use of FTIR spectroscopy for the quantification of IgG levels in camelid serum.

One limitation identified in chapter two of this thesis was the relatively small number of camelid serum samples with low IgG concentrations in the data set. The samples collected for this study were convenience samples obtained during routine herd health visits to alpaca farms in Ontario and New Brunswick, Canada and Adelaide, Australia. Consequently, the majority of samples were from adult alpacas with IgG concentrations in the normal range ( $>1000$  mg/dl) with only 21 of the 175 samples used

in this study having low serum IgG concentrations (<1000 mg/dl) based on RID. This may affect the algorithm's accuracy in predicting IgG values at lower concentrations (as algorithm development was weighted toward higher IgG concentrations) for FTIR.

The focus for the third chapter of this thesis was to develop FTIR based assays for the measurement IgGa, IgGb, IgG(T), IgA, and IgM in equine plasma using enzyme linked immunosorbent assays (ELISA) as the "gold standard" reference test. A second objective was to compare the ELISA IgGa, IgGb, IgG(T), IgA, and IgM concentrations measured in this study to the results of previous studies found in the literature. Methods similar to those used in chapter two were employed to build a calibration model and algorithm which would convert the FTIR spectra obtained from 100 adult equine plasma samples into quantitative values. These results were then compared to IgGa, IgGb, IgG(T), IgA, and IgM concentrations calculated via ELISA assays. With the exception of IgGb, the FTIR-predicted Ig isotypes exhibited a poor correlation with their corresponding ELISA-determined concentrations. It was speculated that this may in part be due to the relatively low plasma concentrations of these isotypes and subclasses relative to total IgG as well as interference from other confounding constituents, such as albumin, which are normally found in high plasma concentrations (8). Absorption bands produced by these confounders may overlap the bands of interest (such as the Ig isotypes or subclasses) on the infrared (IR) spectra, thereby not allowing plasma components with smaller concentrations to be easily identified and measured. These findings indicate that further research is needed to identify preprocessing methods for

Ig isotype/subclass concentration, if FTIR spectroscopy is to be of practical use for the quantification of Ig isotypes or subclasses in equine plasma.

Limited studies to date have attempted to quantify Ig isotypes and IgG subclasses in equine plasma (9-12). Of those studies which were found in the current literature, significant discrepancies were noted between reported concentrations (12). As a result, there is currently no unifying published data regarding the normal concentration ranges of Ig isotypes or IgG subclasses in equine plasma. Therefore, part of the focus for the third chapter of this thesis was to compare the ELISA IgGa, IgGb, IgG(T), IgA, and IgM concentrations measured in this study to the results of previous research. Significant discrepancies were noted between the concentrations found in this study and at least one or more of the Ig isotypes or IgG subclasses measured in each of the previous studies.

Perhaps the most important issue identified in chapter 3 was the significant difference noted between the mean RID IgG concentrations and the ELISA determined total IgG concentrations for the 100 equine plasma samples. For the past number of years, RID assays have been considered the gold standard reference method for the quantitation of serum or plasma IgG (5). As a result, when comparing the ELISA total IgG concentrations to their corresponding “gold standard” RID values, it becomes evident that the ELISA assays inaccurately measured the IgG subclasses by underestimating their true concentrations.

#### **4.2. Future directions**

The present study provided a basis for the potential use of FTIR spectroscopy in camelid IgG measurements. However, as previously mentioned, a significant limitation was the small number of serum samples with low IgG concentrations. An important next step would be to obtain a data set with a larger proportion of cria (particularly those <24 hours of age) serum samples. By doing so, it should increase the number of samples with IgG concentrations <1000 mg/dl. This would allow further modification of the quantitative algorithm which may improve its performance for the measurement of serum samples with lower IgG concentrations.

This study was unable to demonstrate that the concentrations of IgGa, IgGb, IgG(T), IgA, and IgM in equine plasma can be measured by FTIR spectroscopy. It appears more difficult to build an effective algorithm for the FTIR assays when the analyte to be measured is in low concentrations in the blood (due to interference from other higher concentration constituents). More specifically, it is suspected that the absorption bands produced by albumin within the plasma samples of this study were overlapping the Ig bands of interest on the infrared spectra, therefore causing difficulties in developing an effective algorithm for the IgGa, IgGb, IgG(T), IgA, and IgM. Further research investigating the preprocessing of plasma samples to remove albumin is warranted.

Attempts to remove plasma albumin by molecular weight separation via centrifugal filtration were unsuccessful in this project. However, various studies in human literature have outlined other promising methods for albumin depletion of serum samples (13-15). Based on this, a logical next step for future research would be to explore some of these methods and assess their feasibility in albumin depletion of

equine plasma samples. Certain techniques, such as affinity-based methods or immunoaffinity resins, would likely prove inadequate due to their lack of specificity, increased cost or low commercial availability (13-15). However, other methods such as the depletion of albumin component (DOC) protocol outlined by Colantonio et al., may have potential success with equine plasma samples (14). With this chemical based extraction method, which utilizes compounds routinely found in most laboratories, the authors' were able to successfully remove large volumes of serum albumin, while still maintaining the Ig's within the sample (14). The apparent success, ease of use and low cost of this method in human studies make it a promising method to explore with equine plasma samples (14).

Following the success of FTIR spectroscopy for the measurement of IgG concentrations in camelid and equine serum, an additional direction for future research should explore its potential to quantify IgG levels in colostrum samples of these species. Previous research has demonstrated the ability of infrared spectroscopy in the analysis of various bovine milk sample components, therefore it would be logical to assume that similar work can be done with equine and camelid colostrum (16-18). If successful, this could provide a rapid, inexpensive tool to identify foals and crias at risk for failure of transfer of passive immunity (FTPI) (due to inadequate colostrum IgG concentrations in the dam). In doing so, early, proper medical intervention could be provided to minimize the risk of FTPI in the neonate.

A final subject for future research would be to use FTIR spectroscopy for the investigation of serum IgG concentrations in horses of different age groups, breeds and

under different training conditions. This research would also be beneficial for IgA and IgM, if methods to accurately quantify these isotypes using FTIR spectroscopy become established. A study such as this would allow researchers to identify whether different physiological conditions (i.e. age, breed, physical activity level) influence the normal serum Ig isotype concentrations in these animals. As many immunodeficiencies in horses rely upon the measurement of certain Ig levels for diagnosis, establishing normal reference ranges for different equine populations would be an important step to ensure proper diagnoses for these diseases in horses.

### 4.3. References

1. Dubois J, Shaw RA. IR spectroscopy in clinical and diagnostic applications. *Anal Chem.* 2004;76:361A-367A.
2. Jackson M, Sowa MG, Mantsch HH. Infrared spectroscopy: A new frontier in medicine. *Biophys Chem.* 1997;68:109-125.
3. Vijarnsorn M, Riley CB, Ryan DAJ, Rose PL, Shaw RA. Identification of infrared absorption spectral characteristics of synovial fluid of horses with osteochondrosis of the tarsocrural joint. *Am J Vet Res.* 2007;68:517-523.
4. Vijarnsorn M, Riley CB, Shaw RA, et al. Use of infrared spectroscopy for diagnosis of traumatic arthritis in horses. *Am J Vet Res.* 2006;67:1286-1292.
5. Riley CB, McClure JT, Low-Ying S, Shaw RA. Use of fourier-transform infrared spectroscopy for the diagnosis of failure of transfer of passive immunity and measurement of immunoglobulin concentrations in horses. *J Vet Intern Med.* 2007;21:828-834.
6. Benzeddine-Boussaidi L, Cazorla G, Melin AM. Validation for quantification of immunoglobulins by fourier transform infrared spectrometry. *Clin Chem Lab Med.* 2009;47:83-90.
7. Hou S, McClure JT, Shaw RA, Riley CB. Immunoglobulin G measurement in blood plasma using infrared spectroscopy. *J of Applied Spectroscopy.* Accepted November 2013 with anticipated publication in April 2014.
8. Bujacz A. Structures of bovine, equine and leporine serum albumin. *Acta Crystallogr D Biol Crystallogr.* 2012;68:1278-1289.
9. Sheoran AS, Timoney JF, Holmes MA, Karzenski SS, Crisman MV. Immunoglobulin isotypes in sera and nasal mucosal secretions and their neonatal transfer and distribution in horses. *Am J Vet Res.* 2000;61:1099-1105.
10. McFarlane D, Sellon DC, Gibbs SA. Age-related quantitative alterations in lymphocyte subsets and immunoglobulin isotypes in healthy horses. *Am J Vet Res.* 2001;62:1413-1417.
11. Holznagel DL, Hussey S, Mihalyi JE, Wilson WD, Lunn DP. Onset of immunoglobulin production in foals. *Equine Vet J.* 2003;35:620-622.
12. de Camargo MM, Kuribayashi JS, Bombardieri CR, Hoge A. Normal distribution of immunoglobulin isotypes in adult horses. *Vet J.* 2009;182:359-361.
13. Chen YY, Lin SY, Yeh YY, et al. A modified protein precipitation procedure for efficient removal of albumin from serum. *Electrophoresis.* 2005;26:2117-2127.

14. Colantonio DA, Dunkinson C, Bovenkamp DE, Van Eyk JE. Effective removal of albumin from serum. *Proteomics*. 2005;5:3831-3835.
15. Steel LF, Trotter MG, Nakajima PB, Mattu TS, Gonye G, Block T. Efficient and specific removal of albumin from human serum samples. *Mol Cell Proteomics*. 2003;2:262-270.
16. Arunvipas P, VanLeeuwen JA, Dohoo IR, Keefe GP. Evaluation of the reliability and repeatability of automated milk urea nitrogen testing. *Can J Vet Res*. 2003;67:60-63.
17. Hansen PW. Screening of dairy cows for ketosis by use of infrared spectroscopy and multivariate calibration. *J Dairy Sci*. 1999;82:2005-2010.
18. Tsenkova R, Atanassova S, Kawano S, Toyoda K. Somatic cell count determination in cow's milk by near-infrared spectroscopy: A new diagnostic tool. *J Anim Sci*. 2001;79:2550-2557.



## **APPENDIX A. ENZYME-LINKED IMMUNOSORBENT ASSAYS FOR IgGa, IgGb, IgG(T), IgA AND IgM**

### **Section 1. STANDARD DILUTIONS**

#### **Horse IgGa ELISA quantitation set** (Bethyl Laboratories Inc.; Montgomery, TX)

To make standard concentration values of 200 ng/ml, 100 ng/ml, 50 ng/ml, 25 ng/ml, 12.5ng/ml, 6.25 ng/ml, 3.12 ng/ml and 0 ng/ml:

1. Dilute 5 µl of horse reference serum (1.8 mg/ml IgGa) in 9 ml of diluent to make an initial 1000 ng/ml dilution.
2. Dilute 500 µl of the initial (1000 ng/ml) dilution in 2 ml of diluent to make a 200 ng/ml dilution.
3. Serially dilute the 200 ng/ml dilution 1:1 6 times until a dilution of 3.12 ng/ml is reached.
4. Use 500 µl diluent as the zero standard value.

#### **Horse IgGb ELISA quantitation set** (Bethyl Laboratories Inc.; Montgomery, TX)

To make standard concentration values of 200 ng/ml, 100 ng/ml, 50 ng/ml, 25 ng/ml, 12.5ng/ml, 6.25 ng/ml, 3.12 ng/ml and 0 ng/ml:

1. Dilute 5 µl of horse reference serum (9.0 mg/ml IgGb) in 4.5 ml of diluent to make an initial 10 000 ng/ml dilution.
2. Dilute 100 µl of the initial (10 000 ng/ml) dilution in 4.9 ml of diluent to make a 200 ng/ml dilution.
3. Serially dilute the 200 ng/ml dilution 1:1 6 times until a dilution of 3.12 ng/ml is reached.
4. Use 500 µl diluent as the zero standard value.

#### **Horse IgG(T) ELISA quantitation set** (Bethyl Laboratories Inc.; Montgomery, TX)

To make standard concentration values of 1,000 ng/ml, 500 ng/ml, 250 ng/ml, 125 ng/ml, 62.5 ng/ml, 31.25 ng/ml, 15.6 ng/ml and 0 ng/ml:

1. Dilute 5 µl of horse reference serum (3.8 mg/ml IgG(T)) in 19.0 ml of diluent to make an initial 1 000 ng/ml dilution.
2. Serially dilute the 1000 ng/ml dilution 1:1 6 times until a dilution of 15.6 ng/ml is reached.
3. Use 500 µl diluent as the zero standard value.

**Horse IgA ELISA quantitation set** (Bethyl Laboratories Inc.; Montgomery, TX)

To make standard concentration values of 1,000 ng/ml, 500 ng/ml, 250 ng/ml, 125 ng/ml, 62.5 ng/ml, 31.25 ng/ml, 15.6 ng/ml and 0 ng/ml:

1. Dilute 5 µl of horse reference serum (1.5 mg/ml IgA) in 7.5 ml of diluent to make an initial 1 000 ng/ml dilution.
2. Serially dilute the 1000 ng/ml dilution 1:1 6 times until a dilution of 15.6 ng/ml is reached.
3. Use 500 µl diluent as the zero standard value.

**Horse IgM ELISA quantitation set** (Bethyl Laboratories Inc.; Montgomery, TX)

To make standard concentration values of 1,000 ng/ml, 500 ng/ml, 250 ng/ml, 125 ng/ml, 62.5 ng/ml, 31.25 ng/ml, 15.6 ng/ml and 0 ng/ml:

1. Dilute 5 µl of horse reference serum (1.0 mg/ml IgM) in 5.0 ml of diluent to make an initial 1 000 ng/ml dilution.
2. Serially dilute the 1000 ng/ml dilution 1:1 6 times until a dilution of 15.6 ng/ml is reached.
3. Use 500 µl diluent as the zero standard value.

**Section 2. RECOMMENDED STARTING DETECTION ANTIBODY DILUTIONS**

**Horse IgGa ELISA quantitation set** (Bethyl Laboratories Inc.; Montgomery, TX)

To make the manufacturer's recommended 1:35 000 detection antibody dilution:

1. Dilute 2µl of the appropriate HRP-conjugated detection antibody in 2 ml of diluent to make an initial dilution of 1:1,000.
2. Dilute 0.1 ml of the initial (1:1000) dilution in 3.4 ml of diluent (a 1:35 dilution) to make a final dilution of 1:35 000.

**Horse IgGb ELISA quantitation set** (Bethyl Laboratories Inc.; Montgomery, TX)

To make the manufacturer's recommended 1:60 000 detection antibody dilution:

1. Dilute 2µl of the appropriate HRP-conjugated detection antibody in 2 ml of diluent to make an initial dilution of 1:1,000.
2. Dilute 0.1 ml of the initial (1:1000) dilution in 5.9 ml of diluent (a 1:60 dilution) to make a final dilution of 1:60 000.

#### **Horse IgG(T) ELISA quantitation set** (Bethyl Laboratories Inc.; Montgomery, TX)

To make the manufacturer's recommended 1:75 000 detection antibody dilution:

1. Dilute 2µl of the appropriate HRP-conjugated detection antibody in 2 ml of diluent to make an initial dilution of 1:1,000.
2. Dilute 0.1 ml of the initial (1:1000) dilution in 7.4 ml of diluent (a 1:75 dilution) to make a final dilution of 1:75 000.

#### **Horse IgA ELISA quantitation set** (Bethyl Laboratories Inc.; Montgomery, TX)

To make the manufacturer's recommended 1:100 000 detection antibody dilution:

1. Dilute 2µl of the appropriate HRP-conjugated detection antibody in 2 ml of diluent to make an initial dilution of 1:1,000.
2. Dilute 0.1 ml of the initial (1:1000) dilution in 9.9 ml of diluent (a 1:100 dilution) to make a final dilution of 1:100 000.

#### **Horse IgM ELISA quantitation set** (Bethyl Laboratories Inc.; Montgomery, TX)

To make the manufacturer's recommended 1:35 000 detection antibody dilution:

1. Dilute 2µl of the appropriate HRP-conjugated detection antibody in 2 ml of diluent to make an initial dilution of 1:1,000.
2. Dilute 0.1 ml of the initial (1:1000) dilution in 3.4 ml of diluent (a 1:35 dilution) to make a final dilution of 1:35 000.

### **Section 3. DETECTION ANTIBODY DILUTION TRIALS**

#### **Horse IgGa ELISA quantitation set** (Bethyl Laboratories Inc.; Montgomery, TX)

The recommended detection antibody starting dilution of 1:35 000 made the optical density (OD) value for the highest standard fall above the required range of 1.8-2.2. According to manufacturer's instructions, a higher dilution factor was required to lower the OD value. To determine the optimal detection antibody concentration for the IgGa ELISA kit, a trial was conducted:

1. 4 dilutions were made using the HRP conjugated horse IgGa detection antibody: 1:35,000, 1:40,000, 1:45,000 and 1:50 000.
2. These dilutions were each added to duplicate wells containing the three highest standards (200 ng/ml, 100 ng/ml, 50 ng/ml) of the IgGa ELISA kit.

3. The ELISAs were otherwise performed according to manufacturer's instructions.
4. The dilution which best allowed the highest standard to fall within the desired 1.8-2.2 range was chosen for this study.

**Horse IgGb ELISA quantitation set** (Bethyl Laboratories Inc.; Montgomery, TX)

The recommended detection antibody starting dilution of 1:60 000 made the optical density (OD) value for the highest standard fall above the required range of 1.8-2.2. According to manufacturer's instructions, a higher dilution factor was required to lower the OD value. To determine the optimal detection antibody concentration for the IgGb ELISA kit, a trial was conducted:

1. 4 dilutions were made using the HRP conjugated horse IgGb detection antibody: 1:60,000, 1:70,000, 1:75,000 and 1:80,000
2. These dilutions were each added to duplicate wells containing the three highest standards (200 ng/ml, 100 ng/ml, 50 ng/ml) of the IgGb ELISA kit.
3. The ELISAs were otherwise performed according to manufacturer's instructions.
4. The dilution which best allowed the highest standard to fall within the desired 1.8-2.2 range was chosen for this study.

**Horse IgM ELISA quantitation set** (Bethyl Laboratories Inc.; Montgomery, TX)

The recommended detection antibody starting dilution of 1:35 000 made the optical density (OD) value for the highest standard fall above the required range of 1.8-2.2. According to manufacturer's instructions, a higher dilution factor was required to lower the OD value. To determine the optimal detection antibody concentration for the IgM ELISA kit, a trial was conducted:

1. 4 dilutions were made using the HRP conjugated horse IgM detection antibody: 1:40,000, 1:45,000, 1:50 000 and 1:55 000.
2. These dilutions were each added to duplicate wells containing the three highest standards (1000 ng/ml, 500 ng/ml, 250 ng/ml) of the IgM ELISA kit.
3. The ELISAs were otherwise performed according to manufacturer's instructions.
4. The dilution which best allowed the highest standard to fall within the desired 1.8-2.2 range was chosen for this study.

**APPENDIX B. EXPLORATORY TRIALS INTO THE USE OF NANOSEP® CENTRIFUGAL  
FILTRATIONS DEVICES FOR THE REMOVAL OF ALBUMIN FROM EQUINE  
PLSAMA**

**Section 1. FILTRATION DEVICE SIZE SELECTION**

Nanosep® centrifugal filter devices (Pall Life Sciences; Ann Arbor, MI) with 100kDa omega membrane filters were chosen to allow the passage of albumin (molecular weight <100 KDa) through the filter into the filtrate receiver while concurrently trapping immunoglobulins (molecular weight >100 KDa) on top of the membrane within the sample reservoir.

**Section 2. FILTRATION TRIALS**

**2.1 Initial filtration trial**

- 2 equine plasma samples were thawed at room temperature
- 0.4ml of each sample was pipetted into the sample reservoir of a filtration device
- The filtration devices were placed in a fixed-angle centrifuge rotor and spun at 14,000g for 20 minutes (in 5 minute increments)

This attempt to filter plasma with the filtration devices proved unsuccessful as a large portion (> 3/4) of the samples remained unfiltered within the sample reservoir, despite

adequate centrifugation. Potential reasons for this could include a problem with the filtration membrane itself, too high of a starting plasma volume or increased viscosity of the samples to be measured thus not allowing proper filtration through the membrane. Subsequently, results from this initial trial were discarded and additional trials were performed to identify whether one of these problems could account for the poor filtration of our equine plasma samples with the Nanosep® filtration devices.

## **2.2 Filtration trial to test the permeability of the omega membrane within the Nanosep® 100K centrifugal filter devices**

- 0.5ml of sterile saline was pipetted into the sample reservoirs of two filtration devices
- The filtration devices were placed in a fixed-angle centrifuge rotor and spun at 14,000g for 5 minutes

When both of the 0.5ml saline samples were able to pass completely through the membrane and into the filtrate receiver after 5 minutes of centrifugation, it was concluded that the filter membrane was functioning properly.

## **2.3 Filtration trial using 1:1 diluted plasma**

- 2 equine plasma samples were thawed at room temperature
- The plasma samples were diluted 1:1 with sterile saline (0.25ml of plasma + 0.25ml of saline)

- The diluted samples were pipetted into the sample reservoirs of a filtration device
- The filtration devices were placed in a fixed-angle centrifuge rotor and spun at 14,000g for 20 minutes (in 5 minute increments)
- Following centrifugation, the original serum samples, the remaining fluids in the sample reservoirs and the fluids collected in the filtrate receivers of the filtration device were each separately analysed using an FTIR spectrometer:
  - 4µl aliquots were evenly distributed onto the diamond crystal embedded in the steel sampling surface of the spectrometer
  - Samples were dried for four minutes using the 'cool' setting of a hairdryer which was positioned six inches from the sampling surface of the IR machine
  - Absorbance spectra in the IR range of 400-4000  $\text{cm}^{-1}$  were recorded (resolution 4  $\text{cm}^{-1}$ ) for each sample using the FTIR analyzer and its associated software
  - Five sample replicates were analyzed for each of the sample sections
  - Each of the original two (unfiltered) plasma samples were diluted 1:1 with sterile saline (40µl serum + 40µl saline) prior to analysis with the FTIR spectrometer (as outlined above)

For each sample, visual examination and comparison of the residual in the sample reservoir to the original un-filtered spectra indicate a large amount of albumin was still present within the sample. When the two spectra were displayed on the same graph, they overlapped extensively, exhibiting a very similar appearance. Spectra obtained from the filtrate fluid displayed a weak signal, indicating that albumin had not been effectively removed from the sample.

#### **2.4 Filtration trial using a decreased starting plasma volume**

- 1 equine plasma sample was thawed at room temperature
- 0.1ml of sample was pipetted into the sample reservoir of a filtration device
- The filtration device was placed in a fixed-angle centrifuge rotor and spun at 14,000g for 10 minutes (in 5 minute increments)
- Following centrifugation, both the original plasma sample, the remaining fluid in the sample reservoir and the fluid collected in the filtrate receiver of the filtration device were each separately analysed using an FTIR spectrometer (as detailed above in subsection 2.3)

Visual examination and comparison of the residual in the sample reservoir to the original un-filtered spectra indicate a large amount of albumin was still present within the sample. When the two spectra were displayed on the same graph, they overlapped extensively, exhibiting a very similar appearance. Spectra obtained from the filtrate



fluid displayed a weak signal, indicating that albumin had not been effectively removed from the sample.

## **2.5 Filtration trial using an increased plasma dilution**

- 1 equine plasma sample was thawed at room temperature
- The plasma sample was diluted 1:5 with sterile saline (0.1ml of plasma + 0.4ml of saline)
- The diluted sample was pipetted into the sample reservoir of a filtration device
- The filtration device was placed in a fixed-angle centrifuge rotor and spun at 14,000g for 20 minutes (in 5 minute increments)
- Following centrifugation, both the original plasma sample, the remaining fluid in the sample reservoir and the fluid collected in the filtrate receiver of the filtration device were each separately analysed using an FTIR spectrometer (as detailed above in subsection 2.3)

Visual examination and comparison of the residual in the sample reservoir to the original un-filtered spectra indicate a large amount of albumin was still present within the sample. When the two spectra were displayed on the same graph, they overlapped extensively, exhibiting a very similar appearance. Spectra obtained from the filtrate

fluid displayed a weak signal, indicating that albumin had not been effectively removed from the sample.

## **2.6 Additional filtration trial using increased plasma dilutions**

- 3 equine plasma sample were thawed at room temperature
- Each plasma sample was diluted 1:10 (50µl plasma + 450µl sterile saline), 1:20 (25µl plasma + 475µl sterile saline), 1:50 (10µl plasma + 490µl sterile saline) and 1:100 (5µl plasma + 495µl sterile saline)
- The diluted samples were each pipetted into the sample reservoir of a filtration device
- The filtration devices was placed in a fixed-angle centrifuge rotor and spun at 14,000g in 5 minute increments - the 1:50 and 1:100 plasma dilutions were centrifuged for a total of 10 minutes and the 1:10 and 1:20 plasma dilutions were centrifuged for a total of 15 minutes
- Following centrifugation, the remaining fluids in the sample reservoirs and the fluid collected in the filtrate receivers of the filtration devices were each analysed using an FTIR spectrometer (as detailed above in subsection 2.3)

For each sample, visual examination and comparison of the residual fluid in the sample reservoir to the original un-filtered spectra indicated a large amount of albumin was still present within the sample. When the two spectra were displayed on the same graph,

substantial overlap was still present and they exhibited a similar appearance, yet, mild changes were apparent indicating some compounds have been removed from the filtered spectra. However, spectra obtained from the filtrate fluid still displayed a weak signal, indicating that albumin had not been effectively removed from the sample.

## **2.7 Filtration trial using washed omega membranes**

Further experimentation was conducted to determine whether washing the Nanosep® 100K centrifugal filters prior to their use with plasma samples would improve the performance of the filtration device.

- 2 equine plasma sample were thawed at room temperature
- To wash the filtration devices:
  - 500µl of millipore water was pipetted into the sample reservoirs of the filtration devices
  - The filtration devices were placed in a fixed-angle centrifuge rotor and spun at 14,000g for 10 minutes
  - The water collected in the filtrate receiver was discarded
  - The wash procedure was repeated a second time
- 0.5ml of each plasma sample was pipetted into the sample reservoir of a washed filtration device
- The filtration devices were placed in a fixed-angle centrifuge rotor and spun at 14,000g for 30 minutes (in 5 minute increments)

When it was discovered the plasma was not passing from the sample reservoir through the omega membrane and into the filtrate receiver of the filtration device, these filters were discarded and the volume of sample to be filtered was decreased.

- 0.25ml of each plasma sample was pipetted into a sample reservoir of a washed filtration device
- The filtration devices were placed in a fixed-angle centrifuge rotor and spun at 14,000g for 25 minutes (in 5 minute increments)
- Following centrifugation, the remaining fluids in the sample reservoirs and the fluid collected in the filtrate receivers of the filtration devices were each analysed using an FTIR spectrometer as detailed above (in subsection 2.3) with the following exceptions:
  - The remaining fluid in the sample reservoirs was diluted 1:1 with sterile saline before analysis with the FTIR spectrometer (as the plasma was not diluted prior to filtration)
  - Only 3 sample replicates were analyzed for each of the sample sections

For each sample, visual examination and comparison of the residual fluid in the sample reservoir to the original un-filtered spectra indicated a large amount of albumin was still present within the sample. When the two spectra were displayed on the same graph, substantial overlap was still present and they exhibited a similar appearance, yet, mild changes were apparent indicating some compounds have been removed from the

filtered spectra. However, spectra obtained from the filtrate fluid still displayed a weak signal, indicating that albumin had not been effectively removed from the sample.

## **2.8 Second filtration trial using washed omega membranes**

- 2 equine plasma sample were thawed at room temperature
- Filtration devices were washed as outlined above (in subsection 2.7)
- 150 µl of each plasma sample was pipetted into the sample reservoir of a washed filtration device
- The filtration devices were placed in a fixed-angle centrifuge rotor and spun at 14,000g in 5 minute increments until all fluid appeared to have filtered through the membrane (total spin time was 40 minutes)
- 250 µl of sterile saline was added to the sample reservoir which was then manually agitated in an attempt to reconstitute the immunoglobulins which should have remained on the filter
- The fluids in the sample reservoirs and the fluid collected in the filtrate receivers of the filtration devices were then each analysed using an FTIR spectrometer as detailed above (in subsection 2.3) with the following exceptions:
  - The remaining fluid in the sample reservoirs was diluted 1:1 with sterile saline before analysis with the FTIR spectrometer (as the plasma was not diluted prior to filtration)

- Only 3 sample replicates were analyzed for each of the sample sections
- One of the plasma sample was also diluted 1:1 with sterile saline (125µl serum + 125µl saline)
- The diluted sample was pipetted into the sample reservoir of a filtration device
- The filtration device was placed in a fixed-angle centrifuge rotor and spun at 14,000g for 20 minutes (in 5 minute increments)
- Following centrifugation, the remaining fluid in the sample reservoir and the fluid collected in the filtrate receiver of the filtration device were each analysed using an FTIR spectrometer (as detailed above in subsection 2.3)
- Following analysis with the FTIR spectrometer, all fractions obtained from the filtrate receivers in this filtration trial were analyzed using a commercial equine IgG RID assay (Kent Laboratories, Bellingham, WA) to assess whether any immunoglobulins had passed through the filter

For each sample, visual examination and comparison of the residual fluid in the sample reservoir to the original un-filtered spectra indicated a large amount of albumin was still present within the sample. When the two spectra were displayed on the same graph, substantial overlap was still present and they exhibited a similar appearance, yet, mild changes were apparent indicating some compounds have been removed from the

filtered spectra. However, spectra obtained from the filtrate fluid still displayed a weak signal, indicating that albumin had not been effectively removed from the sample.

With the RID assays used in this filtration trial, no discernible rings of precipitation were identified for any of the fluid samples from the filtrate receivers. This confirms that no immunoglobulins had passed from the sample reservoir through the omega membrane and into the receiver of the filtration devices.